

University of Milan
Department of Health Sciences
Pharmacology Laboratory, Polo Universitario S. Paolo



Doctorate in
Physiopathology, Pharmacology, Clinical and
Therapeutic Approaches of Metabolic Disorders
(XXVIII ciclo)

**Post Mortem Neural Precursors Cells therapeutic intervention
promote neural tissue sparing and recovery of function in
Central Nervous System neurodegenerative models.**

Dottorando: Toniella Giallongo
Matricola: R 10212

Coordinatore: Chiar.mo Prof. Alfredo GORIO
Tutor: Chiar.mo Prof. Alfredo GORIO

A.A. 2014-2015

Index

Abstract.....	pg. 6
1. Introduction.....	pg. 9
1.1 Regenerative Medicine.....	pg. 10
1.2 Spinal cord injury.....	pg. 13
1.2.1 Spinal cord injury types.....	pg. 13
1.2.2 Diagnosis.....	pg. 16
1.2.3 Epidemiology.....	pg. 18
1.2.4 Physiopathology of Spinal Cord Injury.....	pg. 20
1.2.4.1 Primary Injury Phase.....	pg. 21
1.2.4.2 Secondary Injury Phase.....	pg. 22
1.2.4.3 Immediate phase.....	pg. 22
1.2.4.4 Acute phase.....	pg. 23
1.2.4.5 Intermediate phase.....	pg. 27
1.2.4.6 Chronic phase.....	pg. 27
1.3 Spinal cord injury therapies.....	pg. 29
1.3.1 Pharmacological therapies.....	pg. 29
1.3.1.1 Methylprednisolone.....	pg. 29
1.3.1.2 Ganglioside GM-1.....	pg. 30
1.3.1.3 Opioid receptor antagonist.....	pg. 31
1.3.1.4 Thyrotropin releasing hormone (TRH).....	pg. 31
1.3.1.5 Antagonists for glutamate receptor (GluR antagonists).....	pg. 31
1.3.1.6 Calcium channel inhibitors.....	pg. 32
1.3.1.7 Inhibition of sodium channel.....	pg. 32

1.3.1.8 Caspases inhibitors.....	pg 32
1.3.1.9 Monoclonal antibody (MoAb).....	pg. 33
1.3.1.10 Cyclosporine A (CsA).....	pg. 33
1.3.1.11 Minocycline.....	pg. 33
1.3.1.12 Erythropoietin (EPO).....	pg. 34
1.3.1.13 Estrogen.....	pg. 34
1.3.1.14 Progesterone.....	pg. 36
1.3.1.15 Cyclooxygenase inhibitors.....	pg. 36
1.3.1.16 Antioxidant.....	pg. 36
1.3.2 Cell therapy.....	pg. 37
1.3.2.1 Schwann cells.....	pg. 38
1.3.2.2 Human Olfactory Ensheathing Stem Cells (hOESCs).....	pg. 38
1.3.2.3 Embryonic Stem Cells (ESCs).....	pg. 39
1.3.2.4 Mesenchymal Stem Cells.....	pg. 40
1.3.2.5 Bone Marrow Derived Stromal Cells (MSCs).....	pg. 40
1.3.2.6 Adipose Derived Stem Cells (hADSCs).....	pg. 40
1.3.2.7 Neural Stem Cells.....	pg. 41
1.3.2.8 Post Mortem Neural Precursors Cells (PM-NPCs).....	pg. 42
1.4 Parkinson Disease.....	pg. 43
1.4.1 Synthesis and Metabolism of Dopamine.....	pg. 43
1.4.2 Dopamine neurotransmission.....	pg. 46
1.4.3 Animal models of Parkinson’s disease: classical toxin-induced rodent models.....	pg. 47
1.4.3.1 6-Hydroxydopamine (6-OHDA).....	pg. 48
1.4.3.2 1-methyl-4-phenyl-1,2,3,6-tetrahydropyridine (MPTP).....	pg. 50
2. Aim of the study.....	pg. 53
3. Materials and methods.....	pg. 56
3.1 Animals.....	pg. 57
3.2 Post Mortem Neural Precursor cells isolation.....	pg. 57
3.2.1 Neural precursors in culture.....	pg. 58
3.2.2 Spheroids immunofluorescence.....	pg. 58

3.2.3 Neuronal differentiation of PM-NPCs.....	pg. 60
3.2.4 Fixing of differentiated cells.....	pg. 60
3.2.5 Cells Immunofluorescence.....	pg. 60
3.2.6 Cell count.....	pg. 61
3.2.7 Cell freezing.....	pg. 62
3.2.8 Cell defrosting.....	pg. 62
3.2.9 PKH26 cells labelling.....	pg. 62
3.2.10 Hoechst cells labelling.....	pg. 64
3.3 Animal treatment for Spinal Cord Injury.....	pg. 64
3.3.1 Preparation of mice for surgery and transplantation.....	pg. 65
3.3.2 Preparation for surgery.....	pg. 65
3.3.3 Laminectomy.....	pg. 65
3.3.4 IH Impactor device protocol (Contusion).....	pg. 66
3.3.5 Sutures and post-care.....	pg. 67
3.4 Tail vein injection of cells.....	pg. 68
3.5 Behavioural Tests and hind limb function.....	pg. 68
3.6 Animal treatments for Parkinson's disease.....	pg. 70
3.7 Behavioural Tests for Parkinson's disease.....	pg. 71
3.8 MR in vivo.....	pg. 72
3.9 Perfusion.....	pg. 72
3.10 Tissue collection and processing.....	pg. 73
3.10.1 Cresyl-violet staining.....	pg. 74
3.10.2 Immunoistochemistry.....	pg. 74
3.10.3 Immunofluorescence.....	pg. 75
3.10.4 Assessment of Myelin preservation.....	pg. 77
3.10.5 Fluororuby staining.....	pg. 77
3.10.6 Confocal microscopy.....	pg. 78
3.10.6.1 Specimen Preparation and Imaging.....	pg. 79
3.10.6.2 Critical aspects of Confocal microscopy.....	pg. 79
3.11 Inflammation.....	pg. 79

3.11.1 Neutrophils quantification.....	pg.80
3.11.2 RNA extraction.....	pg. 80
3.11.2.1 Real-time RT-PCR analysis.....	pg. 80
3.11.2.2 Degradation of genomic DNA and reverse transcription-PCR (RT-PCR).....	pg 81
3.11.2.3 Real-time RT-PCR	pg. 82
3.11.2.4 Real-time RT-PCR conditions.....	pg. 86
3.12 Statistical Analysis.....	pg.86
3.13 Determination of dopamine and metabolites in Parkinson’s disease.....	pg.86
4. Results.....	pg.88
4.1 Derivation of GFP positive Post-Mortem Neural Precursor Cells and Characterization of their Self- Renewal capability.....	pg.89
4.2 Differentiation features of GFP positive PM-NPCs.....	pg. 91
4.3 GFP PM-NPCs neurospheres features before transplantation.....	pg. 93
4.4 PM-NPCs transplanted in Spinal Cord Injury.....	pg.94
4.4.1 PM-NPCs Improve Recovery of Hind Limb Function.....	pg 94
4.4.2 PM-NPCs mediated tissue sparing.....	pg.95
4.4.3 PM-NPCs Homing to Site of Injury, Survival and Differentiation.....	pg.100
4.4.4 PM-NPCs mediates chemokine and growth factor expression in the injured cord.	pg.106
4.4.5 Inflammatory Cell Migration to the Lesion Site.....	pg.107
4.4.6 PM-NPCs promote neural markers expression in recipient injured spinal cord.....	pg.109
4.4.7 Monoaminergic fibers in the injured cord.....	pg.110
4.4.8 PM-NPCs treatment results in increased expression of GAP-43.....	pg.113
4.4.9 Enhanced axonal sparing/regeneration by PM-NPCs.....	pg.114
4.5 PM-NPCs transplanted in Parkinson’s disease.....	pg.117
4.5.1 Loss of function correlate with loss of striatal dopamine.....	pg.117
4.5.2 PM-NPCs transplantation and recovery of function.....	pg.118
4.5.3 Reduced striatal levels of dopamine.....	pg.121
4.5.4 Localization of transplanted PM-NPCs.....	pg.123
4.5.5 Astrogliosis and cytokines changes.....	pg.124
4.5.6 PM-NPCs migratory processes.....	pg.127

4.5.7 Expression of typical markers by transplanted PM-NPCs.....pg.128

4.5.8 Is PM-NPCs action mediated by EPO?.....pg.130

5. Discussion..... pg. 132

6. Bibliography..... pg. 141

7. Pubblicaions pg. 170

Abstract

Regenerative medicine is a branch of translational research focused on the discovery of new approaches for replacement of cells tissue and organs used to improve the recovery in neurodegenerative or traumatic disease.

Spinal cord injury (SCI) is a debilitating clinical condition, characterized by a complex of neurological dysfunctions.). SCI disabilities range from cognitive impairment to loss of sensation and partial to complete paralysis.

We have isolated a subclass of neural progenitors, kept from SVZ 6 hours after animal death capable of surviving a powerful ischemia insult. These cells were named Post Mortem Neural Precursors Cells (PM-NPCs). Differentiation yield mostly neurons (about 30-40%) compared to regular NPCs (about 10-12%). Also the cholinergic yields is higher. Their EPO-dependent differentiation abilities produce a significantly higher percentage of neurons than regular NSCs.

The potential of PM-NPCs in terms of replacement therapy was investigated in a mouse model of contusive spinal cord injury lesioned at T9 level with intensity equal to 70 kDyne, by means of Infinity Horizon Impactor device. 1×10^6 PM-NPCs, were administered intravenously within two hours after the traumatic injury of the cord then the functional recovery and the fate of transplanted cells were studied.

Animals transplanted with PM-NPCs showed a remarkable improved recovery of hind limb function evaluated by Basso Mouse Scale up to 90 days after lesion. This was accompanied by reduced myelin loss, counteraction of the invasion of the lesion site by the inflammatory cells, and an attenuation of secondary degeneration. PM-NPCs migrate mostly at the injury site, where they survive and differentiate predominantly into cholinergic neurons, reconstitute a rich axonal and dendritic network and favors preservation of myelin fibers and promotes tyrosine hydroxylase and serotonergic fiber formation at lesion site. Moreover, the molecular analysis of the lesion site show that PM-NPCs induce a modulation of inflammatory response and release of neurotrophic factors. Pro-inflammatory cytokines (IL-6, MIP-2 and TNF-alpha) levels significantly decrease after 48 hours from spinal cord injury and PM-NPCs transplantation.

Moreover, our results show that transplantation of PM-NPCs facilitated significant axonal sparing/regeneration. This is associated with an increased amount of intact tissue at the lesion site. Anterograde tracing revealed statistically significant increased numbers for supraspinal tracts in PM-NPCs treated animals. Consequently, axons that regenerate across the lesion bridge and reach the caudal interface may mediate improvement in hindlimb movement

Cell therapies has been proposed as a regenerative approach to compensate the loss of specific cell populations in neurodegenerative disorders, where symptoms can be ascribed to the degeneration of a specific cell type. Parkinson's disease (PD) is the second most common neurodegenerative disease, caused by midbrain dopaminergic neurons degeneration in the Substantia Nigra (SN). Stem cell transplantation has emerged as a promising therapeutic approach. The other aim of this work was to evaluate the curative effects of PM-NPCs in a mouse model of PD. The degeneration of dopaminergic neurons was obtained with 1-methyl-4-phenyl-1,2,3,6-tetrahydropyridine (MPTP) administration in C57BL/6 mice at the dosage of 36 mg/kg intraperitoneally. Then the lesion was stabilized by a second injection (i.p.) of the drug at the dosage of 20 mg/kg. 1×10^5 of PM-PCs-GFP were administered to C57/BL mice by stereotaxic injection unilaterally in the left striatum 3 days after the second MPTP administration. The effects of transplanted cells were determined by means of performance tests aimed at detecting behavioral improvements. Our results show that animals treated with GFP-PM-NPCs had a remarkable improvement of parameters measured by means of both horizontal, vertical grid and olfactory tests starting with the third day after transplantation. These improvements were very significant and the average values were close to control. This was maintained throughout two weeks of experimental observation. This was likely promoted by PM-NPCs-derived erythropoietin (EPO), since the co-injection of cells with anti-EPO or anti-EPOR antibodies had completely neutralized the positive outcome. At the end of observational period, most of the transplanted PM-NPCs were vital, and were able to migrate ventrally and caudally from the injection site, reaching the ipsilateral and contralateral Substantia Nigra. Transplanted cells were differentiated into dopaminergic, cholinergic, and gabaergic neurons.

In conclusion, we purified a new class of neural precursors able to survive after a powerful ischemic insult (PM-NPCs). We found that treatment with PM-NPCs can limit the effects of degeneration of the injury both in the spinal cord and in Parkinson's disease. For these reasons these cells represent a liable source for cellular therapy in neurodegenerative disorders, especially on spinal cord injury and Parkinson's disease.

1. Introduction

1.1 Regenerative Medicine

Regenerative medicine is a new branch of translational research focused on the discovery of new approaches towards repair, replacement and regeneration of cells, tissues and organs. It requires a combination of several technologies moving beyond the traditional transplantation and replacement therapies, including genetic engineering, soluble molecules and advanced cell therapy (Greenwood, 2006). The main goal of regenerative medicine is not just replacing what is not functioning in the body, but also inducing and improving the regeneration of intrinsic organism capacity.

Ranking (Score)	Applications of Regenerative Medicine	Examples Identified by the Panelists
1 (415)	Novel methods of insulin replacement and pancreatic islet regeneration for diabetes	Bone marrow stem cell transplantation for pancreatic regeneration Microencapsulation (e.g., poly-lactide-co-glycolide) for immunoisolation of transplanted islets Cultured insulin-producing cells from embryonic stem cells, pancreatic progenitor cells, or hepatic stem cells Genetically engineered cells to stably express insulin and contain a glucose-sensing mechanism
2 (358)	Autologous cells for the regeneration of heart muscle	Myocardial patch for cardiac regeneration Direct injection of autologous bone marrow mononuclear cells for cardiac repair Stromal cell injection for myocardial regeneration Localized angiogenic factor therapy through controlled release systems or gene therapy
3 (339)	Immune system enhancement by engineered immune cells and novel vaccination strategies for infectious disease	Genetically engineered immune cells to enhance or repair immune function Single-injection DNA vaccines
4 (272)	Tissue-engineered skin substitutes, autologous stem or progenitor cells, intelligent dressings, and other technologies for skin loss due to burns, wounds, and diabetic ulcers	Bilayered living skin constructs (e.g. Apligraf) Engineered growth factors (e.g. rbbFGF, rhEGF) applied in conjunction with topical treatments (e.g. SD-Ag-Zn cream) Intelligent dressings composed of a slow-releasing growth hormone polymer Epithelial cell sprays
5 (238)	Biocompatible blood substitutes for transfusion requirements	Polyhemoglobin blood substitutes for overcoming blood shortages and contamination issues
6 (200)	Umbilical cord blood banking for future cell replacement therapies and other applications	Preserved umbilical cord blood stem cells to provide future cell replacement therapies for diseases such as diabetes, stroke, myocardial ischemia, and Parkinson disease Pooled cord blood for the treatment of leukemia
7 (157.5)	Tissue-engineered cartilage, modified chondrocytes, and other tissue engineering technologies for traumatic and degenerative joint disease	Matrix-induced autologous chondrocyte implantation for cartilage repair Tissue-engineered cartilage production using mesenchymal stem cells
8 (121.5)	Gene therapy and stem cell transplants for inherited blood disorders	Genetically engineered hematopoietic stem cells to restore normal blood production in β -thalassemic patients
9 (105.5)	Nerve regeneration technologies using growth factors, stem cells, and synthetic nerve guides for spinal cord and peripheral nerve injuries	Synthetic nerve guides to protect regenerating nerves Embryonic stem cell therapy for spinal cord regeneration Growth factor-seeded scaffolds to enhance and direct nerve regeneration
10 (80)	Hepatocyte transplants for chronic liver diseases or liver failure	Microencapsulation of hepatocytes to prevent immunological reaction Derivation of hepatocytes for transplantation from embryonic stem cells Transdifferentiation of hepatocytes for transplantation from bone marrow cells

Table 1.1 Top Ten Regenerative Medicine Applications for Improving Health in Developing Countries (Greenwood et al, 2006)

The United States National Academies of Science Report, *Stem Cells and the Future of Regenerative Medicine*, estimates that more than a hundred million of patients with conditions such as cardiovascular disease, autoimmune diseases, diabetes, cancer, neurodegenerative diseases, and burns would be considered potential patients in the US for stem cell-based therapies (Petit-Zeman, 2001).

Stem cells are a key component of regenerative medicine, as they open the door to new clinical applications. For a successful application of stem cell-based approaches, it is necessary to define the scientific and clinical advances, as well as regulatory, ethical, and societal issues in terms of safety and efficacy (Hyun, 2008). Considering the large number of improved protocols of cells differentiation and the increasing availability of human multipotent stem cells, the prospect of an access to unlimited numbers of specific cell types on demand could become a reality for several diseases. Up-to-date advances in stem cell field are suggesting that the direct use of cells could really be translated into effective therapies for currently unmanageable disorders (Kriks, 2011; Ma, 2012), although the road towards translation in humans is still full of new challenges (Tabar, 2014).

There are three currently used approaches in the field of regenerative medicine (Figure 1.1): the stem cells implantation for new structures formation, the implantation of pre-primed cells already committed to a given direction, and the stimulation of endogenous cells to replace missing structures (Stocum, 2004). Each of the different aspects identified in the first two approaches, the generation of an appropriate cohort of regenerative cells, their regulated division and differentiation, and the restoration of the appropriate part of the structure, must be evoked by endogenous cells.

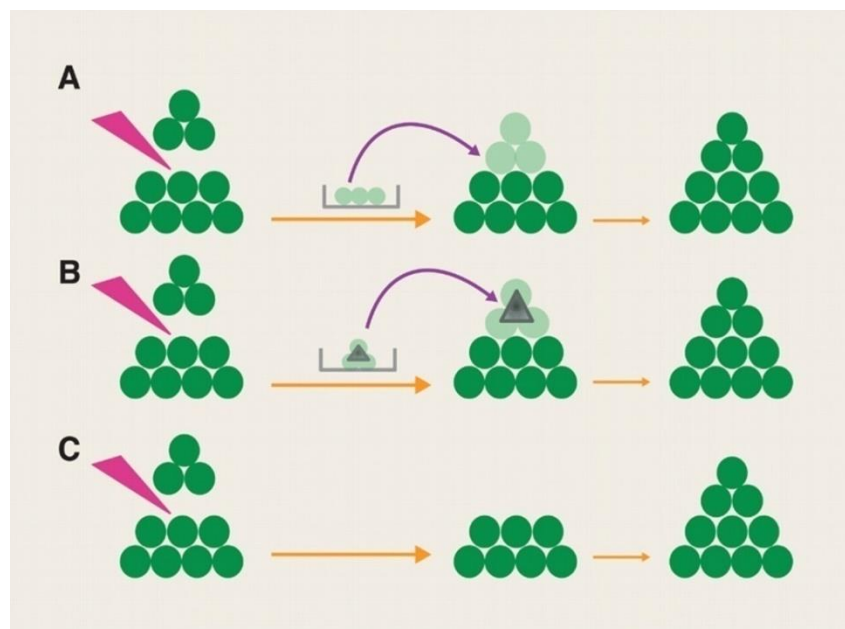


Figure.1.1.Schematic of three approaches to regenerative medicine.

(A) Implantation of stem cells (light green) from culture leads to the restoration of the structure. (B) Stem cells provided with a scaffold (triangle) in order to guide restoration. (C) The residual cells of the structure induced a regenerative response (Stocum, 2004).

So far, stem cell therapy has only been established as a clinical standard of care for diseases of the blood system. However, there is an increasing number of clinics testing stem cell interventions, some of them offer stem cell treatments for a variety of conditions without clear evidence of safety or efficacy. For the successful application of novel stem cell-based approaches, it will be necessary to define the scientific and clinical advances, as well as the associated regulatory, ethical, and societal issues, that need to be addressed in order to deliver treatments safely, effectively, and fairly (Fig. 1.2) (Hyun, 2008).

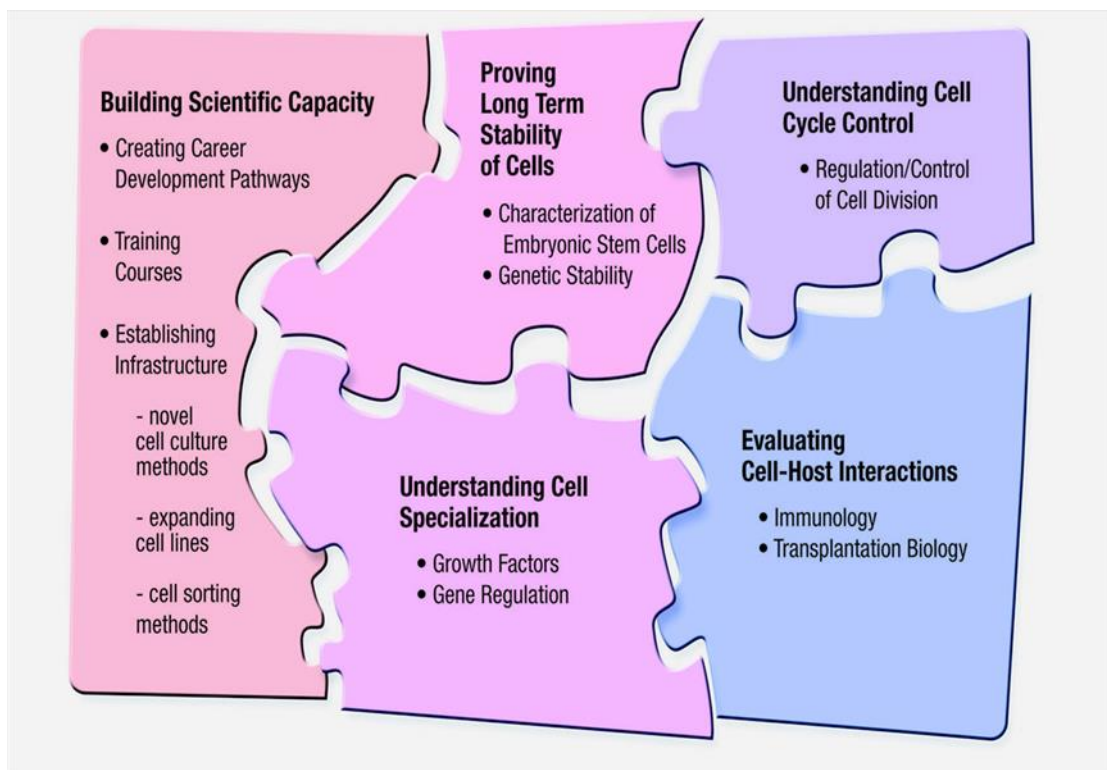


Figure.1.2. The scientific challenges of stem cells research in regenerative medicine

1.2 Spinal cord injury

Spinal Cord Injury (SCI) is a traumatic condition correlated with significant sensory and functional deficits, together with emotional, social, and financial burdens (Venkatesh, 2014). SCI disabilities range from cognitive impairment to loss of sensation and partial to complete paralysis. There are different types of spinal cord injuries depending on the region of the spinal cord and spinal level involved, and the injury may be complete or incomplete. Current therapies for improving clinical outcome include limiting inflammation, preventing secondary cell death and enhancing the plasticity of spared circuits.

1.2.1 Spinal cord injury types

Spinal cord injuries can be classified into three medical cases: the first one is *bone marrow contusion*, which recognizes a minimum anatomical alteration state, which can correspond to a complete alteration of bone marrow function, usually reversible. The trauma is more severe if an edema is present on the lesion site, or with the presence of hemorrhages spots, particularly in the region of the bone (central hemorrhagic lesion). In these conditions, the blood supply is terminal and depends exclusively by the central groove arterial. This is the case of the *spinal cord contusion*, in which the spinal cord injury is often incomplete and its evolution depends on the treatment of the lesion in the first hours after the trauma. In this case, there is no alteration of the bone structure.

On the other hand, a medical case with the more severe prognosis is the *spinal cord laceration*, which is rarely complete and usually involves complications caused by hemorrhagic masses, lacerations and meningeal vascular lesions with secondary ischemia, that make the lesion clearly distinguishable at the macroscopic level (Chirurgia Vol 2, Chirurgia specialistica). Often, immediately after spinal cord injury occurs an event called *spinal shock*, characterized by the complete death of all functional nerves below the injury. This condition can last for six weeks and is not only due to the bruise and edema formed on the spinal cord (caused by the compression of the bone between the vertebrae), but also to the lack of oxygen (caused by the interruption of the blood dispensing to the tissue). It is a physiological block of nerve conduction, which is not necessarily associated with a spinal cord organic damage. Initially occurs a full spinal cord injury, but after a variable interval there is a functional recovery that can become complete (Manuale di chirurgia Vol 1).

Another negative consequence of trauma is the syringomyelia: this is a painful disease that can develop in the first period after spinal cord injury and is caused by the formation of a large space inside the spinal cord fluid full, named *fistula*

Spinal cord injuries can be complete and incomplete.

Complete. There is no sensitive and motor function in the region caudal to the lesion, in the acute phase the limbs are flaccid, the osteotendinous reflexes and the sphincter motility are absent.

Incomplete. There are signals of spinal functions with a better prognosis. There are four types of incomplete lesions:

- Anterior spinal artery syndrome: is the primary blood supply to the anterior portion of the spinal cord. In this condition, there is the interruption in the anterior two-thirds of the spinal cord and medulla oblongata, causing ischemia or infarction of the spinal cord (Fig.1.3). It is characterized by loss of motor function below the level of injury (para- and tetra-paresis/plegia), loss of sensations carried by the anterior columns of the spinal cord (pain and temperature) and preservation of sensations carried by the posterior columns (fine touch and proprioception). Anterior spinal artery syndrome has poor prognosis and is the most common form of spinal cord infarction (Manuale di chirurgia Vol 1, Chirurgia sistemica, fisiopatologia, clinica, terapia Vol. 1, Scivoletto and Di Donna, 2009).

Anterior Cord Syndrome

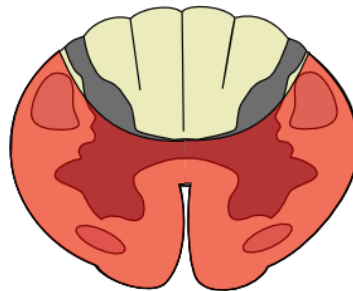


Figure 1.3. Representation of Anterior Cord Syndrome

- Posterior cord syndrome: is a very rare condition. It is caused by lesion of the posterior portion of the spinal cord, is characterized by pain and paresthesia of the limbs with modest sensitivity disorders (Manuale di chirurgia Vol 1, Chirurgia sistemica, fisiopatologia, clinica, terapia Vol. 1).
- Brown-Séquard syndrome or Brown-Séquard's paralysis: is caused by hemisection of the spinal cord with complete interruption of the motor and sensory tract, resulting in paralysis and

loss of proprioception on the ipsilateral side of the injury. In the contralateral side there are temperature sensation and pain sensitivity deficits, tactile discriminative sensation is conserved and there is dissociation of sensibility (Fig. 1.4) (Manuale di chirurgia Vol 1, Chirurgia sistemica, fisiopatologia, clinica, terapia Vol. 1, Scivoletto and Di Donna, 2009).

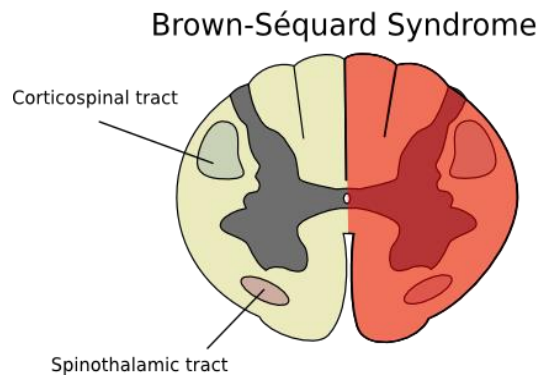


Figure 1.4. Representation of Brown-Séquard syndrome

- Central cord syndrome: is most common in the older persons because osteoarthritis in the neck region causes impairment of the vertebrae. The motility disorder is prevalent in the upper limbs than in the lower limbs, with variable sensory loss (Fig. 1.5) (Manuale di chirurgia Vol 1, Chirurgia sistemica, fisiopatologia, clinica, terapia Vol. 1, Merriam, 1986, Newey, 2000).

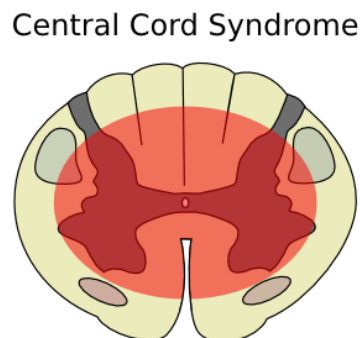


Figure 1.5. Representation of Central Cord Syndrome

A traumatic lesion is not the only cause of spinal cord injury because other factors could be implicated as infection, cysts and tumors. Complete spinal cord injuries result in complete paraplegia or complete tetraplegia.

Complete paraplegia is a complete lesion of the spinal cord at the thoracic or lumbar level and involves lower limbs paralysis and sphincter disorders.

Complete tetraplegia is a complete lesion of spinal cord at cervical level, causing the paralysis of all the limbs and neuro-vegetative disorders.

Para-paresis and tetra-paresis are characterized by incomplete paresis, respectively in the lower limbs, and the upper and lower limbs.

1.2.2 Diagnosis

The presence of a spinal injury requires a rapid and careful diagnosis to minimize to the patient possible posttraumatic complications and to decide the appropriate therapy to use, depending on the type and the degree of the lesion.

The main diagnostic tools used with patients with spinal cord injury is a radiological and neurological diagnosis.

As regards the radiological diagnosis, all patients with suspected spinal lesions should be subjected to radiography of the spinal cord in at least two positions (antero-posterior and lateral), with the inclusion of the first seven cervical and the first thoracic vertebrae. The axial computed tomography (TAC) should be performed in all cases of suspected or confirmed bone injury with simple radiography. The most important diagnostic technique for spinal cord injury is the magnetic resonance (RMN) because it allows the evaluation of the bone marrow structures, estimating possible involvements in the traumatic processes (Chirugiavol2, Chirurgiaspecialistica, Chirurgia sistemica, fisiopatologia, clinica, terapia Vol. 1, Fehlings, 1999). Neurological evaluation of the patient with spinal cord injury must consider not only the presence and site of motility disorders, but also motility and sphincter functions. Neurological examination is very important from the beginning and aims to establish a neurological level, where there are obvious motor or sensitivity deficits. The neurological examination should be conducted as early as possible and repeated frequently, especially in the first days after trauma for the high possibility of positive or negative changes (Chirugiavol 2, Chirurgiaspecialistica). Once the neurological level has been established, it is important to make an accurate description of the neurological deficits. In the past, there were scales

assessment defining the neurological condition of patients that were comparable between different therapy centers. The most widely used and accepted scale is currently the proposal from the American Spinal Injury Association (ASIA) (Fig. 1.6), which includes a standard neurological classification of spinal injury by motor score, based on the evaluation of some key muscle and one sensory groups. Based on the results of the neurological classification of patients, standards are further classified using the ASIA impairment scales, defining therefore the degree of deficiency of the patient (MSKTC, 2014).

The examination must be conducted bilaterally as they can be major differences between the two sides of the body.

Patient Name _____
 Examiner Name _____ Date/Time of Exam _____

ASIA AMERICAN SPINAL INJURY ASSOCIATION **STANDARD NEUROLOGICAL CLASSIFICATION OF SPINAL CORD INJURY** **ISCOS**

MOTOR
KEY MUSCLES
(scoring on reverse side)

	R	L	
C5	<input type="checkbox"/>	<input type="checkbox"/>	Elbow flexors
C6	<input type="checkbox"/>	<input type="checkbox"/>	Wrist extensors
C7	<input type="checkbox"/>	<input type="checkbox"/>	Elbow extensors
C8	<input type="checkbox"/>	<input type="checkbox"/>	Finger flexors (distal phalanx of middle finger)
T1	<input type="checkbox"/>	<input type="checkbox"/>	Finger abductors (little finger)

UPPER LIMB TOTAL (MAXIMUM) + =
 (25) (25) (50)

Comments: _____

L2	<input type="checkbox"/>	<input type="checkbox"/>	Hip flexors
L3	<input type="checkbox"/>	<input type="checkbox"/>	Knee extensors
L4	<input type="checkbox"/>	<input type="checkbox"/>	Ankle dorsiflexors
L5	<input type="checkbox"/>	<input type="checkbox"/>	Long toe extensors
S1	<input type="checkbox"/>	<input type="checkbox"/>	Ankle plantar flexors

LOWER LIMB TOTAL (MAXIMUM) + =
 (25) (25) (50)

SENSORY
KEY SENSORY POINTS

0 = absent
 1 = impaired
 2 = normal
 NT = not testable

	R	L		
C2	<input type="checkbox"/>	<input type="checkbox"/>		
C3	<input type="checkbox"/>	<input type="checkbox"/>		
C4	<input type="checkbox"/>	<input type="checkbox"/>		
C5	<input type="checkbox"/>	<input type="checkbox"/>		
C6	<input type="checkbox"/>	<input type="checkbox"/>		
C7	<input type="checkbox"/>	<input type="checkbox"/>		
C8	<input type="checkbox"/>	<input type="checkbox"/>		
T1	<input type="checkbox"/>	<input type="checkbox"/>		
T2	<input type="checkbox"/>	<input type="checkbox"/>		
T3	<input type="checkbox"/>	<input type="checkbox"/>		
T4	<input type="checkbox"/>	<input type="checkbox"/>		
T5	<input type="checkbox"/>	<input type="checkbox"/>		
T6	<input type="checkbox"/>	<input type="checkbox"/>		
T7	<input type="checkbox"/>	<input type="checkbox"/>		
T8	<input type="checkbox"/>	<input type="checkbox"/>		
T9	<input type="checkbox"/>	<input type="checkbox"/>		
T10	<input type="checkbox"/>	<input type="checkbox"/>		
T11	<input type="checkbox"/>	<input type="checkbox"/>		
T12	<input type="checkbox"/>	<input type="checkbox"/>		
L1	<input type="checkbox"/>	<input type="checkbox"/>		
L2	<input type="checkbox"/>	<input type="checkbox"/>		
L3	<input type="checkbox"/>	<input type="checkbox"/>		
L4	<input type="checkbox"/>	<input type="checkbox"/>		
L5	<input type="checkbox"/>	<input type="checkbox"/>		
S1	<input type="checkbox"/>	<input type="checkbox"/>		
S2	<input type="checkbox"/>	<input type="checkbox"/>		
S3	<input type="checkbox"/>	<input type="checkbox"/>		
S4-5	<input type="checkbox"/>	<input type="checkbox"/>		

TOTALS: + =
 (MAXIMUM) (56) (56) (56) (56)

Any anal sensation (Yes/No) Any anal sensation (Yes/No)

PIN PRICK SCORE (max: 112)

LIGHT TOUCH SCORE (max: 112)

• Key Sensory Points

NEUROLOGICAL LEVEL The most caudal segment with normal function

SENSORY	R	L
MOTOR	<input type="checkbox"/>	<input type="checkbox"/>

COMPLETE OR INCOMPLETE? Incomplete = Any sensory or motor function in S4-S5

ASIA IMPAIRMENT SCALE

ZONE OF PARTIAL PRESERVATION Caudal extent of partially preserved segments

SENSORY	R	L
MOTOR	<input type="checkbox"/>	<input type="checkbox"/>

This form may be copied freely but should not be altered without permission from the American Spinal Injury Association.

REV 03/04

Grade	Ability to move
5	The muscle can move the joint it crosses through a full range of motion, against gravity, and against full resistance applied by the examiner.
4	The muscle can move the joint it crosses through a full range of motion against moderate resistance.
3	The muscle can move the joint it crosses through a full range of motion against gravity but without any resistance.
2	The muscle can move the joint it crosses through a full range of motion only if the part is properly positioned so that the force of gravity is eliminated.
1	Muscle contraction is seen or identified with palpation, but it is insufficient to produce joint motion even with elimination of gravity.
0	No muscle contraction is seen or identified with palpation; paralysis.

ASIA grade	Clinical state (below level of injury)
A	Complete: No preservation of function below level of injury, and no sacral sparing (S4-S5).
B	Incomplete: Sensory but not motor function is preserved below the neurological level and includes the sacral segments S4-S5.
C	Incomplete: Motor function is preserved below the neurological level, and more than half of key muscles below the neurological level have a muscle grade less than 3.
D	Incomplete: Motor function is preserved below the neurological level, and at least half of key muscles below the neurological level have a muscle grade of 3 or more.
E	Normal: motor and sensory function are normal.

Figure 1.6. ASIA evaluation scale.

1.2.3 Epidemiology

Traumatic injury to the central nervous system (CNS) has devastating effects on the quality of life and represents an economic burden for the suffering patient (Abbaszadeh, 2015). Spinal cord injury (SCI), in particular, usually caused by a mechanical damage to the spinal cord and may result in a complete or incomplete loss of neural functions. These two conditions can lead to the loss of motor and/or sensory functions (Li, 2013). The annual incidence of SCI in the US is

approximately 40 cases per million population, not including those who died during the accident. The number of people alive with SCI in the US in 2014 are approximately 276,000, with a range from 240,000 to 337,000 persons (MSKTC, 2014). The mean age of SCI patient has increased during the 70's from 30 years to 42 years in 2010 and it occurs in approximately 70% among male. The most common causes of injury are high velocity/ high impact sports (Fig.1.7)(Li,2013; MSKTC,2014), such as motorcycle and diving, and young subjects usually undergo a worst damage, compared to older victims (Tator, 2000; Sekhon, 2001), because of their higher elasticity in the vertebral ligament and their underdeveloped spinal musculature.

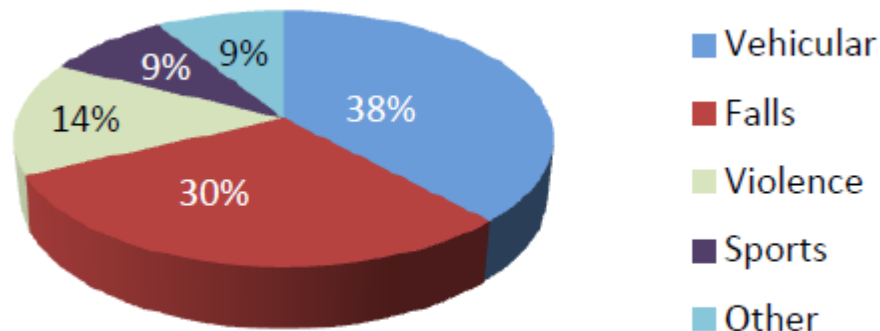


Figure 1.7. Diagram of the main causes of spinal cord injury.

The most frequent neurologic conditions of SCI are incomplete tetraplegia (45%) followed by incomplete paraplegia (21%), complete paraplegia (20%), and complete tetraplegia (14%) (Fig 1.7). Every year in the US are registered 12,000 cases of paraplegia and tetraplegia, caused by spinal cord injury, of which 4000 die before reaching the hospital and 1000 die during their hospitalization. Deaths after admission for acute SCI range from 4,4% to 16,7% (Sekhon and Fehlings, 2001; Kraus, 1980). Considering the relative morbidity associated with acute SCI, this results to be high, with many survivors requiring prolonged or repeated admissions to hospital for complications after the injury (Sekhon, 2001; Heinemann, 1989).

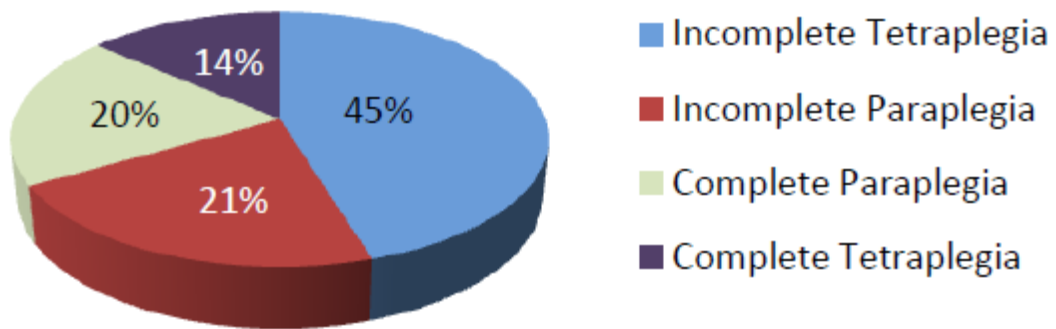


Figure 1.8. Percentage of frequent neurologic conditions of SCI

In Europe the most frequent cause of SCI are road traffic accidents, followed by falls (Werhagen, 2012), with an annual incidence of about 17.5% patients per million, of which 80% are male as in the rest of the world.

1.2.4 Physiopathology of Spinal Cord Injury

The pathophysiological processes underlying SCI, comprise the primary, secondary and chronic phase of injury (Fig. 1.9). In the primary phase, the spinal cord is lacerated by a sharp penetrating force, contused or compressed by a blunt force or infarcted by a vascular insult. The secondary damage is represented by a cascade of biological events that begin from the first minutes after injury and that can lead to neurological damages during the weeks later (Silva, 2014; Li and Lepski, 2011). During the chronic phase, which begins several months from the injury and continues throughout the lifetime of the patient with SCI, there is a remarkable increasing of neurological impairments in both orthograde and retrograde directions (Yiu and He, 2006; Lorber, 2015).

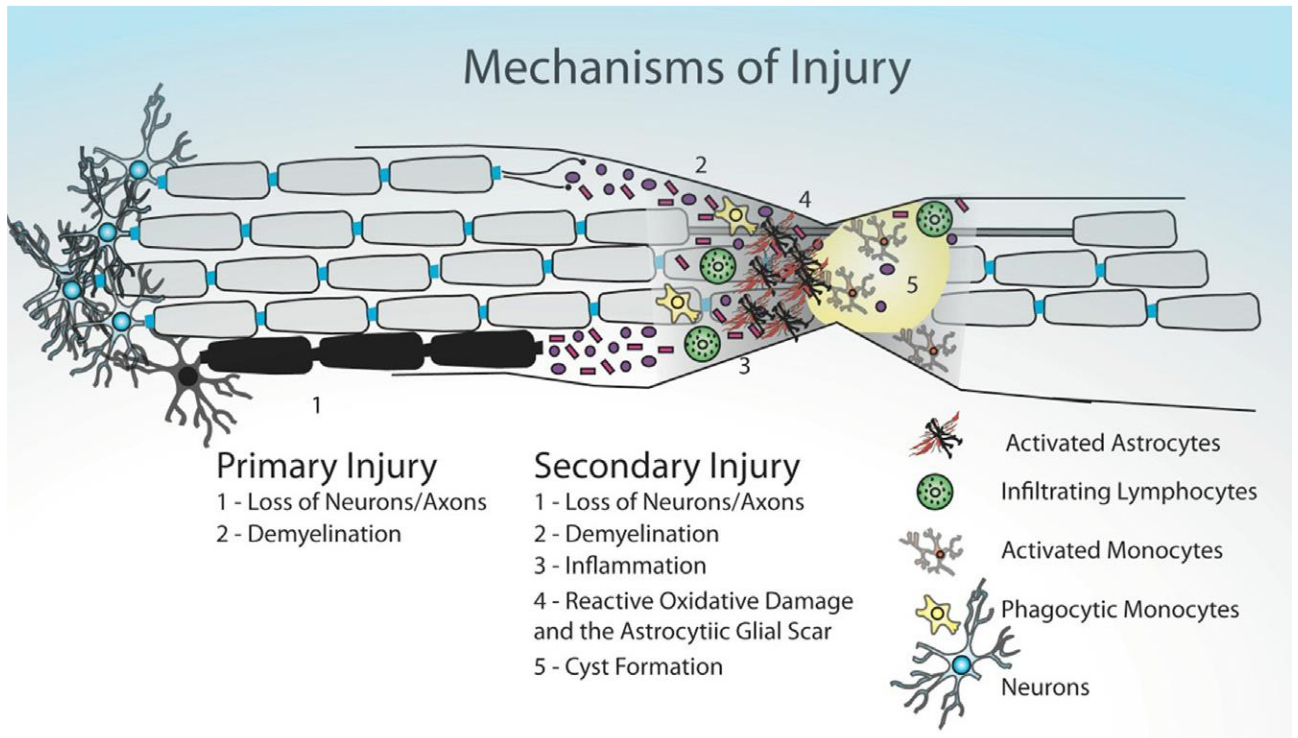


Figure 1.9. Initial spinal cord insult to secondary injury with subsequent glial scar formation. (Anton Y. Jorgensen, 2015)

1.2.4.1 Primary Injury Phase.

This phase refers to the moment of the mechanical trauma to the cord (Li and Lepski, 2013). The typical insult is represented by dislocation, burst fractures, missile injuries and acutely ruptured discs (Sekhon and Fehlings, 2001) and the consequent disruption of axons, blood vessels and cell membranes. Axons are commonly found to traverse the lesion site, often occupying a “subpial rim” of spared yet demyelinated or demyelinated long tract axons (Rowland, 2008). The spinal cord damage in this moment is made by a combination of the initial impact as well as subsequent persisting compression. At the morphological level, spinal cord resident cells are destroyed and a further delayed damage can induce death to cells that survived to the original trauma (Oyinbo, 2011).

1.2.4.2 Secondary Injury Phase.

The secondary phase begins in minutes after injury and lasts for weeks, usually inducing a reduction of autonomic activity (instead of abolishment) and gradually increasing the tone muscle leading to the onset of spasticity movements (Tanhoffer, 2007). The area of trauma distinctly enlarges; there is a prosecution of the events begun during the primary phase, as well as new ones, as free radicals formation, delayed calcium influx, immune system response, inflammation and apoptotic cell death (Oyinbo, 2011). All the events characterizing the secondary phase can be usefully divided in other four phases: immediate, acute, intermediate and chronic stages of SCI.

1.2.4.3 Immediate phase.

The immediate phase begins at the time of injury and is characterized by a traumatic axons severing, an immediate death of neurons and glia, all accompanied by these called 'spinal shock', which is the results of an instantaneous loss of function at the level below the injury. The first detectable pathological change is a generalized swelling of the spinal cord, often accompanied with central gray matter hemorrhage. In this condition, mechanical disruption of cell membranes, or ischemia, resulting from vascular disruption, start to induce necrotic cell death and hemorrhage (largely petechial) in the surrounding white matter. Hemorrhage and swelling, combined, produce cord ischemia that may involve several spinal segments, both in the rostral and caudal direction from the injury (Fig. 1.10) (Rowland, 2008).

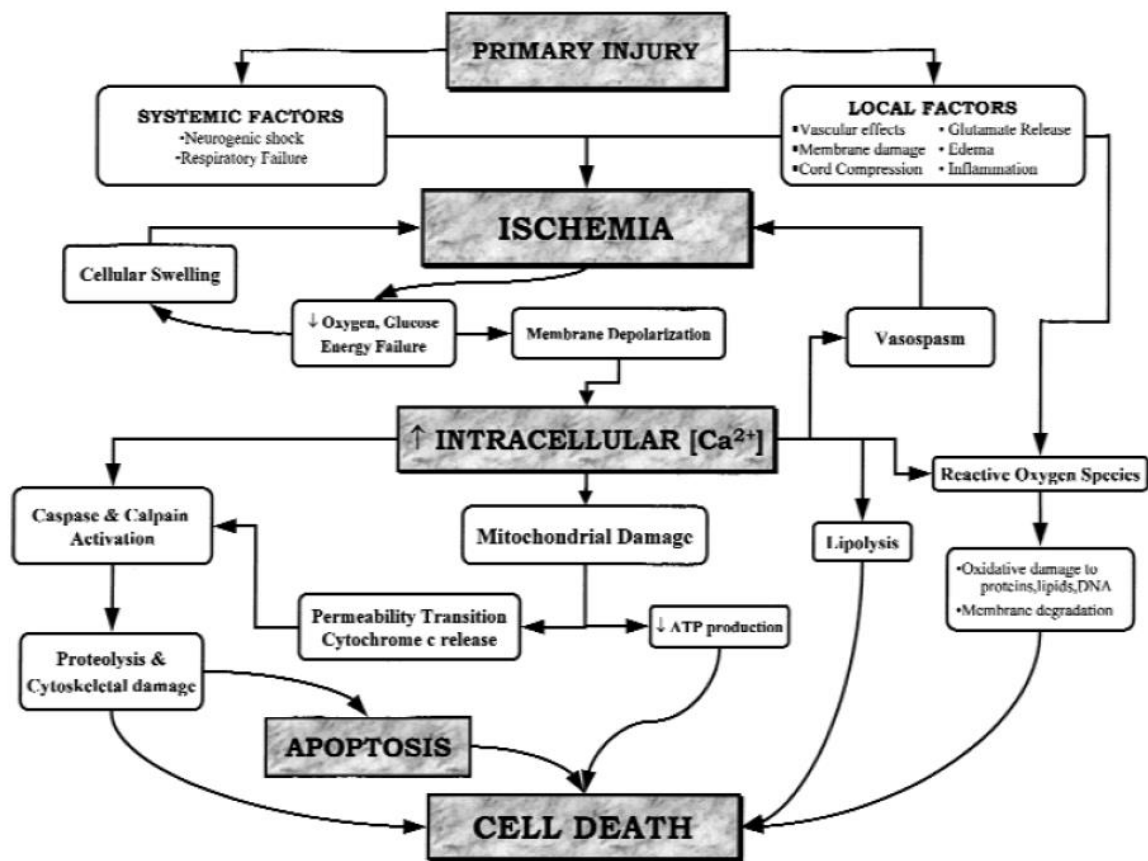


Fig 1.10. Scheme of the main mechanisms responsible for secondary damage after spinal trauma. Acute Spinal Cord Injury, Part I: Pathophysiologic Mechanisms

1.2.4.4 Acute phase.

The acute phase is the period in which the secondary injury processes become dominant. It is divided in two phases: early acute and subacute phase. The early acute phase starts 2 hours post injury and lasts until 48 hours. It is characterized by continuing hemorrhage, increasing edema and inflammation. In these moments there is also the onset of additional processes that contribute to further axonal injury and cell death, as free radical production, ionic dysregulation, glutamate-mediated excitotoxicity and immune-associated neurotoxicity. Vascular disruption, hemorrhage, and resulting ischemia are central constituents of this secondary injury cascade (Rowland, 2008).

Ionic dysregulation. Disruption of cell membranes due to trauma, depolarization of calcium channels due to ischemia, and excitotoxin-mediated activation of calcium channels are

associated with an intracellular shift of calcium ions. Happel and colleagues (Happel, 1981) showed an increase of total tissue calcium in contused spinal cord injury animal by two-fold at 2 hours and five-fold after 5 hours (Tator, 1991). Immediately after SCI, a loss of ionic homeostasis and excitotoxicity occur, and there is evidence that these closely related processes significantly contribute to the propagation of cellular injury after SCI.

Under pathophysiological conditions such as anoxia, ischemia, or trauma, intracellular Na^+ concentration rises and membranes depolarize as a result of energy failure, leading to reverse Na^+ - Ca^{2+} exchange and causing Ca^{2+} accumulation in the intracellular compartment (Li, 2000).

Excitotoxicity. It is a pathological condition caused by an excessive or prolonged exposure to glutamate that often leads to neuronal and glia cell death in many forms of neurotrauma, including SCI (Park et al, 2004). Imbalanced and de-regulated overactivation of glutamate receptors in motor neurons leads to the influx of Na^+ and Ca^{2+} through the N-methyl-D-aspartate (NMDA) and alpha-amino-3-hydroxy-5-methylisoxazolepropionate/kainate receptors (AMPA/kainate), resulting in excitotoxicity (Gerardo-Nava, 2013). When an injury occurs, extracellular level of glutamate increases and energy-dependent transporters fail, especially the Na^+/K^+ ATPase, leading to the swelling of the cell and the loss of K^+ (Lipton and Rosenberg, 1994). The result of all these processes is the overproduction of proteolytic enzymes, induction of lipid peroxidation, ROS (Reactive Oxygen Species) and RNS (Reactive Nitrogen Species) formation, and in triggering apoptosis, which is one of the main mechanisms of cell death in neurologic diseases (Emerit, 2004).

Free radicals mediated injury. Free radicals are highly reactive molecules characterized by an extra electron in the outer orbit and that are produced when oxygen interacts with certain molecules. In central nervous system injury, there is evidence of their pathophysiologic importance and their early occurrence in triggering cell membrane lipid peroxidation (Sekhon and Fehlings, 2001). Several oxidants and derivatives are generated after a damage, including superoxide anions (O_2^-), formed by incomplete electron transport in mitochondria, hydrogen peroxide (H_2O_2) and hydroxyl radicals (OH) (Cornelius, 2013). Hydroxyl radicals (OH) is induced by lowered pH whereas H_2O_2 is produced in the presence of free iron such as the one released from hemoglobin, transferrin or ferritin. In lesioned regions, where pH is lower, conditions are favorable for the potential release of iron from storage proteins (Halliwell, 2009) and hemoglobin itself stimulates oxygen radical reaction (Cornelius, 2013). Activated microglia and infiltrating neutrophils and macrophages provide additional sources of O_2^- at later time points. Enhanced production of reactive oxygen/nitrogen species (ROS/RNS) cause oxidative/nitrosative stress (Juurlink and Paterson, 1998) leading to damage in lipids, proteins,

and nucleic acids (Povlishock and Kosov, 1992). These, if unchecked, can cause geometrically progressive lipid peroxidation, spreading over the cellular surface and causing impairment of phospholipid-dependent enzymes, disruption of ionic gradients and membrane lysis. The level of ROS starts to elevate 12 hours after injury and remains high for ~ 1 week, returning to basal level after 4–5 weeks (Rowland et al, 2008).

Permeability of blood brain barrier (BBB): In uninjured central nervous system (CNS), the BBB is a highly selective permeability barrier that separates the circulating blood from the brain extracellular fluid (BECF). The BBB acts like a filter, limiting the transport of molecules throughout the CNS parenchyma. The blood–brain barrier not only allows the passage of water, some gases and lipid-soluble molecules by passive diffusion, but also avoid the entry of lipophilic molecules and potential neurotoxins protecting the brain from bacterial infections (Rowland, 2008). When a neurological injury occurs, the BBB permeability increases because of the mechanical disruption and the numerous inflammatory mediators released by endothelial cells. Moreover, the breakdown of the BBB results in abnormal leakage of proteins leading to vasogenic edema formation and brain pathology. In addition, two inflammatory cytokines, TNF and IL-1 β , are upregulated after SCI (Pineau, 2007) and their effects known to increase vascular permeability. In rats with SCI induced by a contusion, the peak of vascular permeability disruption of the BBB is 24h after the lesion, restoring physiological values in two weeks (Noble, 1989). In human, the maximum reduction of spinal cord blood flow (SCBF) is seen within 15 min in the traumatized region, in particular in the caudal segment, suggesting that release of vasoactive substances following trauma influences local blood flow impairments (Sharma, 2005). Molecules released by glial and inflammatory cells at the injury, as ROS, nitric oxide (ON), histamine, matrix metalloproteinases and elastase are believed to have a role in vascular permeability of the BBB (Donnelly and Popovich, 2008). The passage of water throughout the BBB consequently lead to the formation of edema, building up around the ependymal canal or at the level of the white matter, leading to nerve compression.

Changes in spinal cord blood flow (SCBF) and the perturbation that follow are an important part of the alterations induced by acute SCI these events can be divided into systemic and local. Hemorrhage may promote ischemia, or thrombosis may occur via platelet aggregation. Finally, excitatory amino acids, particularly, glutamate, may be involved. Ischemia may play a role in the formation of local cord edema and it results in cytotoxic cell swelling that effects both neurons and glia. In the normal situation, gray matter to white matter blood flow is maintained at a 3:1 ratio. White matter perfusion typically decreases within 5 minutes of an acute SCI and begins to return to normal within 15 minutes. In central gray matter typically occur, as early as 5 minutes

after an acute SCI. Traumatized spinal cords show severe hemorrhages predominantly in gray matter, and it may be obstruction of these anterior sulcal arteries that leads to the hemorrhagic necrosis and subsequent central myelomalacia seen at the site of injury. Endothelial damage occurs early, with the formation of craters, adherence of non-cellular debris, over-riding of endothelial cell junctions, and microglobular formations occurring 1 to 2 hours after acute SCI. Acute SCI is one of the causes of neurogenic shock, typically being related to the magnitude and severity of the cord injury (Sekhon and Fehlings, 2001). Oxidative stress, caused by ischemia-reperfusion and inflammatory byproducts, contributes to cell death cascades after traumatic and ischemic CNS injury. Neutrophils, microglia and macrophages produce superoxide anion and nitric oxide, which combine to form the highly reactive and toxic compound peroxynitrite (Xiong, 2007). Free radicals produced during these processes induced apoptosis in neurons and glia via the irreversible oxidation of proteins, lipids and nucleic acids (Donnelly and Popovich, 2008).

Cell death. In chronic neurodegenerative diseases, such as Alzheimer's disease, amyotrophic lateral sclerosis, Parkinson's disease and Huntington's disease and also Spinal Cord Injury, selective neural cell loss by apoptosis is common (Choi, 2003). Numerous studies have provided convincing evidence that apoptosis is present in neurons, oligodendroglia and microglia after SCI (Yip and Malaspina, 2012). Apoptosis usually occurs through intrinsic and extrinsic apoptotic pathways (Rios, 2015). The Bcl-2 family of proteins regulates the intrinsic apoptotic pathway, starting with pathological overload of calcium, opening of the mitochondrial permeability transition pore (mPTP) and activation of caspases-9 and caspase-3 (Precht, 2005). The extrinsic apoptotic pathway is mainly triggered by ligation of death receptors, such as Fas and tumor necrosis factor (TNF) (Choi, 2015 / Rios, 2015). The cytokine tumor necrosis factor- α (TNF- α) is present in the CNS at low levels but it is upregulated more than 100 fold in the ischemic brain (Barone, 1997; Liu, 1994; Tarkowski, 1997; Wang, 2004), suggesting a role in modulating cellular damage. In particular, there are evidence that the activation of apoptosis depends on TNF- α -induced activation of caspase-8 and -3, without affecting caspase-9 (Badiola, 2009).

Inflammation mediators and cellular immune response. The early acute phase after SCI involves infiltration of inflammatory cells, activation of resident microglia and of numerous other cell populations, including astrocytes, microglia, T cells, neutrophils, and invading monocytes. TNF α , interferons and interleukins also play important roles. In particular, neutrophils and macrophages invade the damaged spinal cord with a maximum peak respectively at 12-24 hours and 5-7 days after SCI (Popovich, 1999; Taoka, 1997). It has been reported that anti-inflammatory

treatments selectively interrupted the early, destructive, leukocyte-mediated actions in the injured cord, but leaving an opportunity for later regenerative interventions and wound-healing responses (Marfia, 2014).

The subacute phase starts from 2 days post injury and lasts for 2 weeks. This is the most important period to get better effects of cell therapy. At this stage, phagocytic response is maximal, helping to remove the cellular debris and growth-inhibiting components present on myelin debris in the lesioned area (Donnelly and Popovich, 2008). In subacute period, astrocytes proliferate and activate themselves increasing the expression of glial fibrillary acid protein (GFAP). The reactive astrocytes grow with large cytoplasmic processes that interweave to form the astrocytic scar, which unfortunately represents both a physical and chemical barrier to axonal regeneration (Rowland, 2008). Despite the scar formation, astrocytes also have a positive function in SCI condition, as they re-establish ionic homeostasis and integrity of the BBB, which is very important to limit the reabsorption of edema and the infiltration of immune cells (Herrmann, 2008).

1.2.4.5 Intermediate phase.

The intermediate phase is characterized by the evolution of the astrocytic scar, astrogliosis and regenerative axonal sprouting (Hill, 2001). Astrogliosis repairs the blood-brain barrier and protects neurons and oligodendrocytes, improving regeneration (Young, 2014). In a mouse model of SCI, axonal sprouting has been found in the corticospinal tract from 3 weeks to 3 months post injury, whereas in the reticulospinal tract between 3 weeks and 8 months after lesion (Hill, 2001). These regenerative attempts are insufficient to produce a functional recovery in a severe SCI, but it is important to remember that regenerative potential does exist in the adult spinal cord.

1.2.4.6 Chronic phase.

The chronic phase begins about 6 months after the lesion and it is characterized by the stabilization of the lesion. During this phase, most rats develop expansions of the central canal, either proximal or distal to the contusion site, forming cysts that look very similar to

syringomyelic cysts observed in humans (Young and Keck, 2002). After 15 days post injury, macrophages have completed the removal of the myelin, although it is possible to observe macrophages containing myelin fragments also after three months from the nerve section (Warden, 2001; Bierowski, 2005). In some cases of severely injured spinal cords, Schwann cells can be seen at the injury site, probably migrating from spinal roots. Schwann cells have the ability to re-myelinate the damaged axons at the level of nodes of Ranvier. Although there could be some improvement in neurological function after several years post injury (McDonald, 2002), it can be assumed that after 1-2 years from the trauma, the neurological deficit has stabilized. At this point, the lesion is physically characterized by a cystic cavity and myelomacia (pathological term referring to the softening of the spinal cord). These events represent the final stage of necrotic death after SCI. The lesion may not remain a static condition, and syrinx formation in as many as 30% of patients with SCI can cause delayed neurological dysfunction and neuropathic pain (Stoodley, 2000; Rowland, 2008).

Phases and Key Events	Time After SCI				
	≤2 Hours	≤ 48 Hours	≤14 Days	≤ 6 Months	≥ 6 Months
injury phase	primary immediate	early acute	secondary subacute	intermediate	chronic/late
key processes and events	primary mechanical injury traumatic severing of axons grey matter hemorrhage hemorrhagic necrosis microglial activation released factors: IL-1 β , TNF α , IL-6, & others	vasogenic & cytotoxic edema ROS production: lipid peroxidation glutamate-mediated excitotoxicity continued hemorrhage & necrosis neutrophil invasion peak BBB permeability early demyelination (oligodendrocyte death) neuronal death axonal swelling systemic events (systemic shock, spinal shock, hypotension, hypoxia)	macrophage infiltration initiation of astroglial scar (reactive astrogliosis) BBB repair & resolution of edema	continued formation of glial scar cyst formation lesion stabilization	prolonged Wallerian degeneration persistence of spared, demyelinated axons potential structural & functional plasticity of spared spinal cord tissue
therapeutic aims	neuroprotection	neuroprotection immune modulation cell-based remyelination approaches glial scar degradation		glial scar degradation	rehabilitation neuroprostheses

Table 1.2. Steps of spinal injury and pathological key events. (Rowland, 2008)

1.3 Spinal cord injury therapies

Although the progress made in the field of spinal cord injury has improved the patients' condition and life expectancy, to date there are no solutions that enable the healing of a spinal cord injury. However, in recent years research has reached encouraging results with regard to the modulation of the inflammatory process without being able to induce the regeneration of the lost as a result of the trauma.

1.3.1 Pharmacological therapies

In the last years many different pharmacological treatment methods have been studied based on the pathophysiological mechanisms of spinal cord injury.

1.3.1.1 Methylprednisolone.

To reduce spinal cord edema corticosteroids are the best choice because of their anti-inflammatory action. It has been supposed that the neuroprotective effect of corticosteroids includes the modulation of inflammatory and immune responses, through inflammatory cytokines as TNF- α and NF- κ B (nuclear factor kappa-light-chain-enhancer of activated B cells) (Xu, 1998), inhibition of lipid peroxidation, healing of vascular perfusion and prevention of calcium entering into the cell (Kokoszka, 2001). A synthetic glucocorticoid, Methylprednisolone (MPS), has been used to reduce SCI and brain edema for many years. It has been suggested that the inhibition of peroxidase is the most important mechanism in the SCI treatment and that MPS appear to act with more efficiency than other glucocorticoid. The widespread use of MPS in patients with SCI is due to the results obtained from three clinical trials, the *National Acute Spinal Cord Injury Studies* (NASCIS) I, II and III. In NASCIS I it has been evaluated the effects of ten days doses of 100 or 1000 mg of MPS administered 48 h after lesion (Bracken, 1984; Yilmaz, 2015): these two groups did not differ in motor and sensory recovery. In animal trials, the maintenance dosage of 30-40 mg/Kg injected intravenously has resulted to be appropriate to obtain effective neuroprotection (Young, 1988). In NASCIS II trials the dosage administered was 30 mg/kg MPS followed by a maintenance dose of 5.4 mg/Kg for 23 h. Patients with SCI were randomized into three groups, methylprednisolone, naloxone (an opioid receptor antagonist, caused functional and electrophysiological improvement and reverse the spinal shock (Winkler, 1994)) or placebo. The MPS injected 8 hours after the lesion has induced sensory and motor improvement in

patients with full and partial SCI. This is the first trial demonstrating the efficacy of pharmacological therapy in spinal cord injury. In NASCIS III, methylprednisolone effect has been compared with tirilazadmesylate (member of the family of 21-aminosteroid, lazaroide, that acts on lipidic peroxidase) considering different administration times. In both treatments, the authors reported sensory and motor improvement within 3 h from the trauma (Bracken, 1990). The results suggest the usage of the drug between 3 and 8 hours, with an increased beneficial effect seen if the infusion is prolonged until 48 hours. However, they found very poor effectiveness in neurological healing when the application of 48 hours accompanied by increased wound infection rates, pulmonary embolism and sepsis, leading to secondary deaths (Yilmaz, 2015). The anti-inflammatory effects of high dose of MPS decrease the neuronal regeneration and axonal growth. This is a possible explanation for the ineffectiveness of the MPS given more than 8 hours after injury (NASCIS II) (Baptiste and Fehling, 2006).

1.3.1.2 Ganglioside GM-1.

Other possible pharmacological therapy for SCI is the use of Ganglioside, a glycosphingolipid of the lipid membranes of the nervous cells that contains sialic acid. Systemic administration of ganglioside GM-1 can induce neuroprotective effect, such as neurite outgrowth, and prevent apoptosis and inhibition of excitotoxicity in SCI. A double blind trial has been done to investigate the efficacy of GM-1 in patients with cervical and thoracic SCI (Geisler, 1991): administration of 100mg of GM-1 in 18-32 doses, starting with the first injection 72 h post trauma. The results of this study showed an increase in post-traumatic recovery only in the lower limb, suggesting that GM-1 promotes the regenerated axonal "crossing" of the lesion site, having no effect in the gray matter of the trauma epicenter (Gorio, 1986). The neuroprotective effect of this drug is maintained after 48 h post injury. These positive results led to realize other randomized trial started in 2001. In this trial patients with SCI were first treated with the same protocol used for NASCIS II, and later were divided into three groups: placebo, GM-1 lower dose (300 mg to start and 100 mg/day for 56 days) and GM-1 high dose (600 mg to start and 200 mg/day for 56 days). The recovery, evaluated with ASIA scale reported an improvement in motor recovery. After three months, patients treated with GM-1 showed complete recovery of motor/sensory and bladder function (Geisler, 2001).

1.3.1.3 Opioid receptor antagonist.

After SCI, there is an increase of the circulating Dynorphin A, an endogenous opioid. Dynorphin A is neurotransmitters, modulator of pain response. In high dose, this peptide is neurotoxic and the activation of subtype K of the opioid receptor is correlated to the decrease of the blood flow in the spinal cord (Long, 1986). Naloxone is a non-specific opioid receptor antagonist, with the important role of improving the blood flow in the spinal cord and reducing edema and allodynia in animal models. However in human (NASCIS II) (Bracken, 1990) this opioid antagonist has not shown any significant neuroprotective effect over placebo, but other studies have indicated that the administration of Naloxone within 8 h post SCI is correlated with a motor recovery in lower limb (Bracken and Holford, 1993).

1.3.1.4 Thyrotropin releasing hormone (TRH).

Thyrotropin is a tripeptide that stimulate hypophysis and is able to antagonize the effect of endogenous opioids, and of all the targets correlated in the SCI secondary damage, such as platelet-activating factor (PAF) and excitatory amino acids. In rats the subcutaneous administration of TRH once a day for 7 days, started 24h or 7 days post trauma, increases neurological functions (Hashimoto, 1991). Clinical trials using TRH with a started dose of 0.2 mg/Kg and a maintenance one of 0.2 mg/Kg/h for 6 h, demonstrate that after 4 months this drug improves the motor recovery in patients with partial SCI, but not in patients with full trauma (Pitts, 1995).

1.3.1.5 Antagonists for glutamate receptor (GluR antagonists).

This pharmacological class can easily pass through the ematospinal barrier (ESB) and are immediately available to decrease the secondary excitotoxic damage. Nevertheless, the GluR antagonists are not used in clinical treatment of CNS pathology like SCI, because of the collateral effects induced by the high dosage required for their effectiveness. In a recent study, the injection at the lesion site of an AMPA/Kainate antagonist (NBQX) within 4 h from the lesion in a rat model of SCI has shown decreased the neurotoxicity without collateral effects. (Gaviria, 2000).

1.3.1.6 Calcium channel inhibitors.

Calcium is an important element in SCI secondary damage because it is responsible for the intracellular excitotoxicity and ischemic vasospasm. In a SCI animal model study, Nimodipina (a drug that blocks the calcium channel dihydropyridine-sensitive (L channels)) therapy was used in combination with dextran, in order to investigate the effect on spinal cord injured blood flow and axonal functionality (Fehlings, 1989). The study demonstrates that Nimodipina administered with dextran improve the axonal function in the sensory and somatosensory tract of the spinal cord. Despite this, in a clinical trial the treatment with Nimodipina has not shown any significant benefit in patients with SCI (Petitjean, 1998).

1.3.1.7 Inhibition of sodium channel.

After spinal cord injury, sodium cell concentration increases (Stys, 2004). These pharmacological inhibitors (QUALI?) reduce the sodium accumulation, preserve the white matter in lesioned spinal cord and reduce the myelin damage (Rosenberg, 1999). The administration of the tetrodotoxine (TTX), inhibitors of sodium channel, into the lesion site of the mouse, decrease the axonal degeneration but there is no positive effect on the survival of glial cells that are rich in sodium channels (Rosenberg, 1999). Other inhibitors of sodium channel, Riluzole, has a neuroprotective properties and promote the neurological recovery in rat SCI. Riluzole reduces degeneration into white and gray matter in the rostral part of the lesion (Schwartz, 2001). However it inhibits the presynaptic glutamate release calcium channels induced (Wang, 2004).

1.3.1.8 Caspases inhibitors.

Caspases activation have a central role in apoptotic cells death after SCI and many molecules interfere with this process. These inhibitors are tri-tetra peptides that mimic the catalytic site of caspases substrates, like z-VAD-fmk or z-YVAD-fmk. These peptides block or inhibits the programming cell death and reduce the functional cells loss.

1.3.1.9 Monoclonal antibody (MoAb).

A most important target for pharmacological therapies for SCI is the inflammatory response. The clinical trials that use MoAb in SCI have shown promising results. MoAbs were used to inhibit the interaction between immune cells and endothelium, or to inhibit the integrin-leukotriene complexes. Taoka et al. use this antibody on P-selectin in an animal model, reducing neutrophil infiltration and improving the functional recovery of hind limb (Taoka, 1997). Gris et al. have demonstrated that selective MoAb on CD11d subunit of the CD11d/CD18 integrin's complex reduces lipid peroxidation, improving neurological function and allodynia (Gris, 2004).

1.3.1.10 Cyclosporine A (CsA).

In addition to drugs that limit leukocyte infiltration to the injury site, agents that suppress the immune response are beneficial in the SCI treatment. Treatment with a low dose of CsA (2,5 mg/Kg) administered within the first 6 h after injury, showed decreased lipid peroxidation in rats (Diaz-Ruiz, 1999). Moreover, it was demonstrated that the CsA has the ability to inhibit the autoimmune cellular reaction, within the injured spinal cord, while promoting a decrease in demyelination and of neuronal death (Ibarra, 2003). Moreover, recently it has been found that subsequent intraperitoneal injections of CsA (2, 6 and 12 h post injury) inhibit the inducible nitric oxide synthase activity, presumably by inhibiting calcineurin CA^{2+} -dependent (Diaz-Ruiz, 2004).

1.3.1.11 Minocycline.

Minocycline is a semisynthetic and highly lipophilic derivative of the tetracycline able to pass the blood-brain barrier, where it exerts its anti-inflammatory properties. This antibiotic inhibits excitotoxicity, oxidative stress, neural death pathways, both caspase-dependent and caspase-independent, and the pro-inflammatory mediator release by activated microglia (Wells, 2003; Stirling, 2004). It has been reported that systemic administration of minocycline showed a significant neuroprotective activity, by decreasing apoptosis of oligodendrocytes and microglial activation, reducing the size of the lesion and improving the neurological deficits. The neuroprotective mechanism proposed for the minocycline can be attributed to its ability to increase the mRNA levels of the anti-inflammatory cytokine IL-10, with a consequent decrease in the levels of TNF-alpha (Stirling, 2004). After acute SCI, minocycline reduces the size of the lesion.

1.3.1.12 Erythropoietin.

Erythropoietin (EPO) is an endogenous cytokine mediator of 34 kDa produced by the kidney with the main function to stimulate erythropoiesis. In addition to this effect, when binds its receptor EpoR, EPO activates a protective response against hypoxia, increasing circulating erythropoietin and maintaining an adequate tissue oxygenation. In addition to its tissue protective effect in the CNS (103), EPO also inhibits apoptosis, decreases inflammation and has an effect in the migration and proliferation of neural stem cells (Sakanka, 1998; Shingo, 2001). Its neuroprotective effects on spinal trauma can be attributed to a variety of mechanisms, including the ability to reduce lipid peroxidation, inflammation and apoptosis (Erbayraktar, 2003). After ischemic or mechanical trauma, the human recombinant erythropoietin (rhEPO), administered systemically, passes the blood brain barrier and prevents cell damage and inflammation (Brines, 2000). In two studies realized using two different animal models, one of crushing trauma and the other of a contusion trauma, administration of rhEPO in the acute phase mitigates the effects on spinal cord injury and significantly increases the functional recovery. Although the experimental evidence support the neuroprotective role of EPO, recent animal studies have focused on the treatment of chronic spinal injury with this protein (Wiessner, 2001). There are studies currently in progress about the synthesis of derivative of EPO without erythropoietic effect (Erbayraktar, 2003; Leist, 2004). Erbayraktar and colleagues have managed to create a molecule that has been shown to be neuroprotective in animal models of stroke, peripheral neuropathy and SCI without effects in red cell mass (Erbayraktar, 2003). Another derivative of EPO was created by carbamylation of EPO lysine residues (Leist, 2004). The resulting molecule, CEPO, lost all hematopoietic potentials but maintains all its neuroprotective properties when use in an appropriate treatment of SCI.

1.3.1.13 Estrogen.

The female hormones may act in the neuroprotection hormone-dependent, increasing the expression of bcl2 and through the activation of protein kinase pathways. They induce a

reduction of secondary tissue damage, macrophage/microglia accumulation and apoptosis but no behavioral recovery (Yilmaz, 2015).

1.3.1.14 Progesterone.

The progesterone reduces the production of inflammatory cytokines, can reduce the production of oxidants and free radicals and provides stability of neurotrophin in SCI (Fu, 2005). This protein alters the traditional neurotransmitters like inhibitory GABA (Thomas, 1999). Was reported that progesterone alters neurotransmitters, gene expression and cell morphology in the spinal cord injury.

1.3.1.15 Cyclooxygenase inhibitors.

Indomethacin and ibuprofen are inflammatory prostaglandins that reduce tissue damage and edema in SCI. Contusion SCI increases the concentration of Cox2 in rats. Inhibiting Cox2 with Cyclooxygenase-2 inhibitor (SC-236) provided neuroprotection and an improvement in behavior deficits in rabbit (Dumont, 2001).

1.3.1.16 Antioxidant.

In the animals with spinal cord injury there is an increasing of free radicals. To reduce the concentration of free radical. The antioxidant such as Melatonin (Kaptanoglu, 2000), vitamin E and selenium (Anderson, 1992), lipopolysaccharide (Davis, 2005) have been shown beneficial for SCI and reduce the concentration of free radicals.

Table 1.3 .Pharmacotherapy of acute spinal cord injury and mechanisms of action

<p>Methylprednisolone</p> <p>Inhibition of lipid peroxidation/antioxidative/anti-inflammatory. Properties decrease ischemia, support energy metabolism, inhibit neurofilament degradation, decrease intracellular Ca, decrease PGF/TxA, increase spinal neuron excitability, decrease cord edema</p>
<p>Ganglioside GM-1</p> <p>Stimulate neurite regrowth/regeneration</p>
<p>Opioid receptor antagonists</p> <p>Antagonize the increase in endogenous opioid levels after SCI (opioid receptor activation can contribute to excitotoxicity)</p>
<p>TRH and its analogs</p> <p>Antagonize endogenous opioids, platelet-activating factor, peptide leukotrienes and excitatory amino acids</p>
<p>Nimodipine</p> <p>Decrease intracellular Ca²⁺ accumulation, attenuate vasospasm</p>
<p>Gacyclidine (GK11)</p> <p>Antagonism of glutamate receptors</p>
<p>Magnesium</p> <p>Replace Mg²⁺ depletion that is common after SCI, diminish intracellular Ca²⁺ accumulation, block N-methyl-D-aspartate receptor ion channel, modulate binding of endogenous opioids</p>
<p>Hypothermia</p> <p>Reduce extracellular glutamate, vasogenic edema, apoptosis, neutrophil and macrophage invasion and activation, and oxidative stress</p>
<p>Minocycline</p> <p>Inhibition of microglial activation, inhibition of cytochrome c release</p>
<p>Erythropoietin</p> <p>Reduced apoptosis and lipid peroxidation</p>

<p>Estrogen</p> <p>Not clearly known</p>
<p>Progesterone</p> <p>Reduce the production of inflammatory cytokines</p>
<p>Cyclooxygenase inhibitors</p> <p>Prevents/antagonizes decreased blood flow/platelet aggregation from production of arachidonic acid metabolites</p>
<p>Riluzole</p> <p>Blockade of voltage-sensitive sodium channels and antagonism of presynaptic calcium-dependent glutamate release</p>
<p>Atorvastatin</p> <p>Prevents neuronal and oligodendrocytic apoptosis</p>
<p>Antioxidants</p> <p>Antagonize deleterious effects of free radicals (lipid peroxidation, reperfusion injury, etc.)</p>

1.3.2 Cell therapy

A recent therapeutic approaches used in the spinal cord injury treatment is the cell transplantation, in particular the use of stem cells. Cell transplantation after SCI has several goals: preserve neural tissue in the lesioned spinal cord, create a favorable environment for axon growth and replace damaged tissue through the differentiation of the transplanted cells. In the last two decades the cell transplantation became more relevant as a treatment for SCI and has been the subject of many pre-clinical studies. Numerous cellular types were used in the spinal cord injury studies for their different characteristics and properties; such as the ability to produce myelin and promote axonal growth. Many cell types are able to secrete trophic factors that may have a neuroprotective effect and can promote plasticity in the spinal cord survived tissue post lesion. The cell types more studied for the treatment of spinal cord injury are: i) Schwann cells; ii) olfactory cells; iii) embryonic stem cells; iv) mesenchymal stem cells; v) neural stem / progenitor cells (adult and embryonic).

1.3.2.1 Schwann cells

Schwann cells form myelinated sheet in the peripheral nervous system (PNS), but were they also can support CNS axon regeneration (Pego, 2012). It has been shown that they are not only able to re-myelinate axons after being transplanted in spinal cord injury, but also create a permissive substrate for the growth of the regenerating axons. They have been previously studied and have shown a proven therapeutic effect in the treatment of SCI (Duncan and Milward, 1995), after being isolated directly from the patient and then injected as autologous transplants. Although, several weeks are needed to expand SCs to obtain a sufficient number of cells for transplantation, thus limiting their use in acute treatments (McCreedy, 2012). After a contusion injury, transplanted Schwann cells can reduced the cavitation, and promote the spinal axons regrowth (Pego, 2012), by mechanisms involving the secretion of various trophic factors, such as NGF, fibroblast growth factor-2 (FGF-2), BDNF or NT-3 (Takami, 2002). In contrary, these cells cause and sharpastrocyte reaction and also require a co-adjuvant treatment to increase the effectiveness, which is a disadvantage of this approach (eg. matrigel; cAMP, neurotrophic factors) (Tetzlaff, 2011).

1.3.2.2 Human Olfactory Ensheathing Stem Cells (hOESCs)

Olfactory mucosa/epithelium is a specialized tissue inside the nasal cavity that is involved in olfactory perception. This tissue is characterized by lifelong regeneration of adulthood and multipotent stem cells, condition that offers the possibility to promote regeneration and reconstruct in regenerative medicine. These cells are easily accessible with minimal invasive techniques (Rawson, 2002; Raisman, 2001). Two types of cells are useful in repairing the nervous system: stem-like progenitors cells and Olfactory Ensheathing cells (OECs) (Bianco, 2004).OECs are a specific glia cells class that are restricted to the PNS and alsoCNS, and share certain characteristics with astrocytes as well as Schwann cells (Ramon-Cueto, 1998). In a previous study, Murrell *et al.* showed that human olfactory *lamina propria* derived stem cells can be (1) grown in large numbers and (2) differentiated into neural and non-neural cell types in vitro and in vivo. For the peculiar properties and the plasticity the hOESCs are used spinal cord human clinical trials. The first pilot clinical study with transplantation of autologous hOESCs (Lima, 2006)has been done in 2006. This pattern of recovery suggested functional regeneration of both efferent and afferent long-distance nerve fibers, also confirmed by imaging and neurophysiological examinations. Based on their apparent ability to integrate into the glial scar

and enhance the growth permissiveness of the injured spinal cord we can say that the Olfactory ensheathing cells are also a promising candidate for combinatorial cell-based strategies. Notably, hOESCs can be used not only to treat SCI, but also other CNS diseases like Parkinson's disease (Wang, 2012; Murrell, 2008) and hippocampal lesions (Nivet, 2011). Although, OECs represent one of the most promising alternative for transplant-mediated repair of CNS, mechanism, of their beneficial effects remain to be clarified. However, the use of these cells in more severe traumatic models does not seem to be so effective (Tetzlaff, 2011).

1.3.2.3 Embryonic stem cells (ESCs)

ESCs are the target of regeneration research for their unique pluripotency, which cannot be seen in any other types of stem cells. They are isolated directly from blastocyst in the early stage of embryonic development by mechanical or laser dissection. Unlike adult stem cells, ESCs are able to self-renew for an unlimited number of times and can give rise to all three germ layers tissues and potentially differentiate into every kind of cells (Conley, 2004). ESCs were firstly extracted from murine blastocyst (Martin, 1981) and it took a decade or two to isolate human (Thomson, 1998) or rat ESCs (Buehr, 2008). Most often ESCs are used for SCI treatment in a state of *in vitro* pre-differentiation into defined cell lines that could promote axonal elongation, myelin formation and remyelination. Thus, neural or glial precursors and mature neurons differentiated from ESCs have been grafted into the spinal cord of different SCI models. Several cocktails of growth factors based on retinoic acid (RA) and Sonic hedgehog (Shh) have been used to promote differentiation of ESCs to motoneurons (Feravelli, 2014), which after their transplantation to the injured spinal cord of mice showed to induce functional recovery (McDonald, 1999). *In vitro* pre-differentiation of oligodendrocytes has also been performed in mice and rats. Grafted cells contributed to the remyelination of SC axons and participated in movement improvement after the lesion (Liu, 2000). So far the greatest achievement was recorded by transplantation of oligodendrocyte progenitors derived from hESCs (Keirstead et al., 2005; Cloutier et al., 2006), which advanced into the clinical trials (Chapman, 2012). The safety study involving patients in the subacute phase of SCI, did not report any safety issues, neither any significant improvement of medical conditions after transplantation of oligodendrocyte progenitors (Lucovic, 2012). Clinical trials provided by Geron Corporation were shut down in 2011 for the economical reasons. Despite the promising results obtained in mice and rats, currently the clinical use of hESCs for SCI treatment seems to have come to a standstill. However, the unquestionable potential of these cells is being further studied and applied for other therapies in regenerative medicine.

1.3.2.4 Mesenchymal Stem Cells

Mesenchymal stem cells (MSCs) are multipotent stromal cells that can differentiate into a variety of cell types (Nardi, 2006) such as osteoblasts, chondrocytes, myocytes and adipocytes. The MSCs are known to present low immunogenicity, have an anti-inflammatory/immunosuppressant effect, do not form tumors, and have a pathotropic action. This differentiate capability has been documented in specific cells and tissues of living animals and their counterparts growing in tissue culture. They are two kinds of MSCs used in Spinal Cord Injury transplant: Bone-marrow-derived stromal cells (BMSCs) and Human Adipose Derived Stem Cells (hADSCs).

1.3.2.5 Bone Marrow Derived Stromal Cells (MSCs)

The BMSCs are essentially a set of stromal cells that support the growth of hematopoietic stem cells and mesenchymal stem cells. These cells are used very frequently in the treatment of SCI and other diseases of ischemic character (Parr, 2007). These cells are easily accessible with minimal invasive techniques and can be used in autologous transplants (both in animal models and in humans), have shown to have an effect on motor recovery in rodents and were used in models of chronic SCI. The BMSCs also appear to have the ability to create a substrate that allows the invasion of endogenous Schwann cells. However, the integration of these cells is extremely limited and show the little tendency to differentiate into neural cells (Tetzlaff, 2011).

1.3.2.6 Adipose Derived Stem Cells (hADSCs)

Recent studies have shown that subcutaneous adipose tissue provides a clear advantage over the other MSCs sources due to the simple possibility to extract the adipose tissue and to isolate the stem cells (Zuk, 2001). Stem cells frequency is significantly higher in adipose tissue than in bone marrow (Musina, 2005). It has been shown that ADSCs are able to differentiate into the classical mesodermal tissues like bone, fat and cartilage (Zuk, 2001; Zuk, 2002), and it is claimed that they can be differentiated into nerve, cardiomyocytes, hepatocytes and pancreatic cells (Safford,

2005). They favor neuronal repair, osteogenesis and vasculogenesis however, the potential of in vivo application of these cells is still unclear. Recent biological studies performed on stem cells suggest the possibility to significantly improve the potentiality of tissue regeneration by using ADSCs. They represent a promising source for the cell therapy, due to the less invasive way of isolation compared to the extractions of bone marrow, possibility to obtain a bigger quantities of tissue from lipoaspirate and their easy expansion in vitro-. The effects and safety of the intrathecal transplantation of autologous ADSCs in patients with SCI were evaluated in the first clinical trial (Hur, 2015). Over the 8 months of follow-up, intrathecal transplantation of autologous ADSCs for SCI was free of serious adverse events, and several patients showed mild improvements in neurological function. Patient selection, dosage, and delivery method of ADMSCs should be investigated further.

1.3.2.7 Neural stem cells (NSCs)

Neural stem cells are defined as multipotent and self-renewing stem cells found in both embryonic and adult tissue. (Pego, 2012). They are usually obtained from the subventricular zone (SVZ) of the brain or the spinal cord, and are amplified in crops such as neurosphere which are formed not only by NSCs but also by neural cells at different stage of maturation (Gritti, 1996). When transplanted after SCI, these cells seem to be able to integrate well into the host spinal cord and the numerous studies evaluating the neurological functional recovery showed an improved behavior. The functional improvement was observed in different experimental models, using different animal species. The limitations in the use of (NSCs / NPCs) are mainly due to their tendency to differentiate preferentially into astrocytes and only minimally in oligodendrocytes and in neurons (Horky, 2006). Moreover, they do not seem to be particularly effective in generating a substrate suitable for axonal regeneration in order to create a neural tissue bridge over the lesion (Tetzlaff, 2011). Recent data using human fetal NSCs shown that, these cells can survive inside the lesion, differentiate into motoneurons and improve motor as well as sensory function after transplantation into a SCI (Romanyuk, 2011). An additional study has shown that NSCs derived from human fetal spinal cord and grafted into a rat model of ischemic spastic paraplegia resulted in the progressive recovery of motor function with a concurrent improvement in motor evoked potentials (Cizkova, 2007). The functional recovery was associated with the long-term survival of the grafted neurons, neuronal differentiation and

the development of a GABAergic phenotype in a sub-population of grafted cells that most probably contributed to the suppression of spasticity. Therefore, in an attempt to reduce these pain behaviours following injury, the transplantation of pre-differentiated ESC cells, serotonergic or GABAergic neural precursor cells has been successfully used in various pre-clinical animal studies (Mukhida, 2007).

1.3.2.8 Post Mortem Neural Precursor Cells (PM-NPCs)

Post Mortem -Neural Precursor Cells (PM-NPCs) present at several hours after mouse death (Marfia, 2011) are cells that have different properties from classic neural stem cell (NSCs), subjected to prolonged global ischemia. It would be of great utility to use for the SCI treatment of a type of neural stem cells that in addition to having the benefits and potential described in the previous paragraph, was also able to survive in the ischemic environment to the spinal cord injury (Molcanyi, 2007; Popovich, 2003). Indeed the microenvironment formed in a spinal cord injury is characterized by an important ischemic area, the cells used for the SCI therapy once arrived in the lesion must survive in a very bad environment, and with a very poor perfusion, at least in the early stages immediate harm. In our laboratory we have been isolated Neural stem cell from the SVZ of adult mice.

PM-NPCs growth under hypoxic microenvironment, in this condition HIF-1 α and β dimerize and migrate to the nucleus; this enhances the expression of several key target genes which acts as regulators of cellular proliferation and differentiation, such as erythropoietin (EPO), vascular endothelial growth factor (VEGF), tyrosine hydroxylase (TH) and OCT4, (Adelman and Simon, 2002). These cells differentiate about 33% β tubulin III- and 36% of MAP2-positive compared to 10–12% of NPCs. After differentiation PM-NPCs show HIF-1 α activation, active voltage-dependent Ca⁺⁺ channels and express both EPO and EPO-R (Marfia, 2011). These cells may represent a more successful approach to the treatment of traumatic CNS injuries and neurodegenerative disease such as Parkinson disease.

1.4 Parkinson Disease

As previously reported cell therapies have long been considered a feasible regenerative approach to compensate the loss of specific cell populations in neurodegenerative disorders, where symptoms can be ascribed to the degeneration of a specific cell type, such as the loss of Substantia Nigra (SN) dopaminergic neurons in Parkinson's disease (PD) (Barker, 2013 and 2014). Parkinson's disease (PD), the second most common neurodegenerative disorder after Alzheimer's disease, was originally described in 1817 by James Parkinson in the classic "Essay on the Shaking Palsy". All the cardinal signs of PD relate to motor dysfunction and include resting tremor, bradykinesia, rigidity and postural reflex impairment. Other manifestations include psychiatric symptoms such as anxiety and depression and dysautonomic symptoms such as hypotension and constipation, paresthesias, cramps, olfactory dysfunction, and seborrheic dermatitis. As the disease progresses, decreased cognitive ability may appear (Marsden et al., Oxford textbook of medicine. Vol 3). The main pathological finding associated with the motor deficits of PD is degeneration of the dopaminergic neurons of the pars compacta of the substantia nigra leading to loss of dopamine in the striatum. Symptoms do not develop until about 50-60% of the nigral neurons are lost and about 80-85% of the dopamine content of the striatum is depleted (Marsden et al., Oxford textbook of medicine. Vol 3).

Dopamine neurons have been successfully derived from human embryonic stem cells, and their transplantation in rat PD models showed positive behavioral outcome (Bjorklund, 2002, Kim, 2002; Kriks, 2011; Yang, 2008; Martínez-Cerdeño, 2010). Previously, also allografts of ventral mesencephalon tissue had been used as implants that survived for a long time, and received and made synapses within the host brain. Their use promote recovery from behavioral deficits in 6-OHDA exposed rats (Lindvall, 1990; Schultzberg, 1984; Haque, 1997; Takahashi, 2007). Following those experiences, clinical observations were made in human patients with the transplantation of cells obtained from human fetal mesencephalon (Barker, 2013). It resulted that transplanted dopaminergic neurons could re-innervate the striatum, restore dopamine release and, at least in some cases, support clinical amelioration of the patient condition. Unfortunately, these positive effects were associated often to disabling side effects such as dyskinesias of orofacial muscles, and upper and lower extremities (Barker, 2013, Hallett, 2014; Kefalopoulou, 2014; Hallett, 2015; Tsui, 2011). Such use of human embryonic or fetal central nervous system tissue gave rise to numerous ethical concerns (Barker, 2014, Barker, 2013). The association of

actual issues and severe side effects enhanced the efforts to adopt other sources, and dopaminergic neurons obtained from induced pluripotent stem cells through somatic cell reprogramming, gave positive results in rodents or non-human primate models of PD (; Werning, 2008; Sundberg, 2013; Doi, 2014; Yu, 2007). Recently, we reported the existence of a subclass of SVZ-derived neural progenitors surviving after donor death (Marfia, 2011). Such post mortem neural precursors (PM-NPCs) show a higher neural-like differentiation, and the process is likely dependent on autocrine erythropoietin (EPO) release, since it is prevented by the exposure to anti-EPO and -EPOR antibodies (Marfia, 2011). When PM-NPCs were administered after traumatic spinal cord injury in the mouse, secondary degeneration and neuroinflammation were greatly attenuated, and the recovery of hind limb function was markedly improved (Carelli, 2014 and 2015). In order to determine the therapeutic potential of PM-NPCs in a pre-clinical experimental model of PD, here we transplanted PM-NPCs, unilaterally into the striatum of symptomatic, and dopamine-depleted 1-methyl-4-phenyl-1,2,3,6-tetrahydropyridine (MPTP)-exposed C57/bl mice. We found that PM-NPCs treated animals had had a rapid behavioral improvement within the third day after cells transplantation. The behavioral recovery was likely mediated by PM-NPCs-derived EPO, as the co-injection of anti-EPO or anti-EPO-R antibodies totally abolished the favorable outcome. The majority of transplanted PM-NPCs were vital and capable of migrating ventrally and caudally throughout the striatum from the injection site, and could reach the ipsilateral SN pars compacta (SNpc). This study confirm the therapeutic potential of PM-NPCs in neurodegenerative conditions.

1.4.1 Synthesis and Metabolism of Dopamine

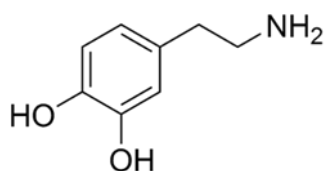


Figure 1.11. Structure of Dopamine, the principal neurotransmitter involved in Parkinson's disease.

The amino acids phenylalanine and tyrosine are the precursors of dopamine (DA) (Fig 1.11). For the most part, mammals convert dietary phenylalanine to tyrosine by phenylalanine hydroxylase (predominantly located in the liver). Tyrosine crosses readily into the brain through uptake;

however, unlike tryptophan, normal brain levels of tyrosine are typically saturating. Conversion of tyrosine to L-DOPA (3,4-dihydroxyphenylalanine) by the enzyme tyrosine hydroxylase is the rate-limiting step in the synthesis of DA. Tyrosine hydroxylase is a mixed-function enzyme that requires iron and a biopterin co-factor; enzyme activity is regulated by phosphorylation and by end-product inhibition. Four alternatively spliced isoforms of tyrosine hydroxylase have been identified in humans, which is in contrast to many non-human primates (two isoforms) and rat (one isoform). At present, it is unclear if these various isoforms play different roles. Once generated, L-DOPA is rapidly converted to DA by L-aminoacid aromatic decarboxylase (AADC), the same enzyme that generates serotonin (5-HT) from L-5-hydroxytryptophan. In the central nervous system (CNS) and periphery, AADC activity is very high, and basal levels of L-DOPA cannot be readily measured.

Metabolism of DA occurs primarily by the cellular L-monoamino oxidase (MAO) enzymes localized on both pre- and post-synaptic elements. MAO acts on DA to generate an inactive aldehyde derivative by oxidative deamination (Fig 1.12), which is subsequently metabolized by aldehyde dehydrogenase to form 3,4-dihydroxyphenylacetic acid (DOPAC).

DOPAC can be further metabolized by catechol-O-methyltransferase (COMT) to form homovanillic acid (HVA). Both DOPAC and HVA, as well as DA, are excreted in the urine. Levels of DOPAC and HVA are reliable indicators of DA turnover; ratios of these metabolites to DA in cerebral spinal fluid serve as accurate representations of brain dopaminergic activity. In addition to metabolizing DOPAC, COMT also utilizes DA as a substrate to generate 3-methoxytyramine, which is subsequently converted to HVA by MAO (Fig 1.12) (Goodman & Gilman's Ed. 12).

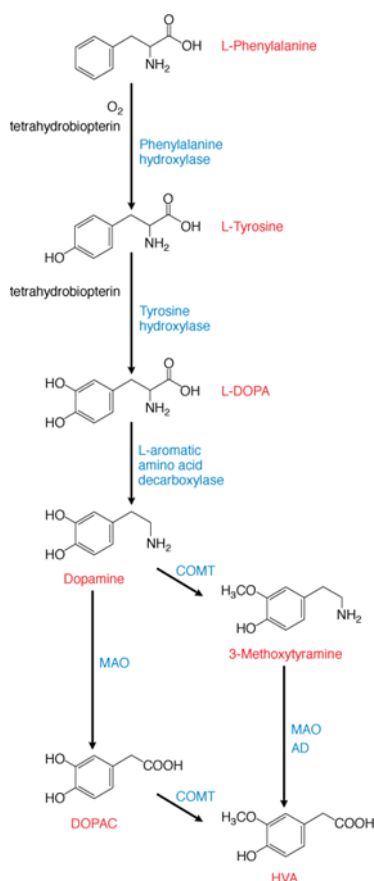


Figure 1.12. Schematic of Dopamine Synthesis and Metabolism (Source Goodman & Gilman's).

1.4.2 Dopamine neurotransmission

The neurochemical events that underlie DA neurotransmission are summarized in Figure 1.13. In dopaminergic neurons, synthesized DA is packaged into secretory vesicles (or into granules within adrenal chromaffin cells) by the vesicular monoamine transporter, VMAT2. This packaging allows DA to be stored in readily releasable aliquots and protects the transmitter from further anabolism or catabolism. Synaptically released DA is subject to both transporter clearance and metabolism. The DA transporter (DAT) is not selective for DA; moreover, DA can also be cleared from the synapse by the norepinephrine (NE) transporter, NET. Reuptake of DA by DAT is the primary mechanism for termination of DA action, and allows for either vesicular repackaging of transmitter or metabolism. DAT activity is regulated by phosphorylation, offering the potential for DA to regulate its own uptake.

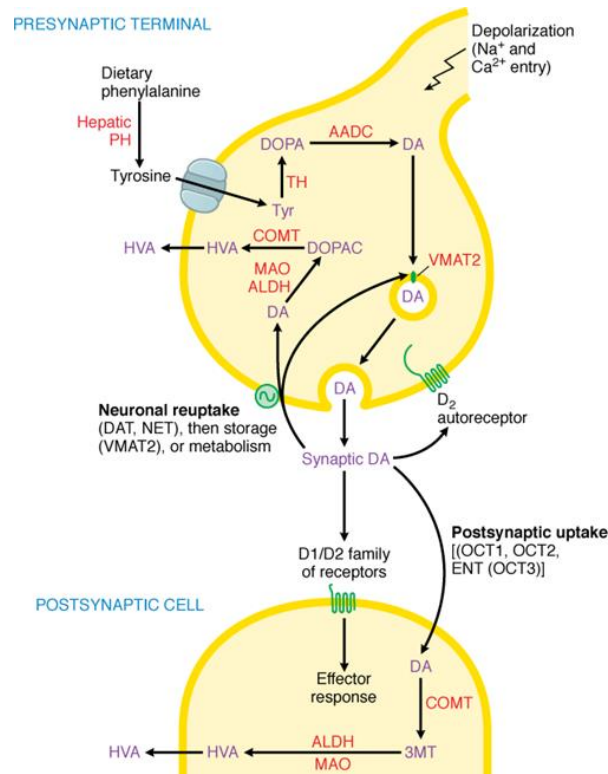


Figure 1.13. Dopaminergic nerve terminal. Dopamine (DA) is synthesized from tyrosine in the nerve terminal by the sequential actions of tyrosine hydroxylase (TH) and aromatic amino acid decarboxylase (AADC). DA is sequestered by VMAT2 in storage granules and released by exocytosis. Synaptic DA activates presynaptic autoreceptors and postsynaptic D1 and D2 receptors. Synaptic DA may be taken up into the neuron via the DA and NE transporters (DAT, NET), or removed by postsynaptic uptake via OCT3 transporters. Cytosolic DA is subject to degradation by monoamine oxidase (MAO) and aldehyde dehydrogenase (ALDH) in the neuron, and by catechol-O-methyl transferase (COMT) and MAO/ALDH in non-neuronal cells; the final metabolic product is homovanillic acid (HVA).

1.4.3 Animal models of Parkinson's disease: classical toxin-induced rodent models

Over the last two decades, significant strides have been made toward acquiring a better knowledge of both the etiology and pathogenesis of PD. Experimental models are of paramount importance to obtain greater insights into the pathogenesis of the disease.

Model	Gradual loss of dopamine neurons in adulthood	Easily detectable motor deficits	Development of Lewy bodies	Based on a single mutation	Short timecourse
6-hydroxydopamine	No	Yes (quantifiable rotation deficit)	No	N.A.	Yes
Rotenone	Yes, but variable individual susceptibility	Yes	Yes	N.A.	Yes
Acute MPTP*	No	Yes	No	N.A.	Yes
<i>Drosophila</i> α -synuclein overexpression	Yes	Yes	Yes	Yes	Yes
Mouse α -synuclein overexpression	Yes, but not in the substantia nigra	Yes	Nuclear as well as cytoplasmic inclusions	N.A.	No (1 year)

*Chronic MPTP administration produces slow evolution of a parkinsonian syndrome and might produce Lewy bodies. (MPTP, 1-methyl-4-phenyl-1,2,3,6-tetrahydropyridine; N.A., not applicable.)

Table 1.3. Characteristics of Animal Models for Parkinson's disease

Thus far, neurotoxin-based animal models have been the most popular tool employed to produce selective neuronal death in both in vitro and in vivo systems. These models have been commonly referred to as the pathogenic models.

The two most widely used rodent models of PD are the classical 6-OHDA-treated rat and the MPTP-treated mouse.

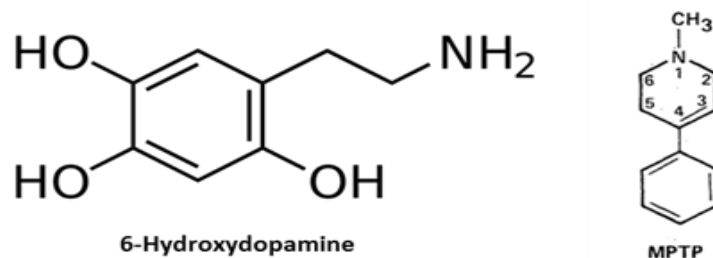


Figure 1.14. Chemical structure of 6-OHDA and MPTP

1.4.3.1 6-Hydroxydopamine (6-OHDA)

The 6-OHDA model has been extensively used as a test bed for novel symptomatic agents as well as providing a means for assessing neuroprotective and neurorepair strategies. Although

unlikely to be the first model of choice for testing symptomatic agents, since its behavioural phenotype is less robust than the 6-OHDA rat, the MPTP-treated mouse provides a useful secondary screening model and has the added advantage of being relatively easy to construct compared with the 6-OHDA rat. The characterization of the hydroxylated analogue of dopamine, 6-OHDA, as a toxin-inducing degeneration of dopaminergic neurons in the nigro-striatal tract (Ungerstedt, 1968) has led to it being a widely used tool to induce Parkinsonism in rodents. Unlike MPTP, 6-OHDA does not efficiently cross the blood–brain barrier and so requires direct injection into the brain. 6-OHDA is injected into the nigro-striatal tract at one of three locations: into the substantia nigra pars compacta (SNpc) where the A9 dopaminergic cell bodies are located; into the median forebrain bundle (mfb), through which the dopaminergic nigro-striatal tract ascends; or into the terminal region, the striatum. Following its injection, 6-OHDA is taken up into the dopaminergic neurons via the dopamine transporter, DAT. Given that 6-OHDA also shows high affinity for the noradrenaline transporter, NET (Luthman, 1989). Although the exact mechanism underlying 6-OHDA toxicity is still under investigation, current understanding is that, once inside dopaminergic neurons, 6-OHDA initiates degeneration through a combination of oxidative stress and mitochondrial respiratory dysfunction. Certainly, 6-OHDA readily oxidizes to form reactive oxygen species (ROS) such as H₂O₂ (Mazzio, 2004), to reduce striatal levels of antioxidant enzymes [total glutathione (GSH) or superoxide dismutase] (Perumal, 1992; Kunikowska and Jenner, 2001), to elevate levels of iron in the SN (Oestreicher, 1994) and to interact directly with complexes I and IV of the mitochondrial respiratory chain, leading to subsequent respiratory inhibition and further oxidative stress (Glinka, 1997). Many of these effects are thought to mirror events occurring in PD brain (Jenner, 1989), thereby supporting a high degree of construct validity for the 6-OHDA model. The 6-OHDA model also mimics many of the biochemical features of PD, including reduced levels of striatal dopamine and tyrosine hydroxylase (TH; rate-limiting step of DA biosynthesis). The 6-OHDA model shares a common failing with many other animal models of PD as it does not lead to the formation of the pathological hallmark of PD, the Lewy body. Lewy bodies are eosinophilic inclusions that contain ubiquitinated proteins such as α -synuclein (Spillantini, 1997 and 1998) and are associated with lipofuscin-containing lysosomes that have also been shown to accumulate α -synuclein in PD brain stem (Braak, 2001). The exact role of Lewy bodies remains to be established, but drugs to reduce aggregate formation are considered a potential future strategy for treating PD. A recent report of parkin-containing aggregate formation in 6-OHDA-lesioned rat (Um, 2010) is therefore an exciting advance but requires confirmation. The one pathological feature of PD robustly displayed by the 6-OHDA model is degeneration of the nigro-striatal

tract. The extent of degeneration can be established post-mortem by assessing the reduction in various parameters in the lesion (ipsilateral) hemisphere, compared with the intact (contralateral) hemisphere including number of nissl-stained cells or TH-positive neurons in the SNpc; levels of TH or DAT immunoreactivity in the striatum and levels of [3H] mazindol binding to DAT in the striatum. Behavioural indices can also be taken as a potential pre-screen for predicted lesion size.

1.4.3.2 1-methyl-4-phenyl-1,2,3,6-tetrahydropyridine (MPTP)

MPTP is a commonly used toxin for inducing both rodent and primate models of PD based on its ability to induce persistent parkinsonism in man (Davis, 1979; Langston, 1983). Subsequent investigations in non-human primates identified that selective destruction of dopaminergic neurons of the nigro-striatal tract was the pathological basis behind the motor deficits observed (Burns, 1983; Jenner, 1984; Langston, 1983), and out of this came the most relevant animal model of PD that persists today. The impact of the MPTP-treated primate model in the PD field is second to none, but first we will focus attention on the use of MPTP in non-primate species. Many species, including rats, are insensitive to the toxic effects of MPTP, possibly due to the relatively rapid clearance of 1-methyl-4-phenylpyridinium (MPP⁺), the toxic metabolite of MPTP (Johannessen, 1985). However, specific strains of mice, notably black C57, and Swiss Webster are sensitive to MPTP (Sonsalla and Heikkila, 1988) and have enabled development of the MPTP mouse model of PD. The mechanism underlying the neurotoxic action of MPTP has been the subject of intense investigation and is relatively well understood. MPTP is a lipophilic pro-toxin that, following systemic injection (usually i.p. or s.c.), rapidly crosses the blood–brain barrier (Riachi, 1989). Once inside the brain, MPTP is converted by MAO-B (principally in glia and serotonergic neurons) into the intermediary, 1-methyl-4-phenyl-2,3-dihydropyridinium (MPDP⁺) before its rapid and spontaneous oxidation to the toxic moiety MPP⁺ (Chiba, 1984). Following its release into the extracellular space, MPP⁺ is taken up via DAT into dopaminergic neurons where cytoplasmic MPP⁺ can trigger the production of ROS, which may contribute to its overall neurotoxicity (Javitch et al., 1985). However, the majority of MPP⁺ is eventually accumulated within mitochondria where the key toxic mechanism occurs. Once inside mitochondria, MPP⁺ impairs mitochondrial respiration via inhibition of complex I of the electron transport chain. This action impairs the flow of electrons along the respiratory chain, leading to reduced ATP production and the generation of ROS, such as superoxide radicals. The

combined effects of lowered cellular ATP and elevated ROS production are most likely responsible for initiation of cell death-related signalling pathways such as p38 mitogen-activated kinase (Karunakaran, 2008), c-jun N-terminal kinase (JNK) (Saporito, 2000) and bax (Hassouna, 1996; Vila, 2001), all of which have been demonstrated *in vivo* following MPTP treatment and may contribute to apoptotic cell death (Jackson-Lewis and Przedborski, 2007) (Figure 1.14). The MPTP-treated mouse has some clear advantages over the 6-OHDA lesion model, not least of all economic benefits in terms of the cheaper costs associated with purchasing and housing mice. Being systemically active, MPTP administration does not require the type of skilled stereotaxic surgery that production of a 6-OHDA lesion requires. The systemic injection also produces a bilateral degeneration of the nigrostriatal tract, more reflective of that seen in PD. The MPTP model also mimics many of the known biochemical features of PD. For example, in addition to the well-known reductions in striatal DA and tyrosine hydroxylase (TH), there are also elevated levels of both striatal preproenkephalin-A (PPE-A) (Gudehithlu, 1991) and ACh (Hadjiconstantinou, 1985). Further downstream in the basal ganglia, extracellular glutamate levels have been shown to be elevated in the SN of MPTP-treated mice, a rise associated with the induction of programmed cell death (Meredith, 2009), also glutathione (GSH) levels are significantly reduced as in PD itself. Finally, in further support of the face validity of this model, inflammatory markers are elevated in the striatum and SN of MPTP-treated mice (Kurkowska-Jastrzebska, 1999; Hebert, 2003), which occurs as a result of reactive microgliosis in PD. The MPTP model does, however, have some clear disadvantages over the 6-OHDA model, particularly in terms of reproducibility and the range of behavioural readouts that can be obtained. Mice are far less sensitive to MPTP than primates, and the higher doses required can be acutely lethal as a result of the peripheral neuro- or cardiotoxicity induced (Jackson-Lewis and Przedborski, 2007). Given that the risk of mortality usually occurs within 24 h of the first dose of MPTP and is dose-dependent, the high rates (up to 50%) seen following acute bolus dosing in the earlier studies can be reduced to acceptable levels (<20%) with reductions in the dose administered and can be almost completely avoided using alternative protocols in which the same or even higher total dose is given in multiple doses (Gibrat, 2009). The various dosing regimens used to generate the MPTP mouse model have been extensively reviewed in Jackson-Lewis and Przedborski, 2007. In many cases, MPTP is given with probenecid (250 mg·kg⁻¹), a uricosuric agent that reduces the renal clearance of MPTP, thereby prolonging its action. The most common protocols and the degree of nigrostriatal tract denervation produced by these can be summarized as follows: acute bolus, 1x30–40 mg·kg⁻¹ giving 80–90% striatal DA depletion; acute multiple, 2x40 mg·kg⁻¹ or 4x12.5–25 mg·kg⁻¹ given at 2 h intervals producing variable

60–90% striatal DA loss; sub-acute, 25-40 mg·kg⁻¹/day for 5 days + probenecid giving 76% loss striatal DA and 60% SNpc cell loss; chronic intermittent, 25 mg·kg⁻¹ twice weekly for 5 weeks + probenecid, giving 95% loss around 1 week, but reducing to a stable 70–80% loss by 12 weeks post treatment (Pothakos, 2009). Chronic infusion can be performed by administration of 20–40 mg·kg⁻¹/day for up to 28 days given via osmotic minipumps, giving most variable degree of cell loss so far ranging from 25% to 80% loss of cells in the SNpc and 28–90% loss of striatal dopamine (Fornai, 2005; Alvarez-Fischer, 2008). The pattern of cell death produced is similar to that seen in humans, with the SNpc affected more than the VTA and chronic infusion may also induce loss of noradrenergic cells in the locus coeruleus, further resembling the clinical picture (Fornai, 2005). However, in all cases, the cell death is rapid in onset, with first signs appearing within 12–72 h, and is maintained for up to 28 days (Novikova, 2006), although striatal dopamine depletion may show signs of recovery when using acute or sub-acute MPTP dosing paradigms (Lau and Meredith, 2003). As noted for the 6-OHDA model, this rapidity of cell death is not reflective of the disease itself and is an obvious weakness of this model.

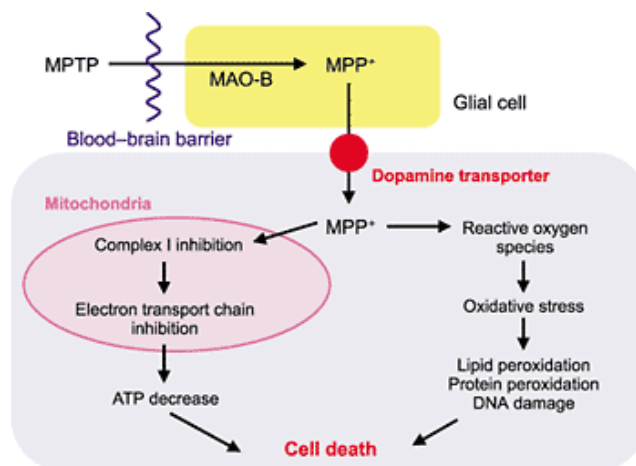


Figure 1.14. The mechanisms by which neurotoxins kill dopamine neurons involve mitochondrial dysfunction and oxidative damage. 6-hydroxydopamine (6-OHDA) is taken up by the dopamine transporter and it then generates free radicals. 1-methyl-4-phenyl-1,2,3,6-tetrahydropyridine (MPTP) is converted by monoamine oxidase B (MAOB) to 1-methyl-4-phenylpyridinium (MPP⁺). MPP⁺ is taken up by the dopamine transporter and can then be accumulated by mitochondria, leading to complex I inhibition and the generation of free radicals, or by the vesicular monoamine transporter, thus reducing toxicity. Rotenone is a direct inhibitor of complex I, which also leads to free-radical generation. MPTP and rotenone treatment increase the expression of alpha-synuclein and, in the latter case, this leads to the formation of Lewy bodies.

2. Aim of the study

In attempt to cure the serious consequences of spinal cord traumatic injury and Parkinson's disease were developed pharmacological treatments that have disregarded the hopes. These procedures are not decisive for the spinal cord injury cure.

Equally most of the experimental therapies of new generation, pharmacological and not, have the purpose of decrease the damage but little benefit accruing to the motor recovery and the neural regeneration.

The stem cell therapy approach is considered a promising tool for CNS regeneration, it seems to be just one of many clinical applications of stem cells. In recent years, the transplantation of embryonic cells represented a major therapeutic hope, however, the difficulty of finding the biological material and the ethical issues, have slowed their use. For this reason the research is concentrate in the direction of stem cells obtained from other source, such as bone marrow, dermis and adult nervous tissue.

The principal aims of this thesis work was to test the potential role of post mortem neural precursors cells (PM-NPCs) in terms to replacement therapy in a mouse model of contusive spinal cord injury and Parkinson's disease. PM-NPCs are a subclass of Sub Ventricular Zone (SVZ)-derived neural progenitors, capable of surviving many hours after donor death (Marfia, 2011). The *in vitro* differentiation of these cells yields more neurons (about 30-40%) compared to neural precursors cells isolated immediately after the animal sacrifice (Gritti, . With the aim to improve the monitoring of cells after transplantation, PM-NPCs will be isolated from the SVZ of mice constitutively expressing the green fluorescent protein GFP.

Detailed aims of the study:

- Isolation and characterization of GFP PM-NPSCs

Post-Mortem Neural Precursor Cells will be isolated from a transgenic mouse strain expressing green fluorescent protein (GFP) under the promoter C of the ubiquitin gene [C57BL/6-Tg(UBC-GFP)30Scha/J]. In particular, cells will be obtained from the SVZ at 6 hours after the mouse death. These cells will be characterized for their growth features, expression of stem markers, spheroids formation capability and *in vitro* neural differentiation potential.

- Stem cells transplantation

As experimental animal models will be used: 1) CD1 mice in which we induced contusive Spinal Cord injury at the T9 level of intensity equal to 70 kDyne, by means of Infinity

Horizon Impactor device;2) C57BL/J mice in which the Parkinsonism will be induced by the administration of MPTP following a specific paradigm (see Materials and Methods).

- In vivo evaluation of stem cells effects

The effect of PM-NPCs transplantation, on motor behaviour will be evaluated by specific animal tests, such as BMS for contusive trauma, horizontal grid, vertical grid and olfactory tests for PD.

- Ex vivo evaluation of survival, homing and fate of transplanted stem cells

At the end of the observational period (30 days for SCI and two weeks for PD) the animals will be sacrificed and perfused, spinal cord and brains will be removed from the different animals, fixed and processed for the immunohistochemical analysis.

By immunofluorescence will be studied the survival, migration and differentiation capabilities of the grafted cells

- Neurochemical changes in Parkinson disease

Animals' brain will be removed and dissected in specific areas (striatum, midbrain and cortex) for evaluate the levels of catecholamines and their metabolites by HPLC analysis.

- Investigate a possible protective mechanism of grafted cells

We will determine the mRNA levels of inflammatory and anti-inflammatory cytokines and neurotrophic factors.

3. Materials and Methods

3.1 Animals

Post-mortem neural precursors were obtained from 2-months old CD1 mice (Charles River, Calco, Italy). The animals were kept in standard conditions for at least 3 days before the experiments ($22 \pm 2^\circ \text{C}$, 65% humidity, and artificial light between 8:00 a.m. to 8:00 p.m.).

Post-mortem neural precursors constitutively expressing green fluorescent protein (GFP) were obtained from 2-months old C57 black mice carrying the transgene for GFP under the control of ubiquitin promoter C (C57BL/6-Tg (UBC-GFP) 30Scha/J; The Jackson Laboratories, Bar Harbor, Maine, USA).

3.2 Post Mortem Neural Precursor cells isolation

Adult CD-1 albino mice and (C57BL/6-Tg (UBC-GFP) 30Scha/J, weighing 25-30 g (Charles River), were anesthetized by intraperitoneal (i.p.) injection of 4% chloral hydrate (0.1 mL/10 g body weight) and sacrificed by cervical dislocation. The cadavers were maintained at room temperature (25°C) for 6 hours. Their brains were removed after the indicated periods and the area encompassing the SVZ and surrounding the lateral wall of the forebrain ventricle was dissected using fine scissors. Primary cultures of NPCs, their maintenance and immunostaining were performed as previously described (*Bottai et al 2008; Gritti et al 1999*).

Tissues derived from a single mouse were used to generate each culture using the following protocol:

1. Transfer the dissected tissue to a phosphate buffer solution containing penicillin and streptomycin 100 U/mL each (Invitrogen, San Diego, CA, USA) and glucose (0.6%) at 4°C until the end of the dissection.
2. To perform the enzymatic dissociation, transfer the tissue to an Earl's balanced salt solution (EBSS) (Sigma-Aldrich, St. Louis, MO, USA) containing 1 mg/mL papain (27 U/mg; Worthington DBA, Lakewood, NJ, USA), 0.2 mg/mL cysteine (Sigma-Aldrich), and 0.2 mg/mL EDTA (Sigma-Aldrich).
3. Incubate for 45 min at 37°C on a rocking platform.
4. Centrifuge tissues at 123g and discard the supernatant.
5. Re-suspend the pellet in 1 mL of EBSS and mechanically dissociate it using an aerosol resistant tip (1000 μL Gilson Pipette). Cells were re-suspended in 10 mL EBSS.
6. Centrifuge at 123g for 10 min, discard the supernatant and re-suspend the pellet in 200 μL of EBSS.

7. Re-suspend the pellet in 1 mL of EBSS and mechanically dissociate it using an aerosol resistant tip (200 μ L Gilson Pipette). Cells were re-suspended in 10 mL EBSS.
8. Centrifuge at 123g for 10 min, discard the supernatant and re-suspend the pellet in Neurobasal[®] Medium (GIBCO[®], Life Technologies Italia, Monza, Italy) containing B-27[®] supplement, 2% L-Glutamine (Euroclone, Pero, MI, Italy), bFGF (human recombinant, 20 ng/mL; Peprotech, Rocky Hill, NJ, USA, or Upstate Biotechnology, Lake Placid, NY, USA) and EGF (human recombinant, 20 ng/mL; Peprotech).
9. Plate the cells at 3500 cells/cm² in the appropriate volume of medium in a 25cm² flask, at 37°C in a humidified 5% CO₂ atmosphere.

3.2.1 Neural precursors in culture

PM-NPCs were plated in growth medium containing bFGF and EGF, after at least 2 weeks in culture gave rise to neurospheres, in absence of serum (*Gritti et al 1996; 1999*). The total number of viable cells was assessed by trypan blue exclusion. The spheres formed were harvested, collected by centrifugation (10 min at 123g), mechanically dissociated by pipetting to a single-cell suspension and re-plated in medium at the density of 10.000 cells/cm². This procedure was repeated every 4-5 days for up to 6 months.

3.2.2 Spheroids immunofluorescence

1. Transfer 1 mL of culture medium containing the spheroids in an eppendorf.
2. Add 100 μ L of 37% PFA for 15' at RT.
3. Centrifuge for 5' at 920 g.
4. Discard the supernatant and add 1mL of Permeabilization solution (300 mM sucrose; 0,2% Triton X-100; PBS) for 15' at RT.
5. Centrifuge for 5' at 920 g.
6. Discard the supernatant and add 1mL of Block Solution (2% BSA; PBS) for 15' RT on a rocking platform.
7. Centrifuge for 5' at 920 g.
8. Discard the supernatant.
9. Add 100 μ L of Binding Buffer (0,2% BSA; PBS) containing the Primary Antibody for 1h on a rocking platform.

10. Centrifuge for 5' at 920 g.
11. Discard the supernatant.
12. Add 100 µL of Binding Buffer containing the Secondary Antibody for 45' on a rocking platform.
13. Centrifuge for 5' at 920 g.
14. Discard the supernatant and wash 2 times with Binding Buffer.
15. Centrifuge for 5' at 920 g.
16. Discard the supernatant and re-suspend the pellet in a solution containing 90% glycerol, 5% PBS 1X, 5% DAPI.
17. Mount:
 - a. Place a drop of the solution with the spheroids on the microscope slide
 - b. Let fall gently the coverslip on the slide
18. Dry overnight at 4°C.
19. Seal the coverslip edges with varnish.

Images were taken using Leica SP2 confocal microscope with He/Kr and Ar lasers (Heidelberg, Germany). In negative control experiments, primary antibodies were replaced with equivalent concentrations of unrelated IgG of the same subclass.

The following primary antibodies were used:

- Anti-Nestin (monocl.1:100; Millipore).
- Anti-microtubuleassociationprotein 2 (MAP2; 1:200; Chemicon).

The following secondary antibodies were used:

- Alexa fluor 543 goat-anti-rabbit IgG (1:1000; Invitrogen, Life Technologies Italia, Monza, Italy).
- Alexa fluor 543 goat-anti-mouse IgG (1:1000; Invitrogen, Life Technologies Italia, Monza, Italy).

3.2.3 Neuronal differentiation of PM-NPCs

In order to verify the multipotency of neural stem cells, the PM-NPCs were subjected to tests *in vitro* differentiation. Neurospheres were mechanically dissociated and cells ($1,5 \times 10^4$ cells/cm²) were seeded into Matrigel®-coated glass coverslips (12 mm diameter) in the presence of bFGF (10ng/ml). After 48 hours, cells were shifted into the differentiation medium in which bFGF were substituted with FBS (1% vol/vol) for 5 days. PM-NPCs attached to the dish and differentiated into the three cell types present in the adult CNS: neurons, astrocytes, and oligodendrocytes in a typical cell lineage ratio (*Marfia et al 2011*).

3.2.4 Fixing of differentiated cells

After seven days of differentiation, the cells were fixed and characterized by immunocytochemical staining.

The fixing procedure includes:

1. Wash with PBS 0.01 M (a phosphate buffer saline containig: 1.5 M NaCl, 20 mM KH₂PO₄ and Na₂HPO₄ 480mM) for 5 min.
2. Add 4% Paraformaldehyde (Sigma) for 10' to fix aldehyde groups in the cell proteins
3. Wash with PBS 1X two times for 10 min.
4. The cells can be stored at 4 °C.

3.2.5 Cells Immunofluorescence

1. Wash with PBS (3 times; 5 min each, room temperature).
2. Incubate the coverslips for 90 min at 37°C (or overnight at 4 °C) in PBS containing 10% normal goat serum (NGS), 0.2% Triton X-100.
3. Wash with PBS.
4. Incubate the coverslips overnight at 4 °C in PBS containing 5% normal goat serum (NGS), 0.1% Triton X-100 and the appropriate primary antibodies or antisera.
5. Wash with PBS.
6. Incubate for 45' (room temperature) with the secondary antibody.
7. Incubate cells with the DNA-binding dye 4'-6'-diamidino-2-phenylindole (DAPI) (2µg/ml in PBS) for 10' at room temperature.

8. Wash 2 times in PBS.
9. Mount using Fluorsave Reagent (Calbiochem, Merck Chemical, Darmstadt, Germany):
 - a. Place a drop of Fluorsave on the microscope slide.
 - b. Let gently fall the glass coverslip with the cells on the slide.
 - c. Keep attention to not make bubbles.
10. Dry overnight at room temperature.

Cells were analyzed by a fluorescence microscope (Leica, Wetzlar, Germany). Acquisition of the stained cells was performed using the image-analysis software (Leica, Wetzlar, Germany) or by confocal microscope Leica SP2 microscope with He/Kr and Ar lasers (Leica, Wetzlar, Germany). Images were taken with a 40X objective lens and 1X zoom (Leica). In control experiments, primary antibodies were either omitted or replaced with equivalent concentrations of unrelated Ig of the same subclass. Moreover, in double labelling experiments, sections incubated with one primary antibody and two secondary anti-sera revealed no appreciable cross-reaction.

Neural differentiation was assessed by immunocytochemistry with antibodies against:

- Anti-NG2 (1:200; Millipore)
- microtubule-associated protein 2 (MAP2; monocl. 1:200; Sigma)
- Glial fibrillary acidic protein (GFAP; monocl. 1:400; Roche, Basel, CH)

The following secondary antibodies were used:

- Alexa fluor 543 goat-anti-rabbit IgG (1:1000; Invitrogen, Life Technologies Italia, Monza, Italy).

3.2.6 Cell count

The quantification of positive cells to neural markers was performed, by confocal microscopy, after specific immunocytochemical staining following 7 days differentiation in culture. Cell counts were performed on a minimum of 9 independent fields (3 fields/3 coverslips/treatment) of photomicrographs captured with 40X objective. Total counts of each neural markers immunoreactive cells were performed and the number of positive cells per culture was expressed as the percentage to the total cells. DAPI supplied the total number of cells being a nuclear staining.

3.2.7 Cell freezing

When the neurospheres amount to the size of approximately 200 μm they are harvested and centrifuged at 700 rpm for 10 min, at this point is drew all the supernatant and the pellet is resuspended in 1.5 ml of colture medium containing dimethyl sulfoxide (DMSO) (Sigma) to a final concentration of 10%. The neurospheres are suspended with a pipette P1000 without being dissociated and transferred criovials (Nalgene). The step of freezing takes place in two stages; initially criovials containing cells are placed in a plastic container that allow a gradual lowering of the temperature of 1 ° C per minute and stored in -80° C freezer.

3.2.8 Cell defrosting

The neurospheres preserved, can be put back into culture after defrosting. The criovial containing the cells of interest is placed in a thermostated bath at the temperature of 37 °C until defrosting occurred that must be as rapid as possible because the DMSO although acting as protection for cells at a low temperature is found to have toxic effects at room temperature. After defrosting the cell suspension is moved in 15 ml tube. Add culture medium previously heated at the temperature of 37 °C until volume of 10 ml and centrifuge at 700 rpm for 10 min. In this passage are washed DMSO residues toxic for the cells. Pellet is resuspended in 1 ml of culture medium by P1000 and placed with adequate medium volume in a T25 flask. After 24 hours the defrosted neurospheres can be dissociated, counted and replated as described before.

3.2.9 PKH26 cells labelling

PKH26 cell linker Kits provide fluorescent labelling of live cells over an extended period, with no apparent toxic effects. Fluorescent linker kits are effective for a variety of cell types and exhibit no significant leaking, or transfer from cell to cell. They provide stable, clear, intense, accurate and reproducible fluorescent labeling of cells (Fig. 3.1).

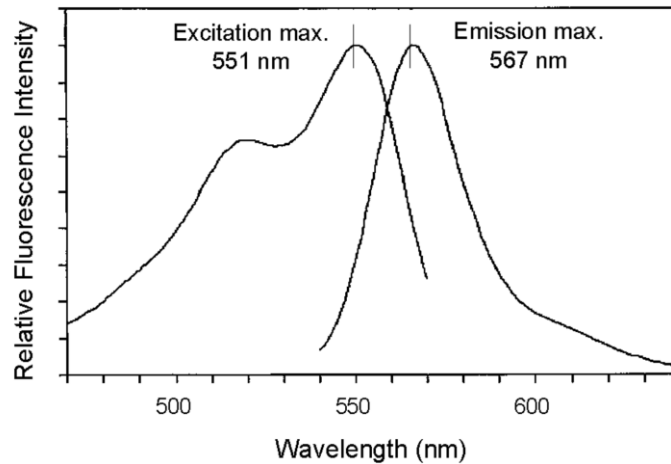


Figure 3.1 Typical wavelength emission of PKH26

For these transplantation experiments, 1×10^6 cells in $150 \mu\text{L}$ were injected in each animal.

Before transplantation, PM-NPCs were labelled with PKH26 and the staining was performed according to the protocol of the manufacturer (Sigma–Aldrich).

The following procedure uses a 2 mL final staining volume containing final concentrations of 2×10^{-6} M of PKH26 and 1×10^7 cells/mL:

1. Resuspend cells to a concentration of 1×10^6 cells/ $150 \mu\text{l}$ (transplant 1×10^6 cells per mouse). Prepare at least 1.2×10^6 cells per mouse because an excess of cells is required for syringe loading purposes.
2. Wash cells 3 times using neural stem cell medium ¹³ in a 10ml conical vial. In each washing step, precipitate cells by centrifugation ($500 \times g$ for 5 min, room temperature).
3. Count the cells before the final spin.
4. Centrifuge the cells ($500 \times g$ for 5 min), and then aspirate the supernatant, being careful not to remove any cells but leaving no more than $25 \mu\text{l}$ of supernatant.
5. Prepare a 2X cell suspension by adding 1ml of Diluent C to the cell pellet and resuspend with gentle pipetting.
6. Immediately before staining, prepare a 2X Dye Solution (4×10^{-6} M) in Diluent C by adding 4ml of the PKH26 ethanol dye solution to 1ml of Diluent C in a tube and mix well to disperse.
7. Rapidly add the 1ml of 2X cell suspension to 1 ml of 2X Dye Solution and immediately mix the sample by pipetting (final cell density will be 1.2×10^7 cells/ml and 2×10^{-6} M PKH26).
8. Incubate the cell/dye suspension for 1- 5 min.
9. Stop the staining by adding an equal volume (2ml) of serum and incubate for 1 min.

10. Centrifuge cells (500 x g for 10 min) and carefully remove the supernatant.
11. Resuspend cell pellet in 10ml of complete medium and centrifuge (500 x g for 5 min).
12. Wash the cell pellet 2 more times with 10ml of complete medium to ensure removal of unbound dye.
13. Resuspend the cell pellet in 10ml of complete medium for assessment of cell recovery, cell viability and fluorescence intensity. If cells are needed for transplantation, wash and resuspend them in a sterile physiological solution at a concentration of 3.3×10^5 cells/50 μ l.

3.2.10 Hoechst cells labelling

Hoechst is a fluorescence DNA binding molecule suitable for the fluorescent microscopy and FACS. This molecule is used for both to display the mitochondria, and identify the nuclei, similarly to the DAPI staining.

For these transplantation experiments, 1×10^6 cells in 150 μ L were injected to each animal.

Before transplantation, PM-NPCs were labelled with Hoechst 33342 (Sigma) and the staining was performed according to the following protocol:

1. Resuspend cells to a concentration of 1×10^6 cells/150 μ l (transplant 1×10^6 cells per mouse). Prepare at least 1.2×10^6 cells per mouse because an excess of cells is required for syringe loading purposes.
2. Add a concentration of 1 μ l/ml of Hoechst to the cell solution used for injected animals.
3. Incubate the cell/dye suspension for 1 hour at 37 °C.
4. Wash and resuspend them in a sterile physiological solution at a concentration of 3.3×10^5 cells/50 μ l.

3.3 Animal treatment for Spinal Cord Injury

The CD1 mice were surged for creating the contusion model of injury, which is analogous to the one of clinical patients and we use Infinity Horizon Impactor device

The procedure consists in following steps.

3.3.1 Preparation of mice for surgery and transplantation

1. Keep the male adult CD1 mice (25–30 g) for at least 3 days before the experiments in standard conditions (22 ± 2 °C, 65% humidity, and artificial light between 08:00 a.m. to 08:00 p.m.).
2. To identify the animal, mark the tail by means of water resistant colored ink.
3. Use an electric clipper to cut the dorsal hair of the mouse from the neck, about at T2 level, to the lumbar area.
4. Sterilize the prepared area with an iodide solution and ethanol (70% in sterile water).
5. Treat the animal with a sub cutaneous (s.c.) injection of 200 µl gentamycin (1 mg/ml in sterile saline solution).
6. Apply ophthalmic lubricant to both animal eyes to prevent desiccation and inject buprenorphine (subcutaneously, 0.03 mg/kg) to alleviate pain.

3.3.2 Preparation for surgery

1. Clean and sterilize surgery equipment.
2. Prepare the surgery area by wiping with an aseptic agent. Set up the IH Impactor device.
3. Prepare the anesthesia equipment: the Active Gas Scavenger with VetScav Filter Weighing Device, continuous flow Induction Chamber, Oxygen Generator, Low Flow O₂ Meter for Mice. Clean the induction chamber and the mask used during surgery.
4. Anesthetize animals with 2.5% (v/v) isoflurane in oxygen (1 L/min), and wait 5 min after the flow induction for the drug to take effect. Check if the whiskers are twitching or if there is slow hind limb withdrawal in response to pinching the footpad. During the surgery, reduce the isoflurane concentration to 2.0% (v/v) isoflurane in oxygen (1 L/min).

3.3.3 Laminectomy

1. Place the mouse on a slide warmer to avoid the problem of hypothermia during the surgery. Position the animal with the dorsal side up.
2. Make a vertical incision with a scalpel over the region of interest from T7 to T12.
3. Hold the skin and superficial fat pad by using standard forceps (usually found in the space between the 5th and 6th thoracic dorsal processes).
4. Count the process under the vessel as T6 then move to T7.

5. Place a little bearing under the ventral side of the mouse to increase the curvature of the spine. Immobilize the spinal cord by blocking it with the Graefe forceps.
6. Cut the paravertebral muscles bilaterally from T7 and T10 vertebral level by using the scalpel until the dorsal surface of the lamina contacts the scalpel tip.
7. Use the scalpel to tick off the junction from T7 until T10. Stop in the space between T8 and T9 spiny protrusions. Cut the tissues between T8-T9 and T9-T10 with the micro scissors.
8. Use the Rongeur to remove the T9 process. Expose the junction by carefully scraping away the muscle layer with the micro scissors. Continue until bone is exposed.
9. Use the forceps to remove muscles from the lamina and open a small space between the vertebrae. Gently insert the micro scissors under the bone, cut the lamina on both sides and remove this part with forceps.
10. Remove the lamina with the forceps to expose the cord. Be sure not to leave any free or jagged bone fragments behind; remove them with the Rongeur.
11. Use the small tip forceps to remove the periosteum as well as any bone fragments or muscles that may be near the incision.
12. Remove the top half of the T9 dorsal process and proceed to the IH Impactor device protocol.

3.3.4 IH Impactor device protocol (Contusion)

1. Place the mouse in the middle of the stabilization platform of the IH Impactor device (Fig. 3.2).
2. Block the animal with the two teeth forceps connected with the stabilization platform by two joint positioning arms (left arm for the thoracic vertebra, right arm for cervical vertebra).
3. Use the rostral arm to grasp the lateral edge of the rostral vertebral body (T8).
4. Manipulate the caudal arm in the same manner to grasp the T10 vertebral body.
5. Place the stabilization platform in the device and lower the tip (diameter 0.75 mm) as close to the cord as possible without touching it.
6. Lift the tip three complete turns before initiating the impact.
7. Perform the contusion with the impactor set to deliver a force of 70 kdyn at 100 mm/s.



Figure 3.2 Infinite Horizon Impactor Device

3.3.5 Sutures and post-care

1. Suture the incision with a 4/0 absorbable suture thread. Cover the exposed spinal cord at the site of removed lamina; suture the tissue at the extremities of the cut by means of a small needle. Put the two stitches immediately above and under the site of spinal cord exposure.
2. Close the skin using two or three Reflex clips without pinching off the underlying muscles.
3. Hydrate the mouse post-surgery with 2 ml of saline solution subcutaneously injected in the lower back.
4. Place the mouse back in a pre-warmed cage to avoid hypothermia during surgical recovery. Place cages on heating pads.
5. Monitor the mice during the acute phase post-injury by checking the size bladder, the suture and the animal weight twice a day. Gently squeeze bladder (twice a day for 7 days) to avoid urinary tract's infections (urine could be cloudy, bloody or containing any precipitates).
6. Treat mice once a day with a saline solution injection (2 ml for two days post-surgery s.c. injection) and antibiotic (gentamycin 0.2 ml; s.c. injection) for five days post injury.
7. Treat mice for post-operative analgesia with buprenorphine (0.1 mg/kg; twice a day) for 3 days post injury.

3.4 Tail vein Injection of cells

In the following step the procedure for injecting the cells into the tail vein is demonstrated. Cells could be also administered with an intraspinal transplant by using a stereotaxic frame (Bottai, 2010; Basso, 2006) or into the cisterna magna (Janowski, 2008). It is important to consider that other cell types could be transplanted with this method, such as mesenchymal stromal cells (e.g., bone marrow mesenchymal stem cells, adipose derived stem cells, amniotic fluid cells). Furthermore, other treatment options such as nanoparticles can be injected via the tail vein after the spinal cord injury.

1. Use 70% ethanol and PBS to clean the needle before use. Handle the needle and the syringe only with sterile gloves.
2. Resuspend the cells in the test tube and load 75 μ l of cells into a 0.3 ml syringe (29 gauge needle and 0.33 cc syringe).
3. Make sure that no bubbles are present within the cell suspension. Keep the syringe in a horizontal position to avoid cell sedimentation.
4. Place the mouse cage underneath the heat lamp to dilate the tail veins.
5. Grab the mouse and gently pull it into the mouse restrainer to visualize the lateral tail vein as a narrow blue line.
6. Clean the tail with an alcohol swab. Once the vein is visualized, grab the tail vein between the middle finger and thumb of the left hand.
7. Bring the needle to the surface at a 15° angle from the horizon and make sure the bevel is up.
8. Inject 50 μ l of cells at a rate of 33 μ l/s. After the injection, delay the retraction of the needle by 10 s. Retract the needle slowly and pay attention to the possible efflux of cell suspension.
9. Clean the syringe as in step 7.1 between loads.

3.5 Behavioural Tests and hind limb function

Neurological function must be tested periodically, from day 3 after injury for 4 weeks. To evaluate locomotor function and hind limb recovery after contusion according to the Basso mouse scale (BMS) (Basso, 2006). During this test the mouse was placed in the open field and two people observe the test. One person records all the data on the score sheet and the other

keeps the animal moving in the open field. Both people watch the animal and call out the movement each sees. One animal is put in the open field at a time and its tested for 4 minute. After each test assigned numerical values from 0 to 9 corresponding to the different behavioral recovery, 9 correspond to the healthy animal.

SCORE	
0	No ankle movement
1	Slight ankle movement
2	Extensive ankle movement
3	Plantar placing of the paw with or without weight support or Occasional, frequent or consistent dorsal stepping but no plantar stepping
4	Occasional plantar stepping
5	Frequent or consistent plantar stepping, no coordination or Frequent or consistent plantar stepping, some coordination, paws rotated at initial contact and lift off (R/R)
6	Frequent or consistent plantar stepping, some coordination, paws parallel at initial contact (P/R, P/P) or Frequent or consistent plantar stepping, mostly coordinated, paws rotated at initial contact and lift off (R/R)
7	Frequent or consistent plantar stepping, mostly coordinated, paws parallel at initial contact and rotated at lift off (P/R) or Frequent or consistent plantar stepping, mostly coordinated, paws parallel at initial contact and lift off (P/P), and severe trunk instability
8	Frequent or consistent plantar stepping, mostly coordinated, paws parallel at initial contact and lift off (P/P), and mild trunk instability or Frequent or consistent plantar stepping, mostly coordinated, paws parallel at initial contact and lift off (P/P), and normal trunk stability and tail down or up & down
9	Frequent or consistent plantar stepping, mostly coordinated, paws parallel at initial contact and lift off (P/P), and normal trunk stability and tail always up.

3.6 Animal treatments for Parkinson's Disease

Parkinsonism was induced by the intraperitoneal (i.p.) administration of 1-methyl-4-phenyl-1,2,3,6-tetrahydropyridine (MPTP) in C57/bl mice following the acute paradigm with a small modification. Figure 11 explain the activity of neurotoxin MPTP.

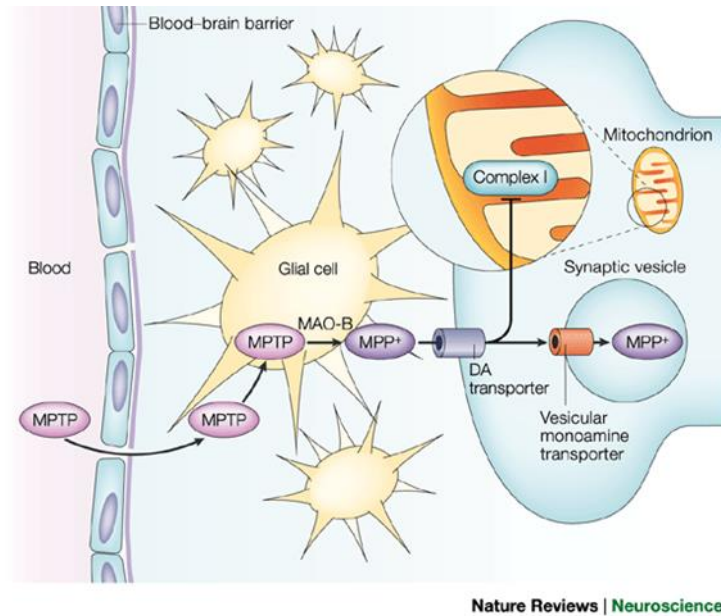


Figure 3.3. Mechanism of neurotoxin MPTP

Briefly, animals were administered of a double dose of MPTP hydrochloride: a first intraperitoneal (i.p.) injection of MPTP (36mg/kg) and a second i.p. injection of MPTP (20mg/kg) after seven days. In order to investigate the stability of the lesion a group of animals were sacrificed 3 days after the second toxin administration (CTRL n=8; MPTP n=8). Animals were transplanted with 5×10^4 cells/ μl (5 μl) GFP PM-NPCs (n=24) or PBS (n=6), according to the following stereotaxic coordinates in relation to bregma: 0.1 mm posterior, 2.4 mm mediolateral and 3.6 mm dorsal at the level of left striatum (Cui, 2011). Fourteen days after transplant, thirteen animals per group were sacrificed by cervical dislocation, and their brains were removed and dissected (Fig 3.4).

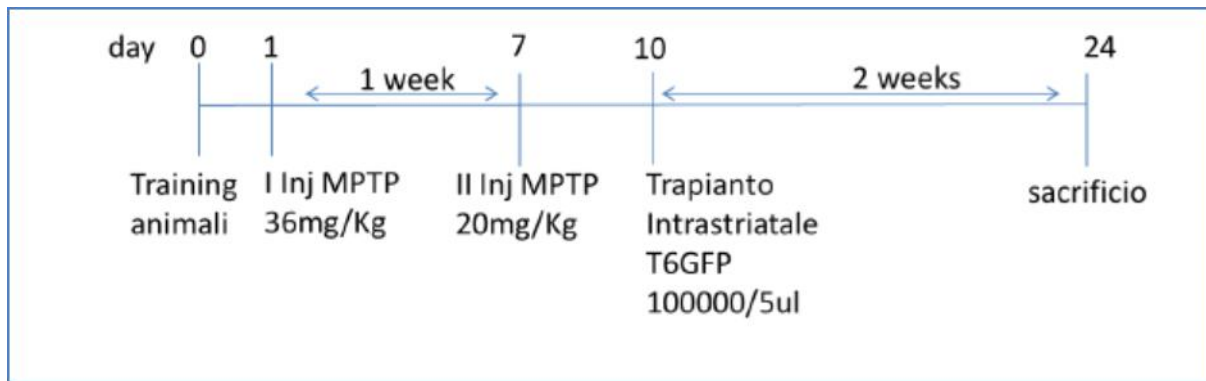


Figure 3.4. Experimental design

Immediately after dissection, the whole striatum, frontal cortex and midbrain were frozen on dry ice until they were assayed. The dissected brain areas of eight mice were used for the neurotransmitters determination (see later). Remaining brains areas (n=5 mice) were used for cytokines and neurotrophic factors gene expression analysis (see later). Ten animals per group were anesthetized by an intraperitoneal injection of sodium pentobarbital (65 mg/kg), perfused through the left ventricle with 50 mL of saline solution and fixed with 200 mL of 4% paraformaldehyde in 0.1 mol/L phosphate-buffered saline (PBS). Brains were subsequently removed from the skulls and then cryoprotected at 4°C in sucrose 300 g/L in 0.1 mol/L PBS solution for further sectioning.

3.7 Behavioral tests for Parkinson's disease

The recovery of motor dysfunction, before and after cell transplantation, was investigated by means of Horizontal grid test (Tillerson and Miller, 2003), Vertical grid test (Kim, 2010), and olfactory test (Schintu, 2009).

Horizontal grid test. The grid apparatus was constructed according to Tillerson and co-workers 2003 (Tillerson and Miller, 2003). The animal was videotaped for 30 s and the videos were replayed for percentage forepaw fault analysis using a recorder with slow motion option. The number of unsuccessful forepaw steps divided by the total number of attempted forepaw steps was evaluated (Tillerson and miller, 2003). Before MPTP administration, the mice were acclimated to the grid twice a day for 1 week.

Vertical grid test. The vertical grid apparatus was constructed according to Kim and co-workers (Kim, 2010). For this test, the mouse was placed 3 cm from the top of the apparatus, facing

upward, and was videotaped while it turned around and climbed down. The score reported was the time required by the mouse to make a turn, climb down and reach the bottom of the grid with its forepaw within 180s (Kim, 2010). Before MPTP administration, the mice were acclimated to the grid twice a day for 1 week.

Olfactory test. Mice were deprived of food for 20 hours before test. A corn chip was buried under the bedding (1 cm) in a cage corner. Each mouse was positioned in the center of the testing cage and the time to retrieve and bite the corn chip was measured (Schintu, 2009).

3.8 MR *in vivo*

All animals were viewed using a tool 7T MRI System (Pharmascan, Bruker Biospin). The animals were anesthetized with isoflurane, positioned supine on the pad and placed in the radio frequency coil (38 mm diameter) inside the magnet. Images were acquired transverse control to confirm correct positioning the region of interest.

Different sequences of magnetic resonance have been used:

- Sequence Spin Echo (MSME), (256x128 matrix; TR / TE: 1200/12 ms; 2 medium; acquisition time: 5 '7' '); with suppression of lipid)
- Sequence gradient echo sequence (FLASH), (256x128 matrix; TR / TE: 1200/10 ms; 2 medium; acquisition time: 5 '7' ')
- Sequence Fast Spin Echo (RARE) (256x128 matrix; TR / TE: 2000/56 ms; 2 medium; acquisition time: 4'16 ")

All animals were acquired in order to obtain sagittal, coronal (5 slices with a thickness of 0.7 mm; field of view (Field of View FOV) 4x4 cm and a spatial resolution of 156 x 312 μ M) and axial (12 slices with a thickness of 0.7 mm; FOV 3x3 cm and spatial resolution of 117 x 234 μ m).

3.9 Perfusion

1. At the end of the experimental period, anesthetize animals by an intraperitoneal injection of sodium pentobarbital (65 mg/kg). Use toe pinches to evaluate the anaesthesia level and proceed only after mouse is unresponsive to the noxious stimuli.
2. Restrain the animal in a supine position on a surgery plane.

3. Cut through the integument and abdominal wall just beneath the rib cage. Separate the diaphragm from the liver.
4. Use the scissors to cut the diaphragm to expose the pleural cavity.
5. Cut the sides of the rib cage until the collar bones.
6. Use the hemostats to clamp the xiphoid cartilage and place the hemostat over the head.
7. Hold the bottom third of the heart on a transversal plane with the forceps. Insert the needle into the left ventricle.
8. Use a hemostat to clamp the heart. This secures the needle and prevents leakage.
9. Use the scissors to cut the right atrium.
10. Allow the PBS to pump (18 ml/min) through the animal. Maintain this pressure throughout the buffer infusion period (3-4 min; corresponding to about 70 ml PBS). Continue until the heart is clean.
11. Switch the stopcock to allow the fixative (4% Paraformaldehyde in distilled water, 4%PFA) through the pump. Allow the 4% PFA to pump through the animal for approximately 8-10 minutes (300 ml). Gradually increase the pressure to reach a maximum of 30 ml/min. A hardened liver is the best indication of a successful perfusion.

3.10 Tissue collection and processing

1. Dissect spinal cords from T5 to L1. Then post-fix the tissue in 6 ml in 4% PFA (overnight at 4 °C).
2. Put the same tissue in a solution with 30% sucrose for 72 h at 4 °C in order to cryoprotect it and to prevent the formation of crystals during freezing.
3. Quick freeze the cord using dry ice cryoprotect with OCT and store it at -80 °C.
4. Section by means of a cryostat with 15 micron thickness and collect sections onto glass slides and continue for Cresyl violet and immunocytochemistry.

3.10.1 Cresyl-violet staining

Cresyl-violet staining is a type of labelling that highlights the cellular architecture of the cut sections in order to see the conformation of white and gray matter after injury.

The staining was performed following this protocol:

1. Wash in PBS 1X pH 7.4 for 5 min.
2. Incubate with a solution of Cresyl –violet for 10 min at 56°C.
3. Refrige for 10 min at room temperature.
4. Wash in EtOH 95%.
5. Wash in Isopropilicalcool for 4 min.
6. Clarify in Xilene for a time to wash the excess of staining.
7. Mounted with Permount and analyze by optical microscope.

3.10.2 Immunoistochemistry

To evaluate the inflammation after the injury in saline and cells injected mice, number of macrophages were estimated in the lesion site, as well as at the rostral and caudal level. The animals were sacrificed after 7 days post injury, the spinal cord was extracted and placed into OCT. The samples were cut with cryostat for 10 µm transversal sections. The procedure of the staining includes following steps:

1. Wash in PBS 1X pH 7.4 three times for 5 min for each
2. Incubate in a solution of Na₄Cl 0.05 M in PBS 1X for 30 min
3. Wash in PBS 1X pH 7.4 three times for 5 min for each
4. Wash with 1% H₂O₂ to block the endogenous peroxidase for 5 min
5. Wash in PBS 1X pH 7.4 three times for 5 min for each
6. Permeabilize each slide with 5% NGS and 0.2% Triton X-100 in PBS 90 min at room temperature.
7. Incubate each slide of primary antibodies (Anti-EB-1, 1:200. SIGMA; Anti TH, 1:800. Millipore) overnight at 4 °C (dilute antibody in 5% NGS; 0.2% Triton X-100 in PBS)
8. Wash in PBS 1X pH 7.4 three times for 5 min for each
9. Incubate with appropriate secondary antibodies (Anti-Rat biotinylated, 1:1000. Sigma; Anti-Rabbit biotinylated, 1:1000. Sigma) for 2 hours at room temperature
10. Incubate with ABcomplex for 45 min at room temperature (prepare the avidinbiotin solution 30 min before use)
11. Wash in PBS 1X pH 7.4 three times for 5 min for each
12. Incubate with 3% DAB diluted in Tris 0.1M pH 7.4 until time to stain the sections.
13. Wash in PBS 1X pH 7.4
14. Dehydrate the section in alcohol scale (5' in ethanol 75%, 5' in ethanol

15. 100%).
16. Clarify in xylene for 3 min.
17. Mount with Permount and analyze by optical microscope

3.10.3 Immunofluorescence

The in vivo immunofluorescence staining was carried out on the slides containing cryosections of the mice tissue perfused in 4% Paraformaldehyde and inserted into OCT. The staining method consisted of the following steps:

1. Rinse sections with 200 μ l of PBS for each slide
2. Permeabilize each slide with 200 μ l of 10% NGS and 0.2% Triton X-100 in PBS for 1 hour at room temperature.
3. Rinse sections with 200 μ l of PBS for each slide (3 times; 5 min each, room temperature).
4. Block non-specific sites with 200 μ l of blocking solution for slide (5% NGS; 0.1% Triton X-100 in PBS) for 30 min (room temperature).
5. Incubate each slide with 200 μ l of primary antibodies overnight at 4 °C (dilute antibody in 5% NGS; 0.1% Triton X-100 in PBS).
6. Wash sections with 200 μ l of PBS for each slide (3 times; 5 min. each; room temperature).
7. Incubate with appropriate secondary antibodies for 2 hours at room temperature.
8. Wash sections with 200 μ l of PBS for each slide (3 times; 5 min. each; room temperature).
9. Stain nuclei with 200 μ l of 4',6-diamidin-2-phenilindole (DAPI) (1 μ g/ml final concentration, 10 min at room temperature).
10. Mount by using the FluorSave Reagent and analyse by confocal microscopy.

In control determinations, primary antibodies must be omitted and replaced with equivalent concentrations of unrelated IgG of the same subclass.

Neural differentiation was assessed by immunohistochemistry using the antibodies against:

- Anti-Anti-beta III Tubulin (β Tub; monoclon. 1:500; Sigma)
- Anti-Anti-Choline Acetyltransferase (ChAT; monoclon. 1:100; Sigma)
- Anti-Tyrosine Hydroxylase (TH; monoclon. 1:500; Sigma)

- Anti-Serotonin (5-HT; monoclon. 1:200; Sigma)
- Anti- Microtubule-Associated Protein 2 (MAP2; monocl. 1:200; Sigma)
- Anti-Glial Fibrillary Acidic Protein (GFAP; monocl. 1:400; Roche, Basel, CH)
- Anti-Growth Associated Protein-43 (GAP-43; monoclon. 1:200; Sigma)
- Anti Neuronal Nuclei (NeuN: monoclonal. 1:100; Millipore)
- Anti Macrophages/Monocyte (MOMA; monoclonal. 1:100; Chemicon)
- Anti Chondroitin Sulfate Proteoglycan (NG2; monoclonal. 1:200; Millipore)
- Anti Nestin (Nestin; monoclonal. 1:200; Millipore)

The following secondary antibodies were used:

- Alexa fluor 543 and 488 goat-anti-rabbit IgG (1:200; Invitrogen, Life Technologies Italia, Monza, Italy).
- Alexa fluor 488 and 594 goat-anti-mouse IgG (1:200; Invitrogen, Life Technologies Italia, Monza, Italy).
- Alexa fluor 647 and 488 goat-anti-rat IgG (1:200; Invitrogen, Life Technologies Italia, Monza, Italy).
- Alexa fluor 546 and 488 donkey-anti- goat IgG (1:200; Invitrogen, Life Technologies Italia, Monza, Italy).

3.10.4 Assessment of Myelin preservation

The FluoroMyelin™ Green fluorescent myelin stain is capable of a selective and rapid labeling of myelin present in the nervous tissue section. By binding to the lipids of axonal sheath via the Lipophilic associations. It is often used for visualization of the myelin distribution and its co-localization with other markers. The procedure of the staining includes following steps:

1. Incubate the cryosections with fluoromyelin diluted 1:300 in PBS for 20 minutes;
2. Wash three times for 10 minutes each with PBS
3. Counted with FluorSave (Merck, Darmstadt, Germany).

Qualitatively and quantitatively analysed by confocal microscopy (Leica TSC2; Leica Microsystems, Heidelberg, Germany)

3.10.5 Fluororuby staining

Fluororuby is a fluorescent rhodamine-conjugated dextran, which has been used to study in vivo axonal transport within the central nervous system. A 10% solution of Fluororuby prepared by dissolving 10 mg of dry powder in 100 µL of PBS, was delivered via intraspinal injection at T6/T7 using a 5 µL Hamilton microsyringe. Injection volumes typically ranged from 0.5-1 µL and were gradually injected over a 10-15 minute interval (Schofield et al., 2007).

3.10.6 Confocal microscopy

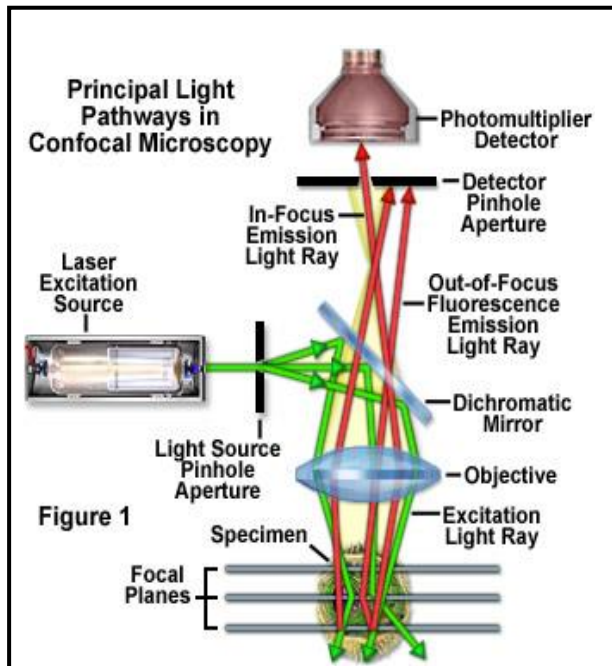


Figure 3.3 Scheme of confocal microscopy

Confocal microscopy offers several advantages over conventional optical microscopy, including controllable depth of field, the elimination of image degrading out-of-focus information, and the ability to collect serial optical sections from thick specimens. The key to the confocal approach is the use of spatial filtering to eliminate out-of-focus light or flare in specimens that are thicker than the plane of focus. In recent years, there has been a tremendous explosion in the popularity of confocal microscopy, due in part to the relative ease with which extremely high-quality images can be obtained from specimens prepared for conventional optical microscopy. In a conventional wide field microscope, the entire specimen is bathed in light from a mercury or xenon source, and the image can be viewed directly by eye or projected onto an image capture device or photographic film. In contrast, the method of image formation in a confocal microscope is fundamentally different. Illumination is achieved by scanning one or more focused beams of light, usually from a laser or arc-discharge source, across the specimen. This point of illumination is brought to focus in the specimen by the objective lens, and laterally scanned using some form of scanning device under computer control. The sequences of points of light from the specimen are detected by a photomultiplier tube (PMT) through a pinhole (or in some cases, a slit), and the output from the PMT is built into an image and displayed by the computer. Although unstained specimens can be viewed using light reflected back from the specimen, they usually are labelled with one or more fluorescent probes.

3.10.6.1 Specimen Preparation and Imaging

The procedures for preparing and imaging specimens in the confocal microscope are largely derived from those that have been developed over many years for use with the conventional wide field microscope. In the biomedical sciences, a major application of confocal microscopy involves imaging either fixed or living cells and tissues that have usually been labelled with one or more fluorescent probes. A large number of fluorescent probes are available that, when incorporated in relatively simple protocols, specifically stain certain cellular organelles and structures. Among the plethora of available probes are dyes that label nuclei, the Golgi apparatus, the endoplasmic reticulum, and mitochondria, and also dyes such as fluorescently labelled phalloidins that target polymerized actin in cells. Regardless of the specimen preparation protocol employed, a primary benefit of the way in which confocal microscopy is carried out is the flexibility in image display and analysis that results from the simultaneous collection of multiple images, in digital form, into a computer.

3.10.6.2 Critical aspects of confocal microscopy

Quantitative three-dimensional imaging in fluorescence microscopy is often complicated by artefacts due to specimen preparation (*e.g.* autofluorescence problems, retractile structures presence, presence or absence of highly stained structures, immersion oil, coverslip thickness etc.), controllable and uncontrollable experimental variables or configuration problems with the microscope (*e.g.* optical component alignment, objective magnification, bleaching artefacts, aberrations, quantum efficiency, and the specimen embedding medium).

In our experimental conditions, the immunofluorescence experiments were assessed by confocal microscopy TSC SP2 Leica.

3.11 Inflammation

Inflammation is part of the complex biological response to the tissue damage or harmful stimuli, such as spinal cord injury. Involves immune cells, blood vessels, and molecular mediators the inflammatory reaction protects the remaining tissue, in order to eliminate the initial cause of cell injury, clear out necrotic cells and tissues damaged from the original insult and the inflammatory process, and to initiate tissue repair.

3.11.1 Neutrophils quantification

After 24 hours post injury, the animals were sacrificed, the spinal cord was placed into OCT and cut transversely into 10 µm thick sections. We proceed to neutrophils quantification not only at the level of trauma, but also rostrally and caudally, to determine the different levels of the inflammation in the mice treated with stem cells and placebo mice.

Consequently we prepared two solutions: the first one containing naphthol (Sigma) (14mg in 1 ml) dissolved in DMSO (Sigma) and Triton X-100 in 9: 1 ratio, and the second one, known as esaziotideparaseabilin, consisting of pararosalina 4% in 2M HCl and NaNO₂ in H₂O 2% mixed 1: 1. The second solution is diluted 1: 200 in 1X PBS for the negative control and in the concentration of 1: 100 in 1X PBS and Naphthol for the staining. The stained sections bone marrow were washed 2 times with 1X PBS for 5 'and subsequently were incubated with appropriate solutions for 1 h at RT. Then the tissue was washed with tap water for 10 'and with distilled water for another 10 '. Nuclei were stained with hematoxylin (Sigma-Aldrich) incubating the sections for 5'. The washing in the tap water was repeated for 15 ' more and the slide coverslip were mounted with 50% glycerol in PBS 1X. Neutrophils were counted in both groups of samples in the dorsal caudal and rostral level of the lesion, using light microscope with 40X magnification.

3.11.2 RNA extraction

3.11.2.1 Real-time RT-PCR analysis

For these experiments, cells were grown and differentiated in 25cm² Petri dishes as described before. Total RNA was isolated by using TRI Reagent® (SIGMA) in accordance with the manufacturer's instructions. In briefly, the procedure used was the following:

- Add 1 ml of TRI Reagent directly on the culture dish. After addition of the reagent, the cell lysate should be passed several times through a pipette to form a homogenous lysate.
- Phase Separation: To ensure complete dissociation of nucleoprotein complexes, allow samples to stand for 5 minutes at room temperature. Add 0.2 ml of chloroform per ml of TRI Reagent used. Cover the sample tightly, shake vigorously for 15 seconds, and allow to stand for 15 min at room temperature. Centrifuge the resulting mixture at 12,000 x g for 15 minutes at 4°C.

Centrifugation separates the mixture into 3 phases: a red organic phase (containing protein), an interphase (containing DNA), and a colourless upper aqueous phase (containing RNA).

- Transfer the aqueous phase to a fresh tube and add 0.5 ml of isopropanol per ml of TRI Reagent used in Sample Preparation and mix. Allow the sample to stand for 10 min at room temperature. Centrifuge at 12,000 x g for 10 min at 4°C. The RNA precipitate will form a pellet on the side and bottom of the tube.
- Remove the supernatant and wash the RNA pellet by adding 1 ml of 75% ethanol per 1 ml of TRI Reagent used in Sample Preparation. Vortex the sample and then centrifuge at 7,500 x g for 5 min at 4°C.
- Briefly dry the RNA pellet for 5–10 minutes by air-drying. Do not let the RNA pellet dry completely, as this will greatly decrease its solubility. Add an appropriate volume of 0.5% SDS water, or to the RNA pellet. To facilitate dissolution, mix by repeated pipetting with a micropipette at 55–60 °C for 10 min.

The RNA quality was verified by running it onto 1% agarose gel and the amount of RNA in the sample was quantified spectrophotometrically. The ratio between A260/A280 was calculated to verify RNA purity. 100 ng/sample was used for cDNA synthesis.

3.11.2.2 Degradation of genomic DNA and reverse transcription-PCR (RT-PCR)

The degradation of contaminating genomic DNA from RNA samples was performed with DNase I (RNase-free) (New England BioLabs) according to manufacturer's instructions. In brief, the procedure used was the following:

- Resuspend 1 µg RNA in 1X DNase I Reaction Buffer to a final volume of 10 µl.
- Add 1 unit of DNase I, mix thoroughly and incubate at 37°C for 10 min.
- Add 0.5 M EDTA to a final concentration of 5 mM. EDTA should be added to a final concentration of 5 mM to protect RNA from being degraded during enzyme inactivation.
- Heat inactivate at 75° C for 10 min. The synthesis of single-strand cDNA was carried out on 1 µg of RNA template, using iScript™ Reverse Transcription Supermix for RT-qPCR (BIO-RAD) following the manufacturer's instructions.

Component	Volume per reaction
5X iScript reverse transcription supermix	4 μ l
RNA template (1 μ g total RNA)	11 μ l
Nuclease-free water	5 μ l
Total volume	20 μ l

Reaction protocol:

Priming	5 min at 25°C
Reverse transcription	30 min at 42°C
RT inactivation	5 min at 85°C

Retrotranscription samples are stored at -20°C, until their use for real time RT-PCR.

3.11.2.3 Real Time RT-PCR

Real-time RT-PCR quantifies the initial amount of the template most specifically, sensitively and reproducibly, and is a preferable alternative to other forms of quantitative RT-PCR that detect the amount of final amplified product at the end-point (Freeman WM et al., 1999). Real-time PCR monitors the fluorescence emitted during the reaction as an indicator of amplicon production during each PCR cycle as opposed to the endpoint detection (Higuchi R et al., 1993), eliminating post-PCR processing of PCR products. This helps to increase throughput and to reduce the chances of carryover contamination. In comparison to conventional RT-PCR, real-time PCR also offers a much wider dynamic range of up to 10^7 -fold (compared to 1000-fold in conventional RT-PCR). The real-time PCR system is based on the detection and quantitation of a fluorescent report (Livak KJ et al., 1995). This signal increases in direct proportion to the amount of PCR product in a reaction. By recording the amount of fluorescence emission at each

cycle, it is possible to monitor the PCR reaction during exponential phase where the first significant increase in the amount of PCR product correlates to the initial amount of target template. The higher the starting copy number of the nucleic acid target, the sooner a significant increase in fluorescence is observed. Currently four different chemistries, TaqMan®, Molecular Beacons, Scorpions® and SYBR® Green (BIO-RAD), are available for real-time PCR. All of these chemistries allow detection of PCR products via the generation of a fluorescent signal.

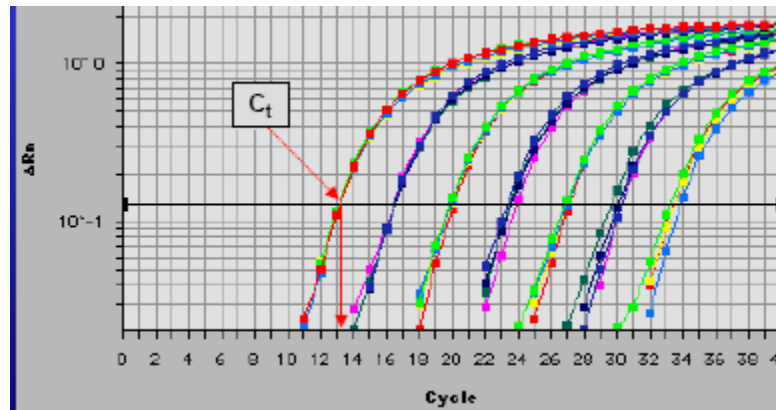


Fig.3.4 Real time PCR curves and Ct value

TaqMan probes, Molecular Beacons and Scorpions depend on Förster Resonance Energy Transfer (FRET) to generate the fluorescence signal via the coupling of a fluorogenic dye molecule and a quencher moiety to the same or different oligonucleotide substrates. SYBR Green is a fluorogenic dye that exhibits little fluorescence when in solution, but emits a strong fluorescent signal upon binding to double-stranded DNA. The threshold cycle or C_t value (Fig. 3.4) is the point when the system begins to detect the increase in the signal associated with an exponential growth of PCR product during the log-linear phase. This phase provides the most useful information about the reaction and the slope of the log-linear phase is a reflection of the amplification efficiency. The efficiency (Eff) of the reaction can be calculated by the formula: $\text{Eff} = 10^{(-1/\text{slope})} - 1$. The efficiency of the PCR should be 90 - 100% ($-3.6 > \text{slope} > -3.1$). A number of variables can affect the efficiency of the PCR. These include length of the amplicon, secondary structure and primer quality. The C_t is an important parameter for quantitation. The higher the initial amount of genomic DNA, the sooner accumulated product is detected in the PCR process, and the lower is the C_t value. The threshold should be placed above any baseline activity and within the exponential increase phase. Some software allows determination of the cycle threshold (C_t) by a mathematical analysis of the growth curve. This provides better runt-

run reproducibility. Two strategies are commonly employed to quantify the real-time RT-PCR data: the **standard curve method** (absolute quantification) and the **comparative C_t method** (relative quantification). In the **standard curve method**, a standard curve is first constructed from an RNA of known concentration. This curve is then used as a reference standard for extrapolating quantitative information for mRNA targets of unknown concentrations, thus generating absolute copy number data. In addition to RNA, other nucleic acid samples can be used to construct the standard curve, including purified plasmid dsDNA, in vitro generated ssDNA or any cDNA sample expressing the target gene. Spectrophotometric measurements at 260 nm can be used to assess the concentration of these DNAs, which can then be converted to a copy number value based on the molecular weight of the sample used. However, cDNA plasmids are the preferred standards for standard curve quantitation. The **comparative C_t method** involves comparing the C_t values of the samples of interest with a control or calibrator such as a non-treated sample or RNA from normal tissue. The C_t values of both the calibrator and the samples of interest are normalized to an appropriate endogenous housekeeping gene. The comparative C_t method is also known as the $2^{-\Delta\Delta C_t}$ method (Livak KJ et al., 2001), where $\Delta\Delta C_t = \Delta C_{t,\text{sample}} - \Delta C_{t,\text{reference}}$. $\Delta C_{t,\text{sample}}$ is the C_t value for any sample normalized to the endogenous housekeeping gene and $\Delta C_{t,\text{reference}}$ is the C_t value for the calibrator also normalized to the endogenous housekeeping gene. For the $\Delta\Delta C_t$ calculation to be valid, the amplification efficiencies of the target and the endogenous reference must be approximately equal. This can be established by looking at how ΔC_t varies with template dilution. If the plot of cDNA dilution versus delta C_t is close to zero, it implies that the efficiencies of the target and housekeeping genes are very similar. This quantification method is described in the Applied Biosystems User Bulletins #2 and #5. Relative gene expression comparisons work best when the expression of the chosen internal control is abundant and remains constant among the samples. By using an invariant endogenous control as an active reference, quantitation of an mRNA target can be normalised for differences in the amount of total RNA added to each reaction. For this purpose, the most common choices are 18S RNA, GAPDH (glyceraldehyde-3-phosphate dehydrogenase) and β -actin. Real-time PCR requires an instrumentation platform that consists of a thermal cycler, a computer, optics for fluorescence excitation and emission collection, data acquisition, and analysis software. These machines, available from several manufacturers, differ in sample capacity (some are 96-well standard format, others process fewer samples or require specialized glass capillary tubes), method of excitation (some use lasers, others broad spectrum light sources with tuneable filters), and overall sensitivity. In our experimental conditions, Real-time PCR was performed in an MJ Opticon 2 using iQTM SYBR Green supermix (BIO-RAD) following the

manufacturer's instructions. 18S rRNA was used as reference housekeeping gene for normalization. We performed an analysis using the $\Delta\Delta C_t$, this procedure can be used since we have determined previously that the replication efficiencies (slopes of the calibration or standard curves) for the genes of interest and housekeeping gene are very close. All the amplification reactions were performed in duplicate. The primers were designed using Oligo Perfect® Designer Software (INVITROGEN).

The nucleotide sequences of the primers for spinal cord injury were:

Gene Name	Forward primer	Reverse primer
GAPDH	CGACTTCAACAGCAACTCCCCTCTCC	TGGGTGGTCCAGGGTTTCTTACTCCTT
BDNF	CATTACCTTCCTGCATCTGTTGG	CGTGGACGTTTACTTCTTTTCATGG
IL-6	GACAACCACGGCCTTCCCTAC	CGTTGTTCATACAATCAGAATTGCC
NGF	TGGGCCCAATAAAGGTTTTGCC	TGGGCTTCAGGGACAGAGTCTCC
TNFα	TCTATGGCCCAGACCCTCACAC	CAGCCACTCCAGCTGCTCCTC
MIP2	ACGCCCCCAGGACCCCACTG	GGACAGCAGCCCAGGCTCCTCC
LIF	AACGTGGAAAAGCTATGTGCG	GCGACCATCCGATACAGCTC

The nucleotide sequences of the primers for Parkinson disease were:

Gene Name	Forward primer	Reverse primer
18S	TTTCGGAAGTGGCCATGATTAAG	AGTTTCAGCTTTGCAACCATACTCC
IL15	CCATCTCGTGCTACTTGTGTTTCCTTCTAA	GAAAGCAGTTCATTGCAGTAACTTTGCAAC
IL-6	TCCAGTTGCCTTCTTGGGACTGATGCTGGT	AGTTTCAGATTGTTTTCTGCAAGTGCATCA
IL1α	ATGGCCAAAGTTCCTGACTTGTGTTGAAGAC	GTTGCTTGACGTTGCTGATACTGTCACCCG
TNF-α	GACGTGGAAGTGGCAGAAGAGGCACTCCC	GAGGCCATTTGGGAACTTCTCATCCCTTTG
NGF	CTCAGCAGGAAGGCTACAAGA	TACAGGCTGAGGTAGGGAGG
BDNF	ACTACCAAAGCCACAAGGCA	GCTGATCCTCATGCCAGTCA

3.11.2.4 Real Time RT-PCR conditions

Amplification reactions were performed in 96-well standard plate. Each sample was analysed in duplicate. Reaction mix for all primers was prepared adding 2 µl of cDNA sample (dilution 1:10) to the following mix:

- 1.2 µl of primer forward (10 µM)
- 1.2 µl of primer reverse (10 µM)
- 10.6 µl of Dnase and Rnase free water
- 15 µl of 2X iQ™ SYBR Green supermix

Amplification conditions were:

• 95°C for 10 min	40 cycles
• 95°C for 15 sec	
• 60°C for 30 sec	1 cycle
• 75°C for 30 sec	

3.12 Statistical Analysis

Data are expressed as means \pm SEM. The two-way analysis of variance (Anova) and Bonferroni's post-test were applied using Prism 5 software (GraphPad Software Inc, La Jolla, USA) assuming a p value less than 0.05 as the limit of significance.

3.13 Determination of dopamine and metabolites in Parkinson's disease

For dopamine and its metabolites analysis it has been followed the protocol described by Vaglini and co-workers (28). Briefly, the striatal tissue samples were homogenized in 600 µL ice-cold 0.1 N perchloric acid containing 10 pg/ILdihydroxybenzylamine (DBA) as the internal standard; an aliquot of homogenate was assayed for protein. The homogenates were centrifuged and the levels of monoamines and their metabolites in the supernatant were determined by reverse-phase HPLC coupled to an electrochemical detector. One liter of mobile phase contained 10.35 g (75 mM) sodium dihydrogen orthophosphate, 0,505 g (2,5 mM) heptan sulfonic acid, 25 mM EDTA,

100 μ L triethylamine and 200 mL acetonitrile, adjusted to a final pH of 3,00 with phosphoric acid. A C18 inertsil ODS-3, 4.6 \cdot 250 mm, 5- μ m, reverse-phase column was used (Beckman, San Ramon, CA, USA). The mobile phase (filtered and degassed) was delivered at a flow rate of 1.2 mL/min; the applied potential was set to -0.10 V (detector 1) and $+0.30$ V (detector 2). For catecholamine assays, a standard curve was prepared using known amounts of DA and metabolites dissolved in 0.1 N perchloric acid containing a constant amount (10 μ g/mL) of the internal standard (DBA) used for tissue samples. The standard curve for each compound (DA or its metabolite) was calculated using regression analysis of the ratios of the peak areas (compound area/DBA area) for various concentrations of each compound recorded at the reducing electrode. An analogous regression analysis was performed for the oxidizing electrode. For DA and its metabolites, results are expressed as the mean \pm SD of at least 5 animals per group.

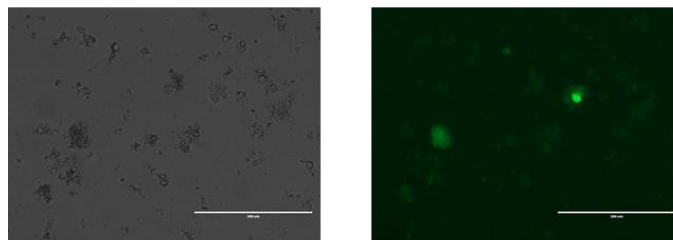
4. Results

4.1 Derivation of GFP positive Post-Mortem Neural Precursor Cells and Characterization of their Self-Renewal capability

Adult C57BL/6-Tg (UBC-GFP) 30Scha/J or CD1 mice were softly anesthetized and killed by cervical dislocation. The cadavers were maintained at room temperature (25°C) for 6 hours, and after this period the animals were decapitated and their brains were removed, the neural precursors were extracted (see Materiali and Methods) from the area including the SVZ surrounding the lateral wall of the forebrain ventricle. PM-NPCs expressing green fluorescent protein (GFP PM-NPCs) (Fig. 4.1A) proliferate in response to the exposure to hFGF and bEGF, and formed typical neurospheres similar to those formed by NPCs and PM-NPCs obtained from CD1 mice (Marfia, 2011) (Fig. 4.1B).

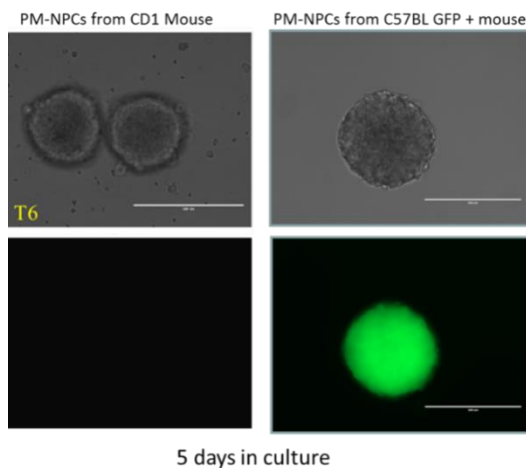
A

PM-NPCs from C57BL GFP + mouse



48 hours after isolation

B



5 days in culture

Figure 4.1. GFP positive PM-NPCs are able to form neurospheres.

Undifferentiated post mortem neural precursors cells isolated from the Sub Ventricular Zone (SVZ) of adult mice that constitutively expresses the green fluorescent protein (GFP) proliferate in response to growth factors (EGF and FGF-2) and form neurospheres. (A) Pictures were taken 48 after cells isolation. Scale bars 200 μm . (B) Picture were taken 5 days post in culture Scale bars 100 μm .

To assess for self-renewal, individual primary spheres were mechanically dissociated, and cells were plated in growth medium at the density of 3000 cells/cm² in 500 μ l. The number of neurospheres formed by GFP-positive PM-NPCs was $169 \pm 7,63$ /well and was similar to the number of spheres formed by both classical neural stem cells (NPCs) and post mortem neural precursors cells from CD1 mice (Marfia, 2011)(Fig. 4.2). This assay was performed at passage 7, 15 and 30 without observing any significant difference.

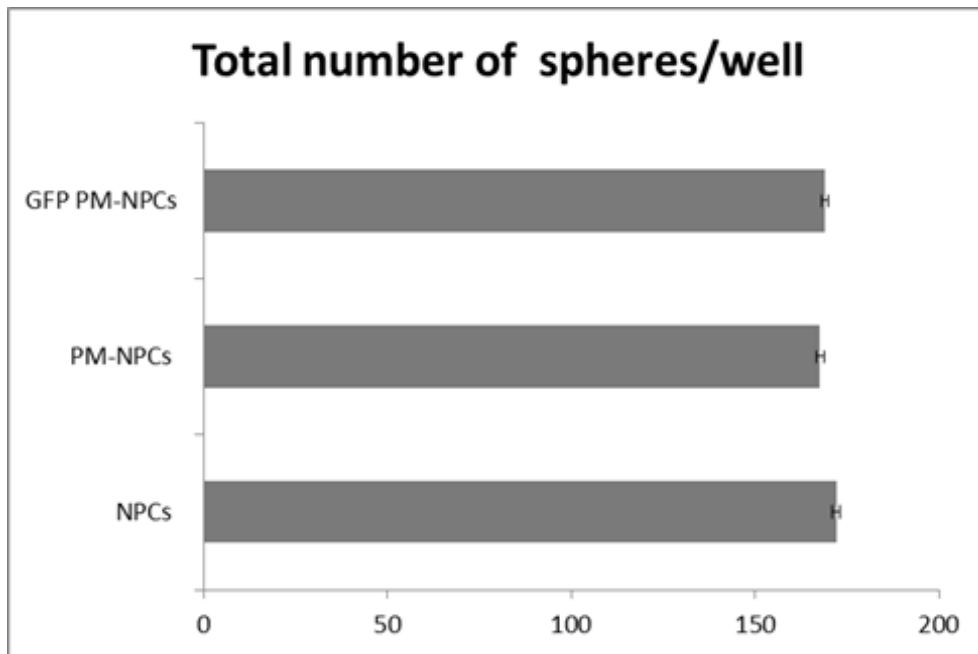


Figure 4.2. Neurosphere assay.

PM-NPCs population analysis was performed by counting the number of neurospheres generated after 10 days of culture. Classical neural stem cells from SVZ of adult CD1 mouse (NPCs; Gritti, 1996), post mortem neural precursors cells from SVZ of adult CD1 mouse (PM-NPCs, Marfia, 2011) and post mortem neural precursors cells from Adult C57BL/6-Tg(UBC-GFP)30Scha/J mouse (GFP+ PM-NPCs) were cultured in the presence of bEGF, and hFGF. The number of spheres formed in each well was counted after 7–12 days. It is represented the number of neurospheres generated by 3000 cells plated in a single well. The experiment was performed three times in triplicate for each cell sources and was repeated at passage 7, 15 and 30 without observing significant differences. Data are expressed as the mean of three independent experiments with similar results \pm standard error.

4.2 Differentiation features of GFP positive PM-NPCs

GFP PM-NPCs were differentiated to assess for multipotency. Neurospheres were mechanically dissociated and cells to the concentration of 1×10^4 cells/cm² were seeded onto Matrigel®-coated glass coverslips (12 mm diameter) in a medium with bFGF and without hEGF. After 48 h cultures were shifted to a differentiation medium containing 1% (FBS) (Invitrogen). PM-NPCs attach to the dish and begin the differentiation process into neurons, astrocytes, and oligodendrocytes, after removal of growth factors and addition of serum and adhesion molecules. 7 and 15 days after differentiation induction the extent of the differentiation was evaluated by monitoring the number of cells expressing MAP-2, GFAP, and NG2 antigens (Fig. 4.3A and C). The quantification of neuronal-like differentiation after 7 days is shown in panel B of the same figure. MAP-2 positive neurons were $39,3 \pm 0,77$ %; GFAP (astrocytes) and NG2 (oligodendrocyte precursors) -positive cells were $60,9 \pm 2,81$ and $12,86 \pm 0,48$ respectively. The extent of the GFP PM-NPCs differentiation confirmed that these precursors cells have similar features of that previously obtained (Marfia, 2011).

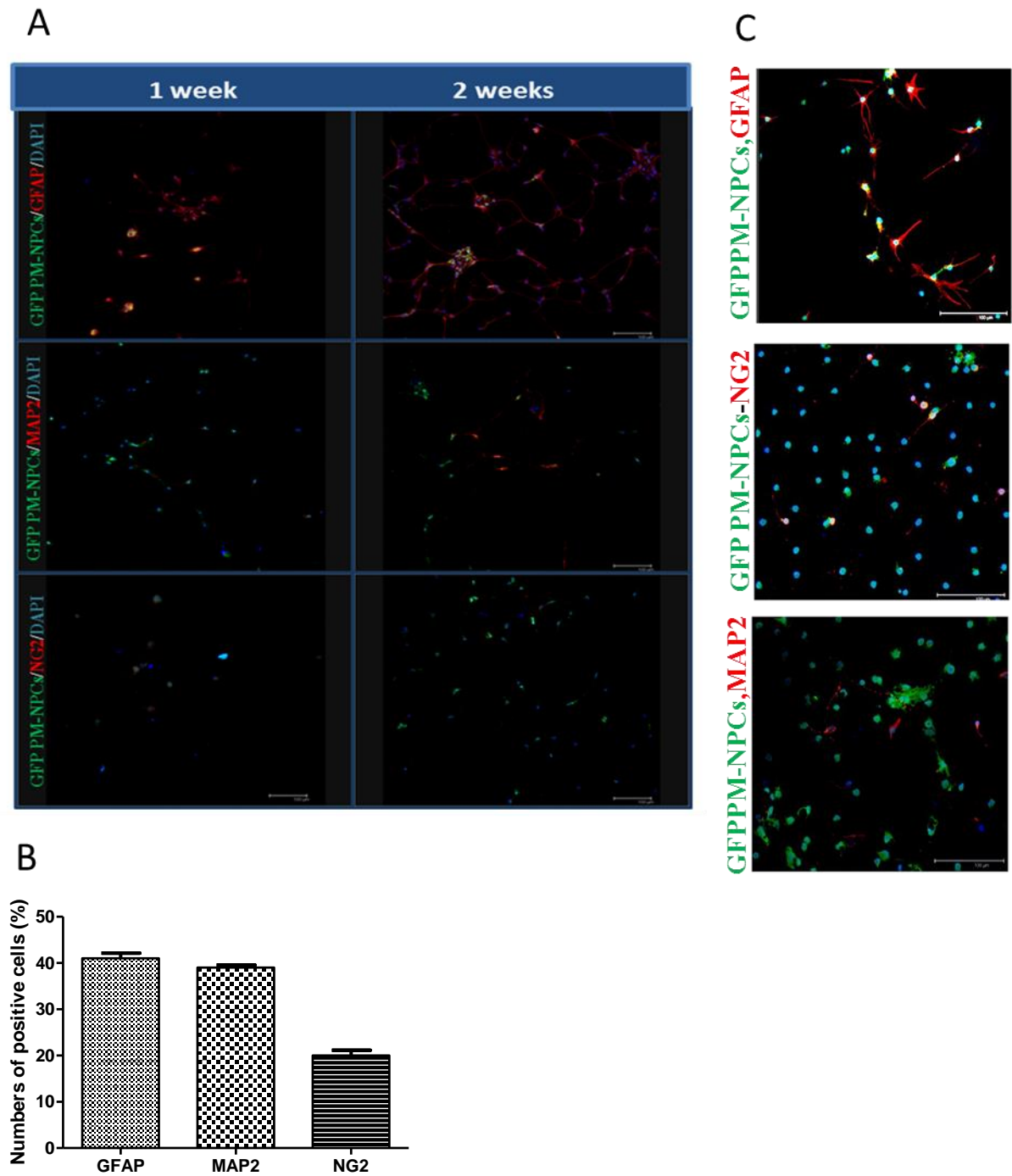


Figure 4.3. Neural marker expression after differentiation. After removal of growth factors, PM-NPCs neurospheres readily differentiates into MAP2 positive neurons, NG2 labelled oligodendrocytes precursors and astrocytes (GFAP). Staining with specific markers is showed in red. Nuclei are stained in blue with DAPI. Bars are 100 μ m(A).A magnified is represented on the right of the figure (C) Quantification was performed by counting the number of cells positive for the staining. Positivity was expressed as a percent of the total cells. The quantification indicates that about 40 % of PM-NPCs differentiates into neurons. Data are expressed as the mean of three independent experiments with similar results \pm SEM(B).

4.3 GFP PM-NPCs neurospheres features before transplantation.

As control, before transplantation was investigated the expression of Microtubule-Associated Protein 2 (MAP2) by immunocytochemistry assay in GFP PM-NPCs neurospheres. MAP2 is important to determine and stabilize dendritic shape during neuron development.

As showed in figure 4.4 by immunocytochemistry the GFP PM-NPCs neurospheres before transplantation do not express Map2 (Fig. 4.4A) but, as expected, are positive to the staining with Nestin (stem cell marker) (Fig. 4.4B)

A

B

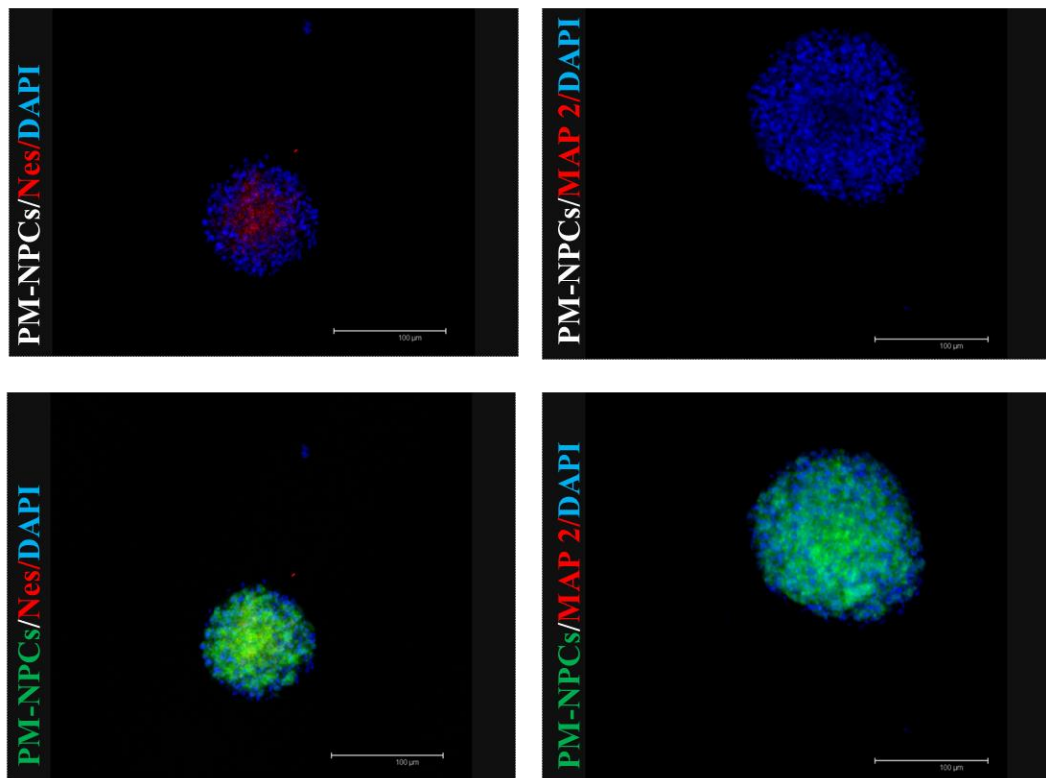


Figure 4.4. PM-NPCs do not express MAP2.

PM-NPCs endogenously express green fluorescent protein and for that reason are showed in green. The labelling for nestin (A) and microtubule association protein 2 (MAP2;B) are showed in red. Nuclei were stained with DAPI and are showed in blue. The experiment was performed in duplicate with similar results and the picture showed here are representative. Scale bars are 100 microns.

4.4 PM-NPCs transplanted in Spinal Cord Injury

4.4.1 PM-NPCs Improve Recovery of Hind Limb Function

PBS-treated mice have a transient loss of ability in hind limb function caused by the 70 Kdyne traumatic impact to the mice cord. This initial loss of hind limb movement followed by a progressive gradual recovery reaching the maximum in 2-3 weeks (3.20 ± 0.08 points of the BMS scale; $n = 15$) (Fig. 4.5). After these weeks animals reach a recovery corresponding to plantar placing of the paw with or without weight support or occasional, frequent, or consistent dorsal stepping, but not plantar stepping (Basso, 2006).

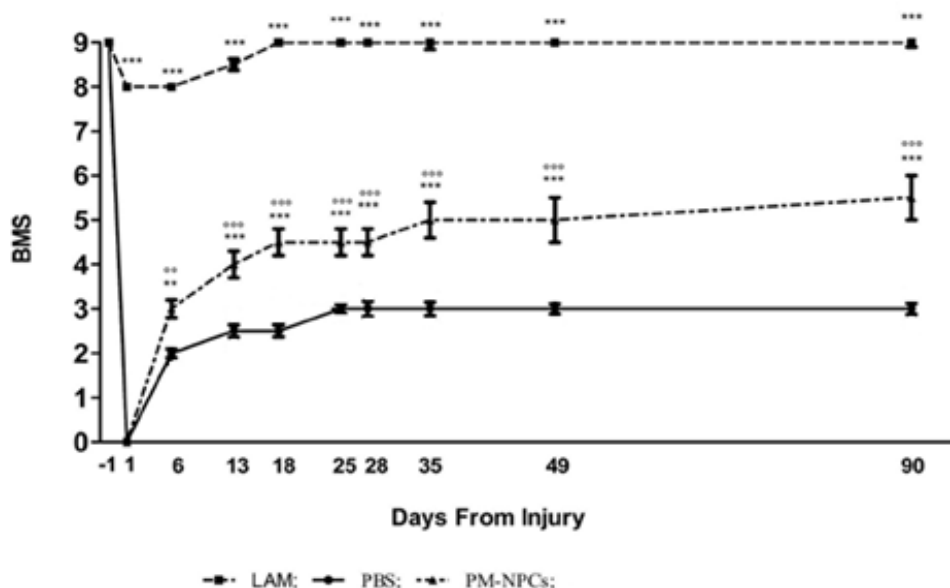


Figure 4.5. PM-NPCs Improve Recovery of Hind-Limb Function.

The open field locomotion was the test employed for the determination of motor function recovery, the score is determined according to the Basso Mouse Scale (Basso, 2006). The experimental animals, tested the day prior to the injury, scored 9 points in the BMS scale (see in Materials and Methods), then the score fell to 0 following SCI and gradually recovered thereafter. The recovery of hind limb function of lesioned mice showed a remarkable and long lasting improvement when animals treated with PM-NPCs. The groups were randomized, the analysis was performed in double blind fashion, and 15 animals composed each group. Values represent average \pm SEM. We determined the statistical differences by means of ANOVA test followed by Tukey's post-test. *** $P < 0.001$; ** $P < 0.01$ vs Saline; °°° $P < 0.001$; °° $P < 0.01$ vs CTRL.

After transplant of PM-NPCs in the injured mice the recovery was earlier and reached a higher recovery extent up to 5.14 ± 0.06 at d 28, corresponding to frequent or consistent plantar stepping without coordination, or frequent or consistent plantar stepping with some coordination (see Materials and Methods). The behavioral improvement was particularly evident between days 7 and 14 after SCI, and then it kept steadily improving up to 90 days (Fig. 4.5). Throughout the observational period no signs of allodynia-like forelimb hypersensitivity (Hoffstetter, 2005) were recorded in any experimental group.

4.4.2 PM-NPCs-mediated tissue sparing

Thirty days after lesioning tissue sparing at lesion site was analyzed by means of quantitative analysis (see Materials and Methods) following thionin staining. The post-traumatic tissue loss is far more evident in the cord of PBS-treated lesioned mice (Fig. 4.6A), than in the cord of the animals treated with PM-NPCs (Fig. 4.6B). This result is confirmed by the quantitative analysis (Fig. 4.6C).

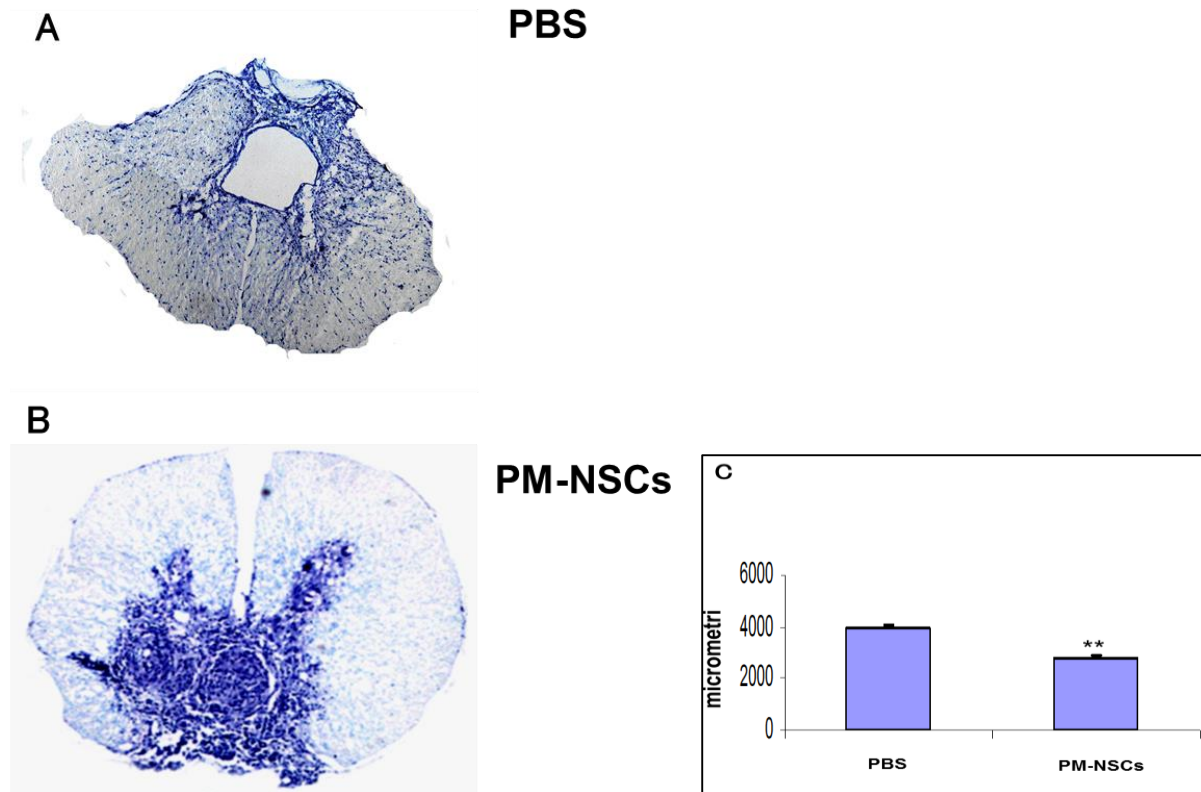


Figure 4.6. PM-NPCs-Mediated Reduction of Post-Traumatic Injury.

Morphology preservation was qualitatively and quantitatively analyzed by means of thionin staining. For qualitative analyses serial cross (T9 level) and longitudinal-sections of spinal cord injury after 30 days from injury were acquired from animals treated with PM-NPCs or PBS. The quantitative analyses of tissue preservation after traumatic injury was performed considering cross sections for at least seven animals for each group and calculating the length of lesion extension. PM-NPCs determine a significant reduction of lesion length through the lesion site compared with PBS treated group. Values represent average \pm SEM; ** $P < 0.01$ vs PBS.

Ten months after lesioning, *in vivo* NMR analysis was performed in saline and cell-treated animals. In Figure 4.7 is shown that spinal tissue in the animals treated with PM-NPCs was preserved. The T2-weighted RARE images show that the spinal cord matter become very thin at the injury site surrounded by a very high hyperintense signal in saline treated mice. This effect is probably due to spinal liquor filling the empty space left by the reduced size of the surviving cord. Spinal cord shrinkage at lesion site and liquor accumulation is a constant finding in all chronically-lesioned untreated animals (Fig. 4.7).

Differently, the spinal cord matter of the PM-NPCs transplanted animals, is rather well preserved at site of injury even 10 months later and the hyperintensive signal is far less intense than in saline-treated animals (Fig. 4.7), it can be observed that the protective effect of the cells is maintained chronically. The reduced tissue loss is likely due to tissue sparing.

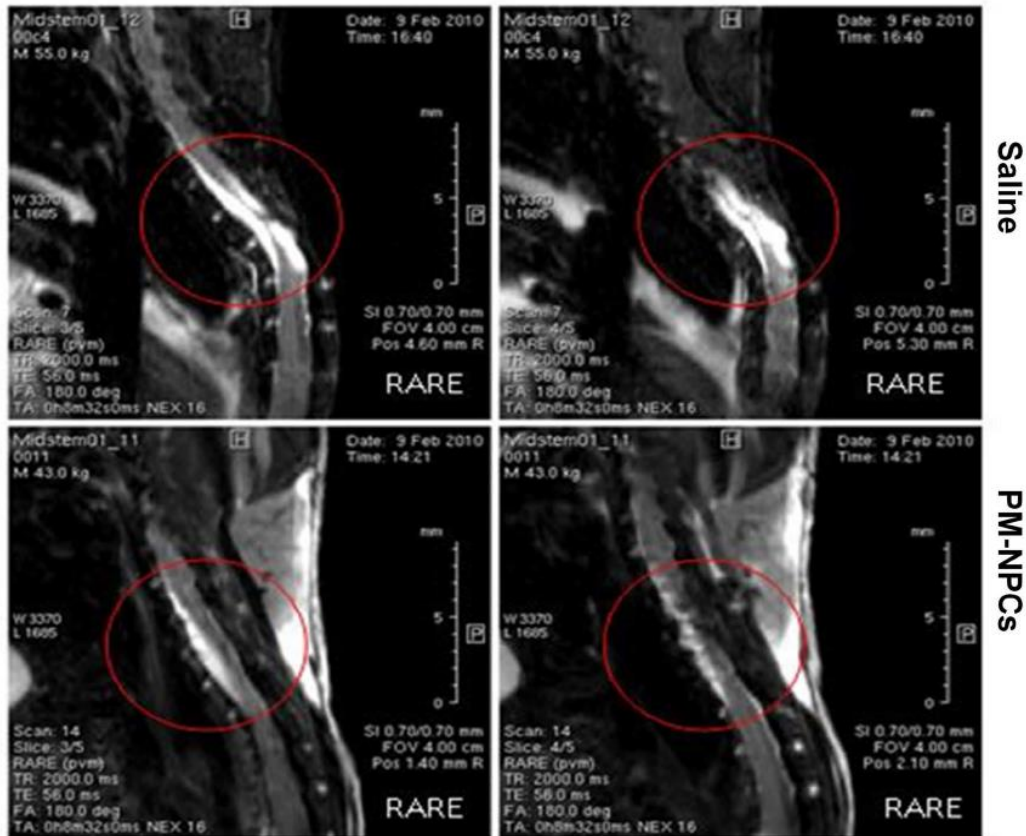


Figure 4.7. In Vivo MRI 10 Months After Spinal Cord Injury.

RARE sequences obtained at 10 months after injury and cells transplantation by means of a 7 tesla NMR (Bruker). It is shown a significantly better parenchymal preservation in PM-NPCs treated animals, while there is only a thin residual tract in saline-treated mice that is accompanied by a major liquor accumulation. The images are representative for 2 mice, but similar images were obtained for at least 4 animals per group.

The reticulospinal tract is an important pathway in eliciting locomotion, by electrophysiological studies it was shown its function in the coordination of rhythmic stepping movements (Bellerman, 2006; Mori, 1998). The preservation of myelin in the reticulospinal tract that descends through the ipsilateral dorso- and ventro-lateral funiculi was studied by means of

FluoroMyelin™ staining followed by confocal quantitative analysis as detailed in Material and Methods (Vitellaro-Zuccarello, 2007; Vitellaro-Zuccarello, 2008). Myelin preservation was quantified 30 days after lesioning, sections were taken at the center of lesion and 2 mm caudally to the lesion site. Only intact myelin was assessed, and the rubble of degenerated myelin was obviously not considered. Inproximityof the lesion, the trauma caused almost 50% loss of myelin and about 70% more caudally. The application of PM-NPCs reduced themyelin loss inremarkable and highly significant manner inbothevaluationpoint, lesion site and caudally. (Figure 4.8).

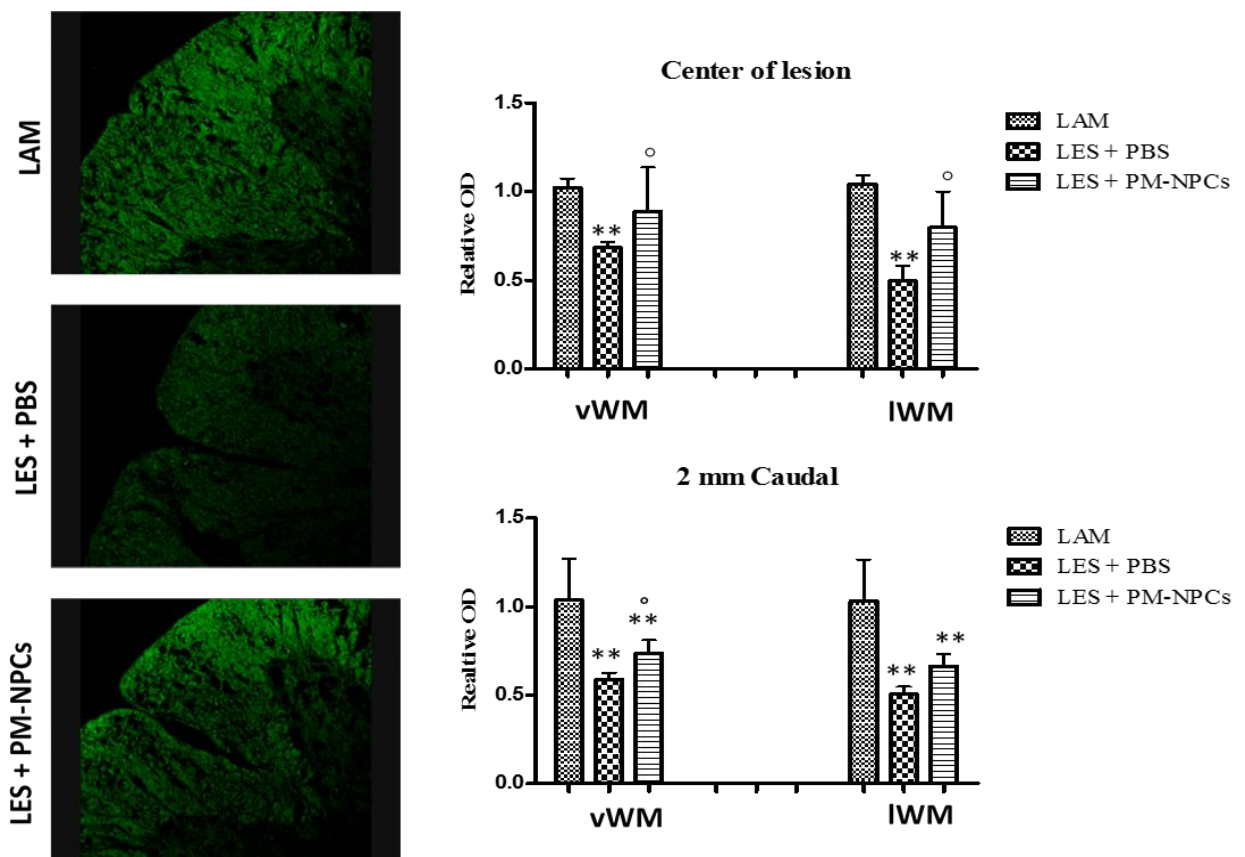


Figure 4.8. Sparing of Myelin in the Injured Cord

The images and the relative quantification show the protective action of PM-NPCs on the myelin tracts in the injured cord. Myelin was quantified by means of Fluoromyelin™ staining (green) performed in sections at the lesion epicenter and 2 mm caudally to the lesion site through quantitative confocal analysis of ventral and lateral white matter as indicated in the graphs. The confocal microscope images for the laminectomy, saline and PM-NPCs-treated mice were obtained using the same intensity, pinhole, wavelength and thickness of the acquisition. As reference we used sections close to the ones analyzed and not treated with fluoromyelin. For the quantification we considered sections from at least six animal per group. Values represent average \pm SEM. We determined the statistical differences by means of ANOVA test followed by Tukey's post-test. $^{\circ\circ}$, $^{***}P < 0.001$; $^{\circ}$, $^{**}P < 0.05$; $^{\circ}$, $^{*}P < 0.01$.

Figure 4.9 show that near the PM-NPCs cluster the post injury reaction of GFAP cellular profiles was markedly reduced. The quantification confirmed that GFAP positive cells were reduced in the site where PM-NPCs are located (Fig. 4.9A) respect the other part of the lesioned cord (Fig. 4.9B). None of the transplanted cells PM-NPCs differentiated into GFAP positive cells different to the in vitro results where about 40-50% of the cells differentiate in oligodendrocytes.

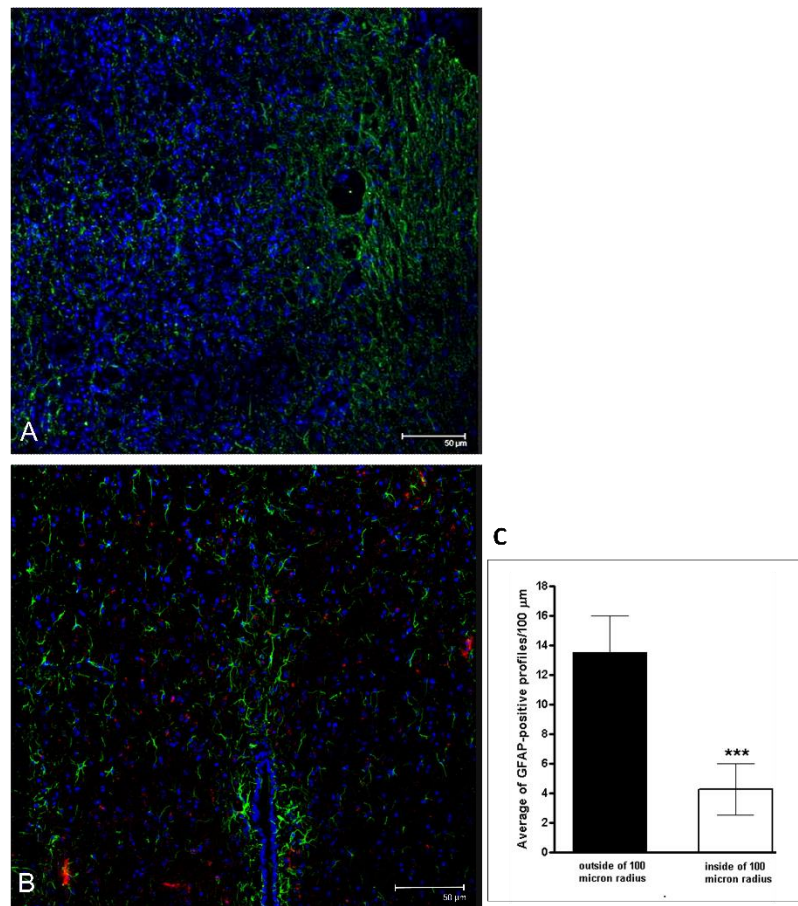


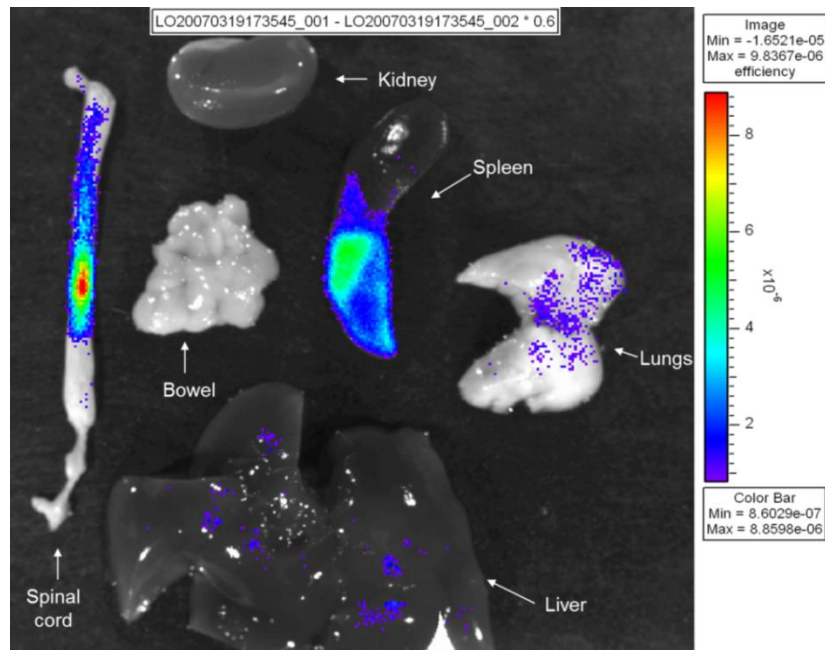
Figure 4.9. GFAP Immunoreactive-Positive Profiles 30 Days after Lesioning

PM-NPCs reduce the extent of gliosis in their microenvironment in the injured cord. Sections were taken at 1 mm caudally to the lesion site from cords of PBS (A) and PM-NPCs-treated (B) mice. Quantification of GFAP-positive profiles (green) in a 100 μm radius around PKH26-labeled PM-NPCs clusters (C). GFAP staining is showed in green and PKH26 labeled PM-NPCs are showed in red. Values represent average ± SEM. ***P < 0.001 vs Saline.

4.4.3 PM-NPCs Homing to Site of Injury, Survival, and Differentiation

PKH26- labeled PM-NPCs transplanted mice were killed after 48 h and CCD camera analysis was performed to isolated following organs: spinal cord, kidney, bowel, spleen, lungs and liver. PM-NPCs were distributed mainly at the center of the lesion site; Figure 4.10 shows a highest detected fluorescence peak in this region, only a smaller positivity was observed in the spleen (Fig. 4.10A). Figure 4.10B shown the comparison of spinal cords from PM-NPCs- and saline-treated where it is can possible to observe a higher and specific signal of fluorescence correlated with the presence of transplanted cells in the former, and the absence of specific signal in the latter. Four weeks after injury, we have also serially sectioned seven cords of treated mice, and detected PKH26- or GFP-positive PM-NPCs by means of confocal microscopy at the edge of the lesion. Total number of positive cells was 260.000 ± 45.000 per cord, that is 100 fold higher than surviving ES cells as reported previously and 10 fold higher than adult NSCs (Bottai et al, 2010; Bottai et al, 2008).

A



B

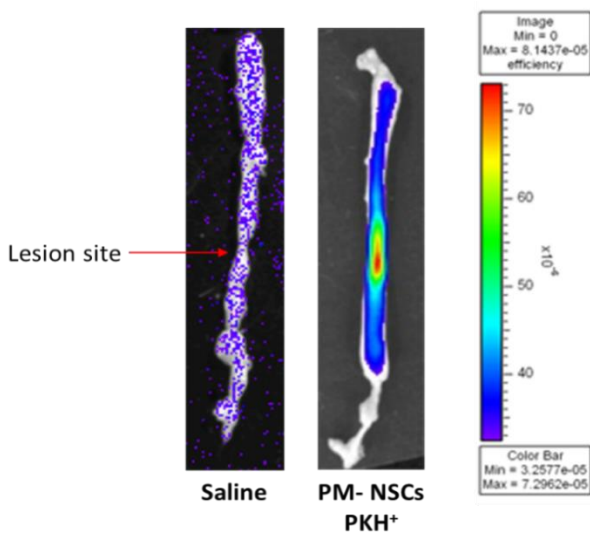


Figure 4.10. Organ distribution of i.v. administered PM-NPCs

PKH26 labeled PM-NPCs distribution 48 hours after injection was investigated by means of CCD camera. Animals were killed and spinal cords and organs extracted and acquired to investigate organ distribution of PM-NPCs. (A) The picture shows the high accumulation of the labeled cells at the lesion site and a lower signal in the spleen. (B) Comparison of spinal cord fluorescence of PM-NPC injected mice and saline-treated animals showed a high fluorescent signal relative to the presence of labeled transplanted cells only in the animals treated with PM-NPCs. Pictures are referred to one PM-NPCs treated mouse, we observed very similar results in at least other six animals.

Most engrafted PM-NPCs accumulated at the edges of the lesion (Fig. 4.11, 4.12, 4.13), where formed clusters since the early days of their administration, then the clusters dispersed along the lesion edges and transplanted cells differentiate assuming gradually the asymmetric cellular conformation of neurons. At one week after lesioning and transplantation small PM-NPCs are grouped along the irregular margins of the lesion and almost 50% of the cells are already positive for MAP-2 and ChAT (Figures 4.11, 4.13).

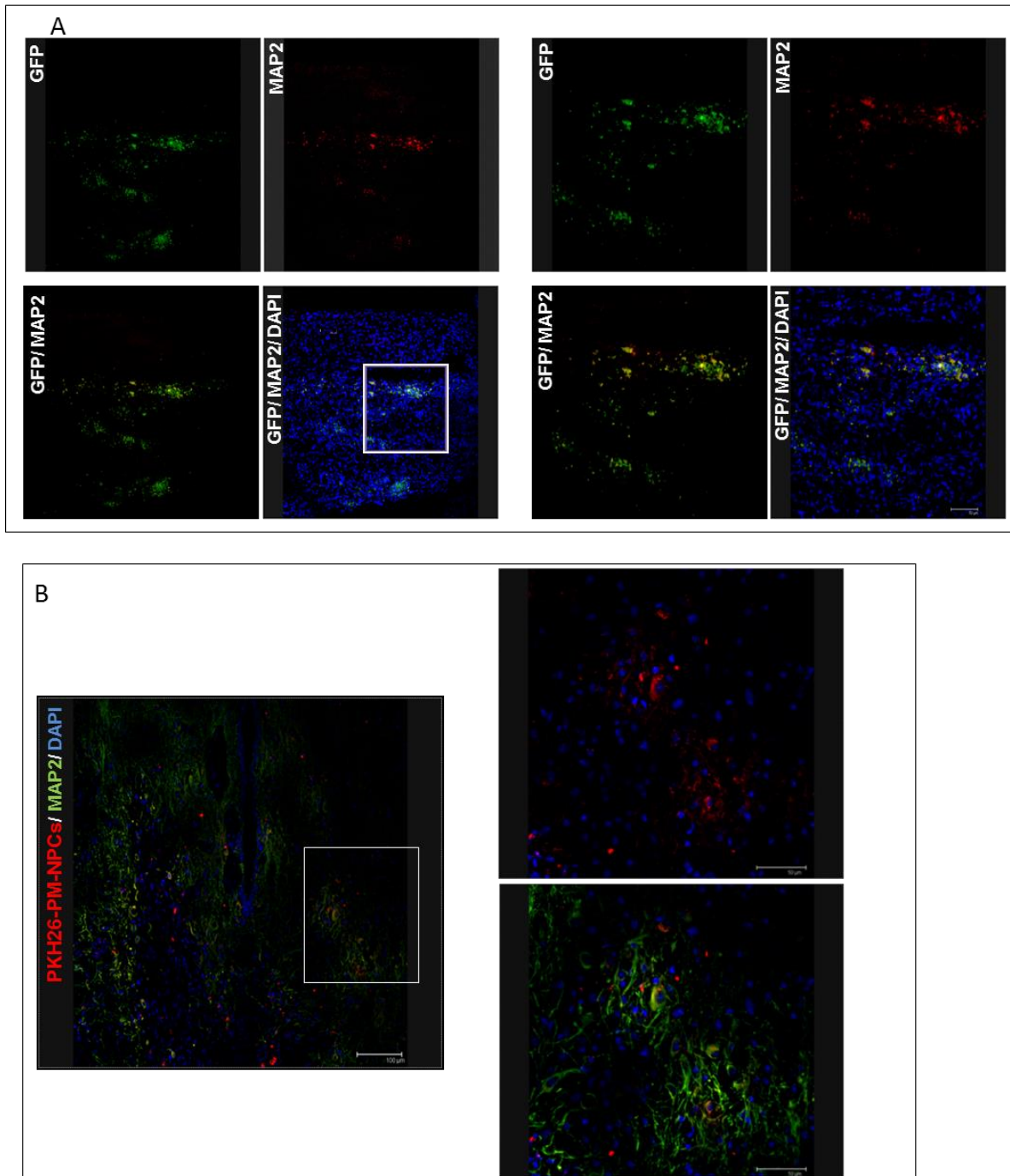


Figure 4.11. PM-NPCs MAP2 trans-differentiation in lesioned cords

GFP-labeled PM-NPCs (A) are clustered at the edges of lesion site at 7 days after their i.v. supplementation to the injured mice, some of them have differentiated in MAP2 positive cells (Bar = 100 μm). A magnified detail is represented on the right side of the figure (Bar = 50 μm). (B) PKH-labelled PM-NPCs (red) are present throughout the edges of lesion site at 60 days after their i.v. supplementation to spinal cord injured mice. Most of them have differentiated in MAP2 positive cells (green; Bar = 100 μm). A magnified detail is represented on the right side of the figure (Bar = 50 μm). Most PKH-labeled PM-NPCs have acquired a neuronal-like shape with dendritic-like processes that intermingle with those of local spinal neurons that survived the lesion. Together they form a rich neuropil. All labeled cells have one nucleus. Nuclei are stained in blue (DAPI).

Analyzing the section of spinal cord transplanted animals at days 30 and 60 after lesioning we can observe that the cell body of PM-NPCS increases in size and most cells extend dendritic like processes that are fully immunostained by the specific antibodies to MAP-2 and β -tubulin III (Figures 4.11, 4.12).

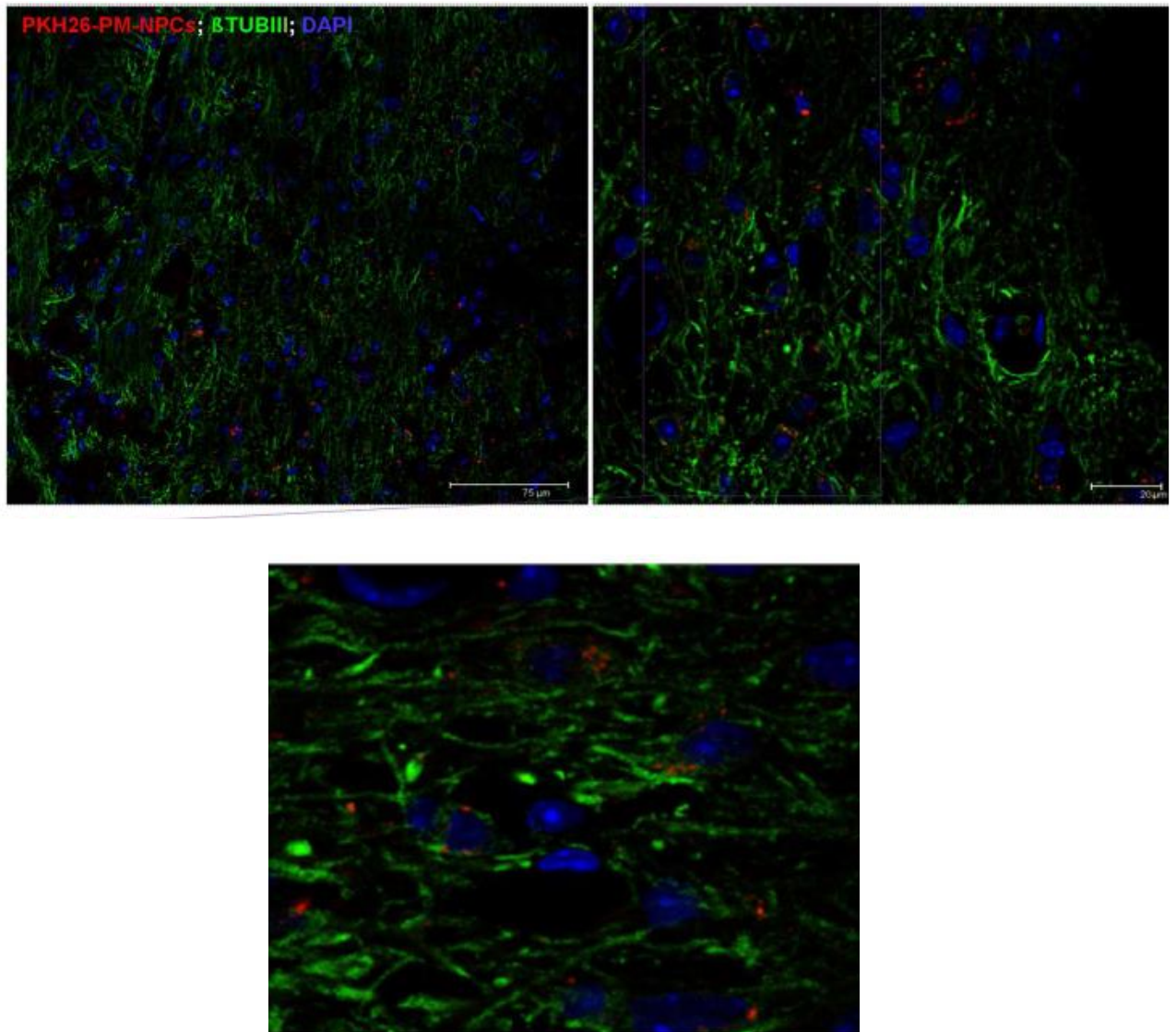


Figure 4.12. β -Tubulin III Expression by PM-NPCs at the Edges of the Lesion

Pictures representing the edges of the lesion at 60 days after i.v. supplementation of PKH26-labeled PM-NPCs. The preparation was immunostained for β tubulin III. Several PM-NPCs are present among the surviving neural profiles, practically all PKH26-labeled cells are positive for β -tubulin III. We show two fields at different magnification (bar = 75 or 20 μ m), and a detailed enlargement that shows clearly how each labeled cell has one nucleus and bears profiles positive for β -tubulin III.

Immunohistochemical staining for Choline-AcetylTransferase (ChAT) revealed that most transplanted PM-NPCs are positive for this enzyme (ChAT), and that the positivity with time is present also in the cellular dendritic-like processes (Fig. 4.13). Such a differentiation into cholinergic neural cells in vivo confirms the earlier in vitro observations (Marfia, 2011).

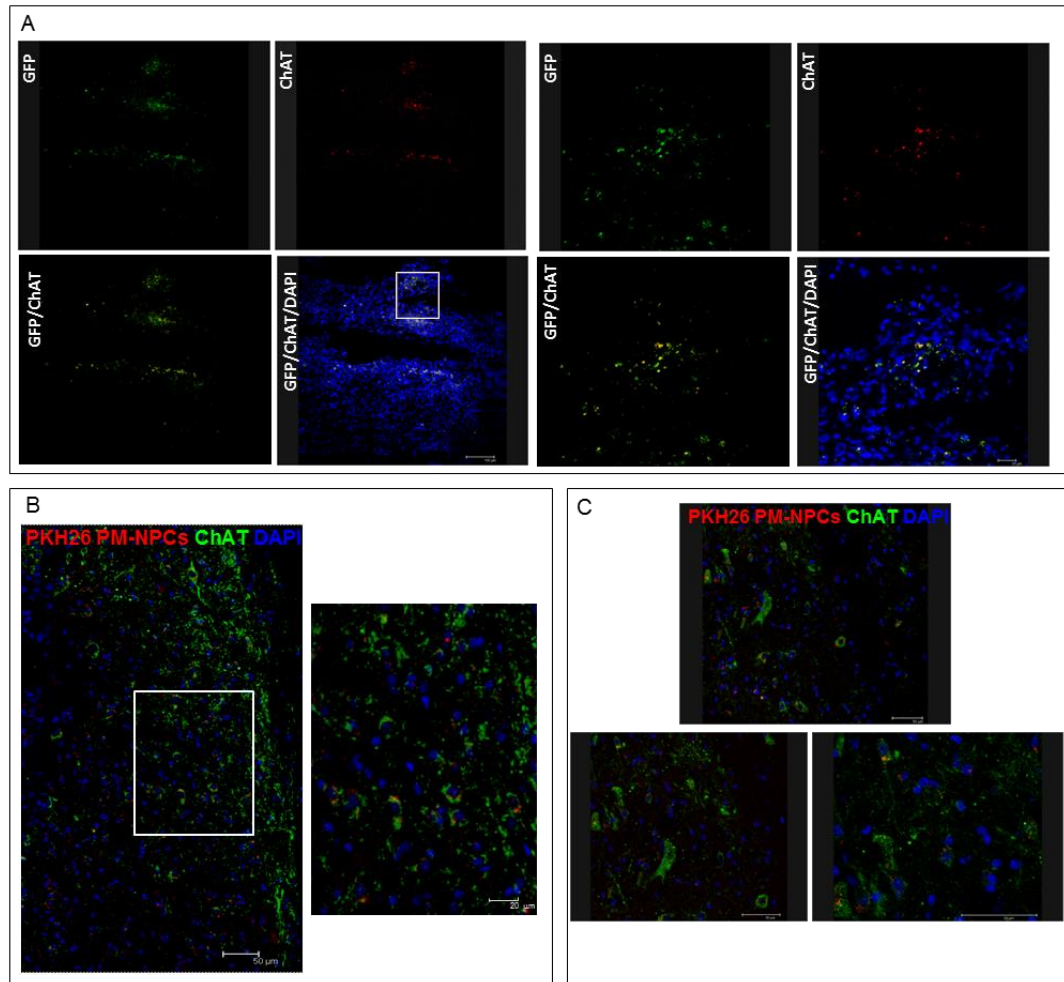


Figure 4.13. PM-NPCs transplanted cells differentiate into cholinergic neurons

(A). Some GFP-labeled PM-NPCs clustered at the edges of the lesion at 7 days after their i.v. administration. Several PM-NPCs are positively immunostained for Choline Acetyl Transferase (ChAT; red). The pictures (bar = 100 μ m) are enlarged in the right part of the panel (bar = 20 μ m). (B) Several PKH26-labelled PM-NPCs (red) are accumulated at the edges of the lesion 30 days after their i.v. administration. Most PM-NPCs are positive for ChAT immunostaining (green) as shown clearly in the enlargement on the right side. ChAT stain is dotted and in most cases perinuclear, although some positive processes are evident (bar = 75 and 20 μ m), (C) PKH26-labeled PM-NPCs clustered at the edge of the lesion 60 days after their administration. All PM-NPCs are positive for ChAT immunostaining as clearly shown by the two consecutive enlargements (bar = 50 μ m). The labeling is now diffused throughout the neuron-like cell bodies and in the cellular processes.

The achievement of morphological complexity and the positivity to ChAT, MAP2, and β -tubulin III by transplanted PM-NPCs is not likely due to fusion with surviving host spinal cord neurons (Figs. 4.11, 4.12, 4.13), this is evident by their clear different morphology and the absence of two nuclei in any single labeled cell. The quantification of such differentiation is shown in Table I, performed on spinal cords 60 days after lesioning and PM-NPCs transplantation.

Markers	% of PM-NPCs Positively Labeled
β -Tubulin III	94.2 \pm 5.1
MAP2	87 \pm 4.5
ChAT	78.5 \pm 3.7

For the quantification we considered at least four fields per marker.
Values represent average \pm SEM.

Table 1. Percentage of transplanted PM-NPCs positive for neuronal markers 60 days after intravenous administration.

4.4.4 PM-NPCs-Mediated chemokine and growth factor expression in the injured cord

Some additional effects of PM-NPCs was suggested by the action of these cells in promoting the recovery of function, therefore, we have assayed the production of neurotrophic factors and inflammatory cytokines that represent the major targets of pharmacological agents aimed at repair in neurodegenerative disorders. The mRNA levels of six different factors was quantitatively evaluated (Fig. 4.14), these factor are nerve growth factor (NGF); tumor necrosis factor α (TNF α); interleukin-6 (IL-6); MIP-2; and leukemia inhibitory factor (LIF). The animals treated with Saline or PM-NPCs was compared. As controls, we assayed the chemokines in the T9 region of the spinal cord of both uninjured and laminectomized animals. As expected in the lesioned animals cord all the assayed chemokines were increased. We observed that MIP 2 expression is diminished by PM-NPCs at 48 hours and 1 week after lesioning; differently IL-6, TNF α , NGF and LIF are reduced at the earlier time, but significantly increased at 1 week compared to saline treated mice. BDNF was increased by PM-NPCs in lesioned mice only at 48 hours (Fig. 4.14).

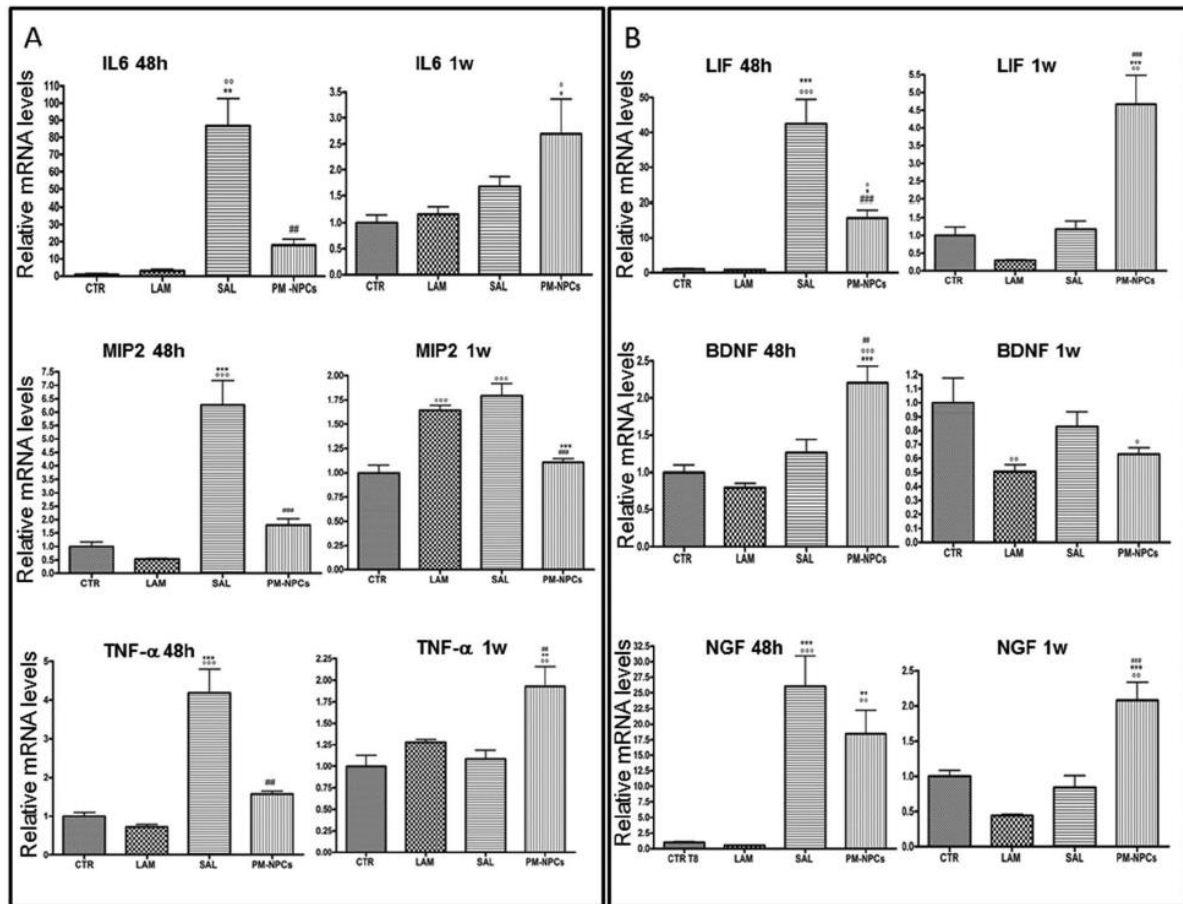


Figure 4.14. PM-NPCs transplanted cells affect local expression of cytokines.

Expression of cytokines mRNA was evaluated by real time RT-PCR. Each group was composed of six mice, and we performed three quantitative (Q)-RT-PCRs in each experiment, we run a duplicate per each sample and a parallel PCR for the gene of interest and the reference gene Glyceraldehyde-3-Phosphate Dehydrogenase. Values represent average \pm SEM. ***, $^{\circ\circ}$, ### $P < 0.001$; $^{\circ\circ}$, **, ## $P < 0.01$; $^{\circ}$, *, # $P < 0.05$; * vs Control (CTRL); $^{\circ}$ vs LAM; # vs Saline

4.4.5 Inflammatory Cell Migration to the Lesion Site

The invasion of the lesioned spinal cord by neutrophils and macrophages was counteracted by the administration of PM-NPCs. Two days after lesioning, neutrophils infiltration was investigated at the site of injury by means of Leder stain throughout the lesion site. As reported previously neutrophils decrease with time (Bottai, 2008). In the better preserved tissue the number of neutrophils is reduced, and the preventive effect PM-NPC is quantitatively very significant (Fig. 4.15).

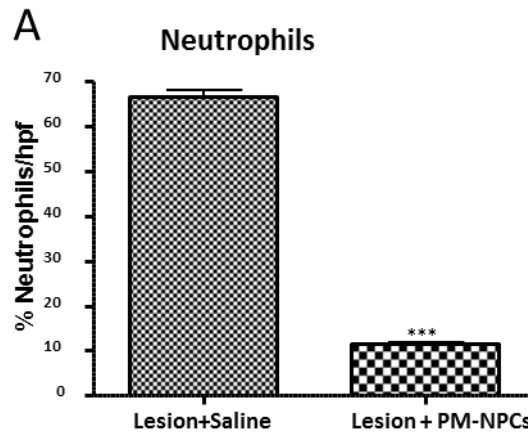


Figure 4.15. Tissue infiltration by neutrophils.

Neutrophil infiltration was quantitatively assessed at lesion epicenter 48 h after lesioning by means of the naphthol AS-D chloroacetate (Sigma-Aldrich) technique for esterase. Results are expressed as number of neutrophils per HPF. The presence of transplanted PM-NPCs greatly reduced the invasion by neutrophils. For the quantification, we considered sections from at least six animals per group. Values represent average \pm SEM. *** $p < 0.001$ versus saline.

Figure 4.16 shown the effect of the transplanted cells monitoring the number of ED-1-positive cells (macrophages) in the site of lesion and rostrally one week after injury. Both qualitatively and quantitatively the counteracting action of PM-NPCs is evident and significant.

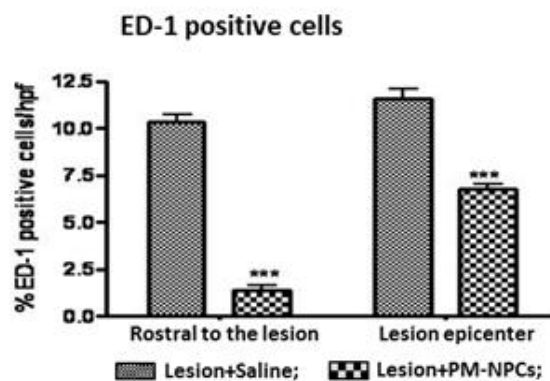


Figure 4.16. Tissue infiltration by macrophages.

Coronal cryostat section of cord lesion epicenter and cord 0.4 mm rostral to the lesion were stained for ED-1, and the number of positive cells was quantitatively evaluated as described in Materials and Methods. Results are expressed as the number of ED-1-positive cells per HPF. For the quantification, we considered sections from at least six animals per group. Values represent average \pm SEM. *** $p < 0.001$ versus saline

4.4.6 PM-NPCs promote neural markers expression in recipient injured spinal cord

Previously was reported that PM-NPCS have a specific distribution reaching at high prevalence the lesion site in the spinal cord. At 30 days after lesion and transplantation, PM-NPCs were still alive and are localized at the lesion site. At this observation time, PM-NPCs cell bodies resulted with a more structured morphology characterized by the presence of dendritic-like processes (Fig. 4.18). This is particularly evident with the immunohistochemical staining for Choline-AcetylTransferase (ChAT) (Fig. 4.17) and MAP-2 and β -tubulin III (Fig. 4.18). Figure 1 reveals that at 30 days after transplantation 75 ± 9.35 percent of transplanted PM-NPCs were positive for ChAT. ChAT immunoreactivity is dotted and in most cases perinuclear, although some positive processes are evident

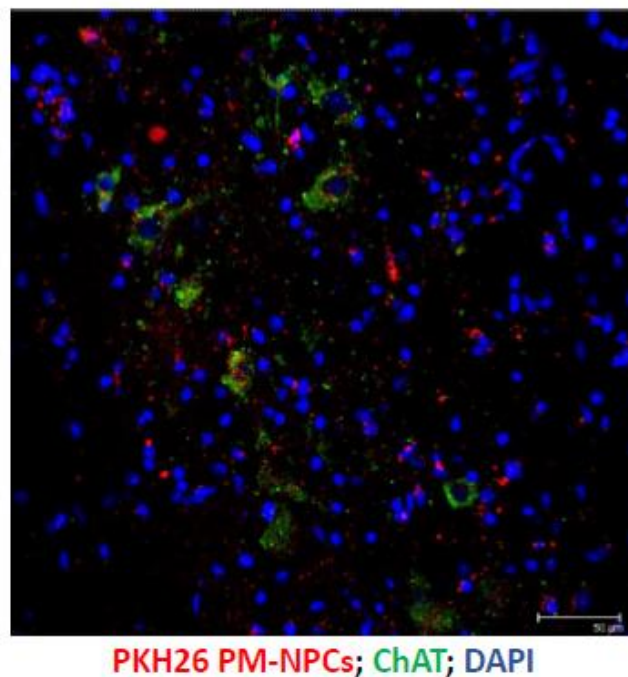


Figure 4.17. PM-NPCs transplanted cells differentiate into cholinergic neurons.

At 30 days after i.v. injection, several PKH26-labeled PM-NPCs (red) were accumulated at the edges of the lesion. Most PM-NPCs were positive for ChAT immunostaining (green) (Scale bar = 50 μ m).

Moreover, transplanted PM-NPCs accumulate at the irregular margins of the lesion and almost 50% of the cells were already positive for MAP-2 and β -tubulin III (Fig. 4.18). This suggests

that transplanted neural precursors attempt to form contacts with the near microenvironment of the host tissue. The quantification of MAP-2 and β -tubulin III staining performed both at distal end (Rostral and caudal) and at the lesion site shows that higher expression of neuronal markers are determined in PM-NPCs treated animals (Fig. 4.18).

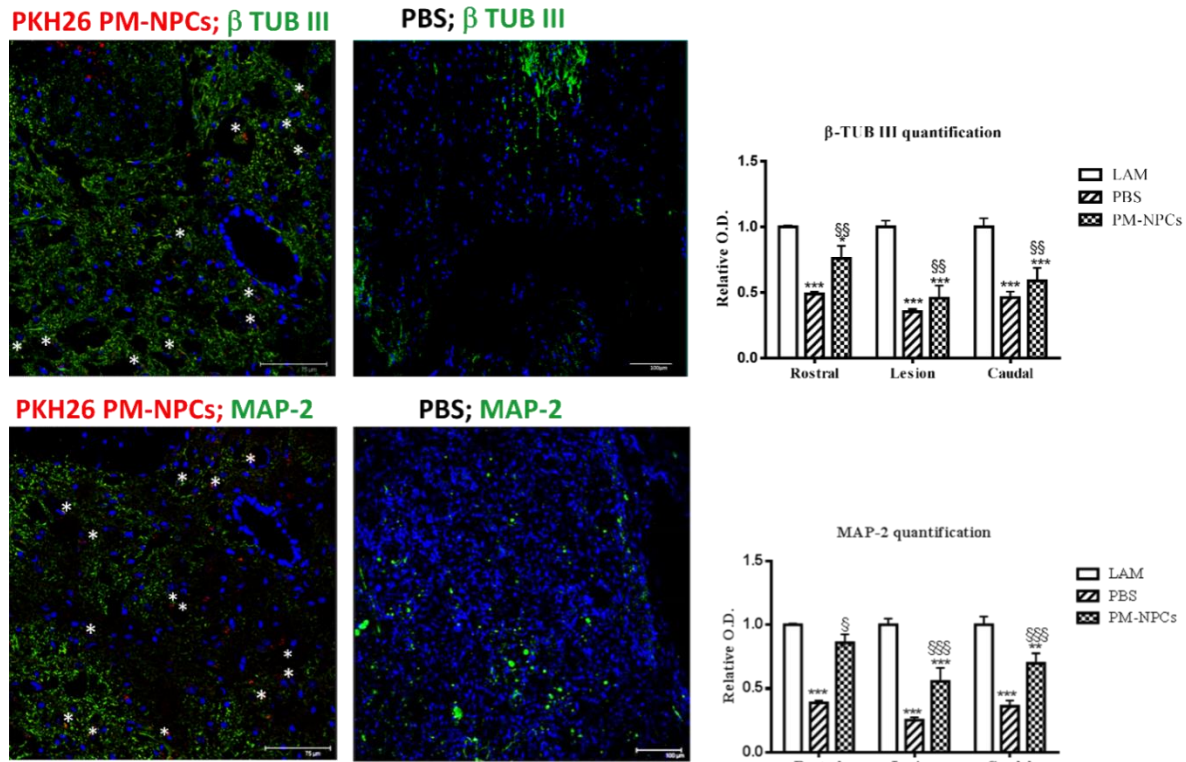


Figure 4.18. PM-NPCs transplantation improves neuronal markers expression in injured spinal cord.

Pictures represent the edges of the lesion at 30 days after i.v. administration of PKH26 – labeled PM-NPCs. Coronal sections of the tissue were immune stained for β tubulin III and MAP-2 (showed in green). PKH26-labeled cells were positive for β -tubulin III and MAP-2 (white stars) (Scale bar=75 and 100 μ m). Immunoreactivity was quantified in sections taken at the lesion epicenter, 1 mm rostral and caudal to the lesion site through quantitative confocal analysis. The confocal microscope images for Laminectomy (LAM), PBS, and PM-NPCs-treated mice were obtained using the same intensity, pinhole, wavelength and thickness of the acquisition. As reference, we used sections close to the ones analyzed. In negative control the primary antibodies were omitted and replaced with equivalent concentrations of unrelated IgG of the same subclass. Values represent average \pm SD. We determined the statistical differences by means of ANOVA test followed by Tukey's post-test. *** $p < 0.001$ vs LAM; \$\$ $p < 0.01$ vs PBS.

4.4.7 Monoaminergic fibers in the injured cord

Both the above findings and our prior ones (Carelli, 2014 and 2015) suggest that injection of PM-NPCs promotes axonal regeneration after SCI. We therefore searched for the identification of mechanisms that could contribute to the functional improvements. Since serotonin (5-HT) can

regulate the CPG and facilitate locomotion (Liu, 2009), we examined the 5-HT immunoreactivity rostral, within, and caudal to the lesion in CD-1 mice comparing the PM-NPCs, PBS and control groups.

Figure 4.19 shows the 5-HT immunoreactivity both in the lesion epicenter (Fig. 4.19A) and distally (2 mm rostral or caudal from the lesion site; Figure 4.19B). Serotonin (5-HT)-positive fibers (green) are present also caudally to the lesion. The quantification, performed 4 weeks after lesioning, shows that labeling is only about 20 % of LAM values in intermediate-lateral gray matter and ventral horns of PBS injected animals. Differently, the extent of 5-HT innervation is more than doubled when lesioned animals were treated with PM-NPCs (Fig. 4.19).

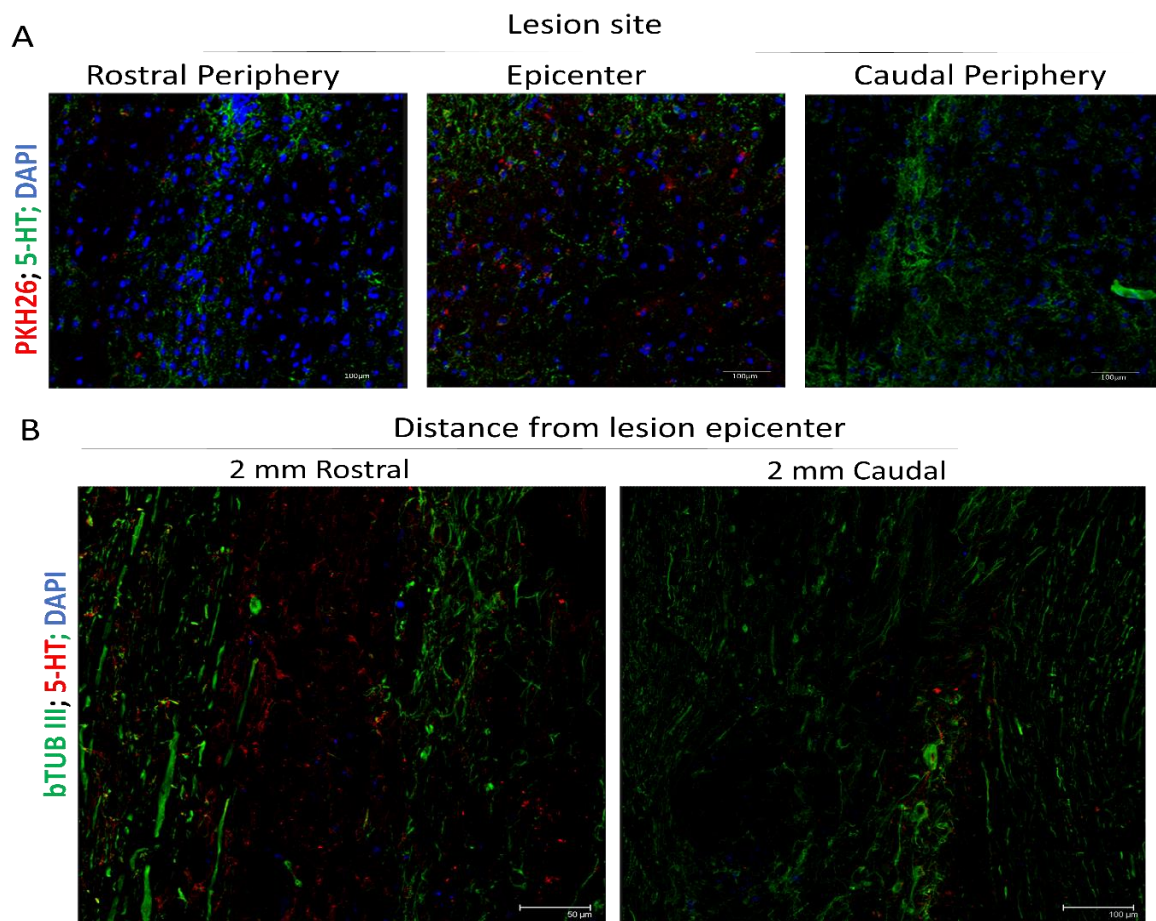


Figure 4.19. PM-NPCs promote serotonergic fibers sprouting through the lesion site

Serotonergic (5-HT) fibers were investigated at the lesion site (panel A) and 2 mm away from the lesion (panel B) 4 weeks after PM-NPCs infusion in lesioned mice. In panel A, PM-NPCs are shown in red and 5-HT is shown in green. Nuclei were counterstained with DAPI (blue). In panel B, 5-HT staining is shown in red and neuronal fibers were identified with beta-tubulin

A comparable analysis was conducted also for Tyrosine Hydroxilase (TH)-positive fibers (red) of the intermediate-lateral gray matter and ventral horn areas caudally to the lesion (Fig. 4.20 and Fig. 4.21).

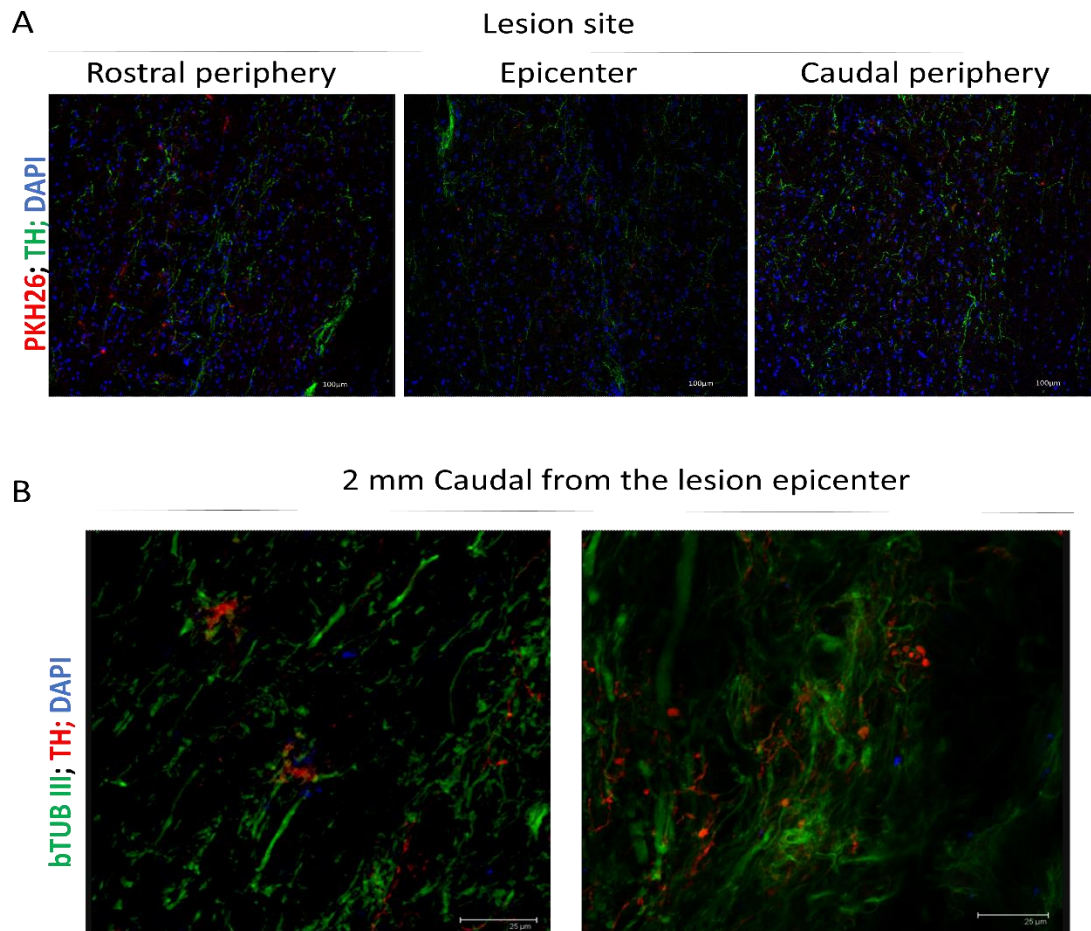
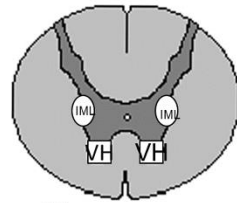


Figure 4.20. PM-NPCs promote Tyrosine Hydroxilase (TH)-positive fibers sprouting through the lesion site

Tyrosine Hydroxilase (TH)-positive fibers were investigated at the lesion site (panel A) and 2 mm caudal from the lesion (panel B) 4 weeks after PM-NPCs infusion in lesioned mice. In panel A, PM-NPCs are showed in red and TH is showed in green. Nuclei were counterstained with DAPI (blue). In panel B, TH terminals are showed in red and neuronal fibers were identified with beta-tubulin III (green). Nuclei were counterstained with DAPI (blue). Scale bars = 25 μm.

In saline treated animals, the loss of TH-positive fibers was significant but quantitatively not as large as we observed for 5-HT. TH-positive innervation of these areas was quantitatively similar to healthy animals when lesioned animals were treated with PM-NPCs (Fig. 4.21). Thus transplantation of PM-NPCs promotes sparing and perhaps regrowth of monoaminergic fibers in the distal portions of the traumatically injured cord.



VH= ventral horns; IML= intermediolateral

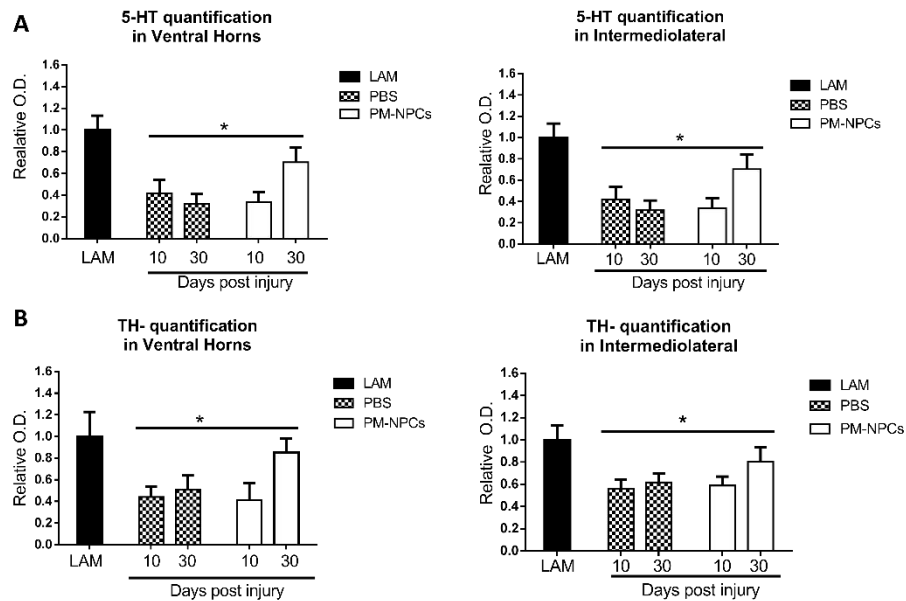


Figure 4.21. Quantification of serotonergic and Tyrosine Hydroxylase (TH) immunoreactivity.

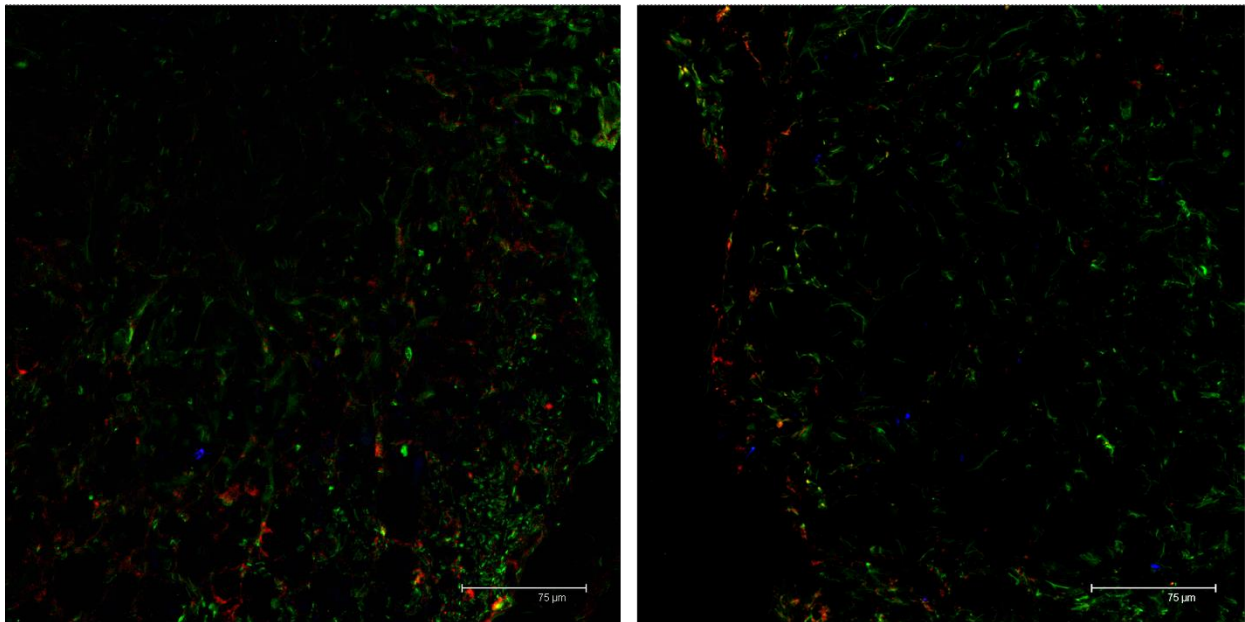
Serotonergic (5-HT) and Tyrosine Hydroxylase (TH) fibers quantification was performed at 4 weeks after PM-NPC transplantation in lesioned animals. The quantification was performed in spinal cord coronal sections ($n=3$ for each animal; at least 3 animal per group) as described in detail in M&M section in intermedio-lateral and ventral horns (please see the representation). Values represent average \pm SD. We determined the statistical differences by means of an ANOVA test followed by Bonferroni's post-test. *** $p < 0.001$ vs PBS; °°° $p < 0.001$, °° $p < 0.01$, ° $p < 0.05$ vs LAM.

4.4.8 PM-NPCs treatment results in increased expression of GAP-43

Growth-associated protein 43 (GAP43) it is expressed at high levels in neuronal growth cones during development, during axonal regeneration and it is considered a well-known marker of neurite outgrowth (Skene, 1986). To corroborate the above evidences on PM-NPCs stimulation of neurons regeneration, cryostat sections of spinal cord of cells injected animals, taken at 2 mm from the lesion epicenter, were examined for the GAP-43 expression at 30 days after cells injection (Fig. 4.22). The immunoreactivity of GAP-43 was especially noticeable in bundles

positive to staining with beta-tubulin III and GAP-43 staining resulted near the PM-NPCs localization (Hoechst).

2 mm from the lesion epicenter



GAP43/b TUB III/PM-NPCs (Hoechst+)

Figure 4.22. GAP43 expression in PM-NPCS transplanted cord.

Qualitative picture of GAP43 expression investigated 2 mm away (rostral and caudal) from the cord lesion site of lesioned animals transplanted with PM-NPCs. GAP 43 is showed in red and neuronal fibres were detected with beta-tubulin III staining (green). In order to perform double staining in these experiments PM-NPCs were labelled with Hoechst (blue). Scale bars = 75 μ m. Pictures are representative of at least three different immunostaining experiments.

4.4.9 Enhanced axonal sparing/regeneration by PM-NPCs

To evaluate anterograde axonal sparing/regeneration twenty days after injury fluororuby was injected rostrally at T6/T7 level (Fig. 4.23, 4.24 and 4.25) and animals were sacrificed 5 day later (25 days after PM-NPCs infusion). Fluororuby was picked up by intact axons and transported caudally (Fig. 4.24). The extent of dorsal tract labeling is high at the point of injection then it gradually decreases. Axonal fluororuby labeling is practically absent at the lesion site (Fig. 4.25 and 4.24) in saline-treated mice, while a significant fluorescence can be detected across and

caudally to the lesion in PM-NPCs treated lesioned mice (Fig. 4.23, 4.25 and 4.24). The detail of lesion epicenter is reported in Figure 4.23. The labeling is also higher rostral to the lesion suggesting a powerful axonal sparing by PM-NPCs (Fig. 4.23 and 4.24). The quantification fluorescence labeling at the lesion site (Fig. 4.25) shows that PM-NPCs-treated animals show 10 fold more labeled axonal profiles than in saline-treated. In addition, it can be noted that the number of labeled profiles decreases moving from injection site to the lesion in saline-treated animals, while it remains almost resistant in PM-NPCs treated mice.

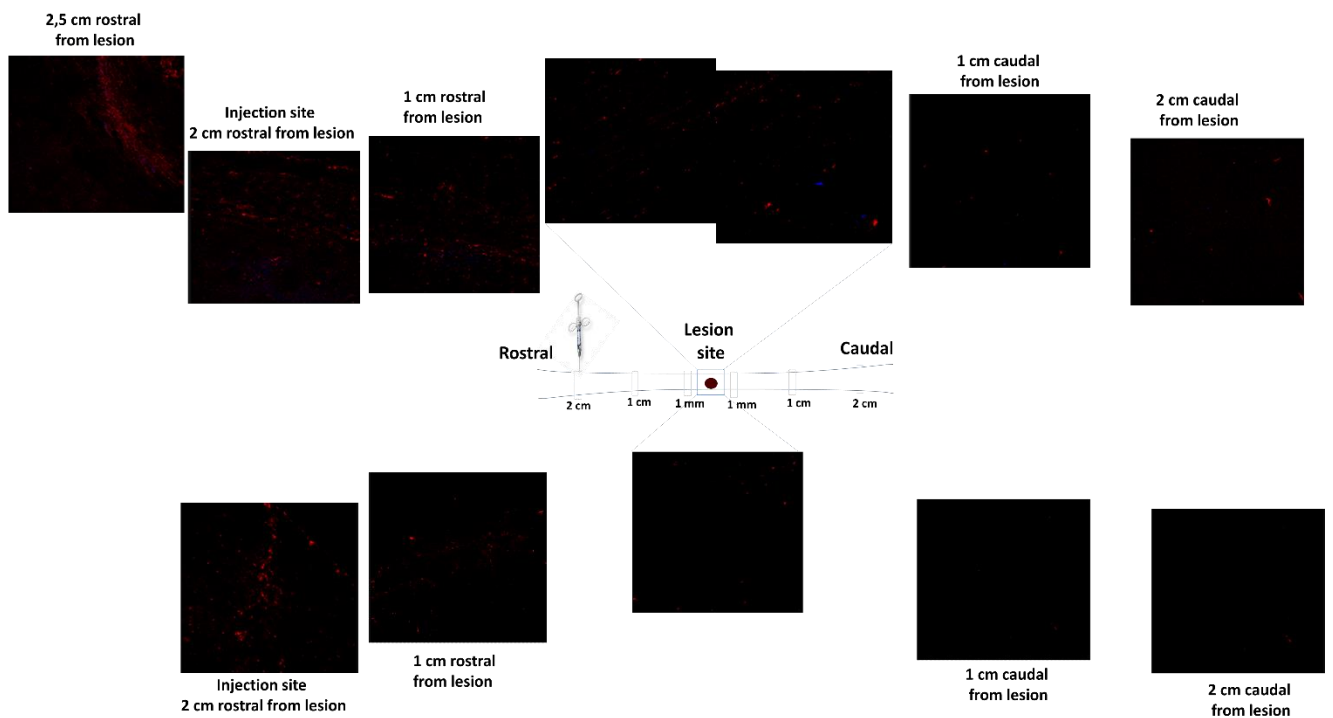


Figure 4.23. In vivo axonal transport recovery in spinal cord of animal transplanted with PM-NPCs.

Anterograde axonal transport was studied, by fluororuby injection at T6/T7, 30 days after PM-NPCs transplantation. Reconstruction of longitudinal sections of lesion site epicenter (T9) and 1 μ m away from the lesion from animals transplanted with PM-NPCs. Scale bars = 100 μ m.

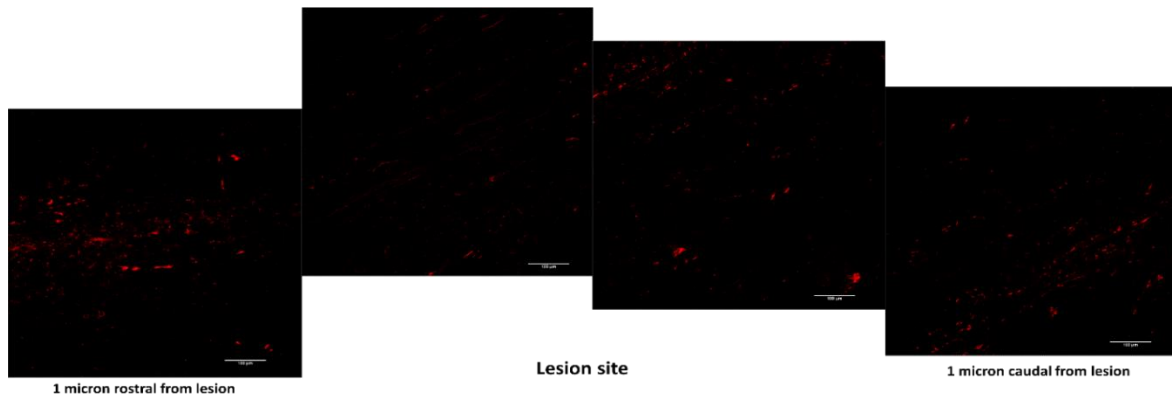


Figure 4.24. In vivo reconstruction of axonal tracer transport in spinal cord of animal transplanted with PM-NPCs. Qualitative image of anterograde axonal transport was 30 days after lesion. As described in material and methods section fluororuby was injection at T6/T7 at day 25 after lesioning and animal sacrificed five days later. Schematic reconstruction of spinal cord longitudinal sections of lesioned (below) and lesioned+PM-NPCs (above) treated animals. PM-NPCs were stained with Hoechst (blue).

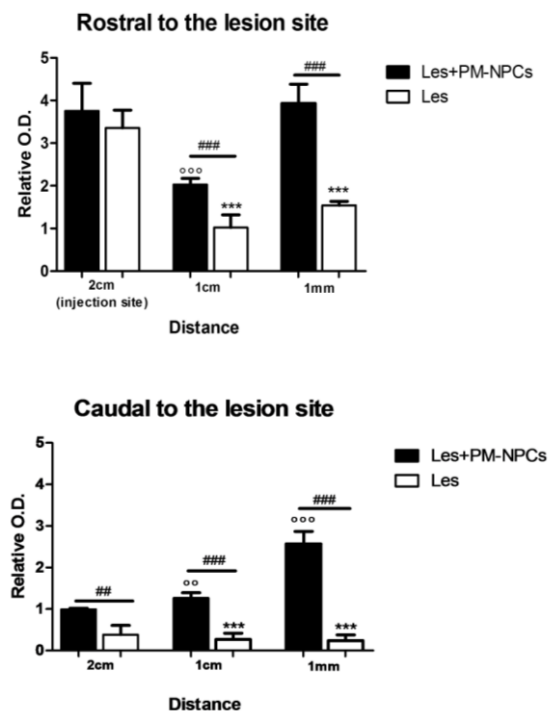


Figure 4.25. Quantification of Fluororuby immunoreactivity in spinal cord of animal transplanted with PM-NPCs. Quantification of fluorescent areas 2 cm, 1 cm and 1 mm away from the lesion from animals transplanted with PM-NPCs was performed in three animals per group. We determined the statistical differences by means of an ANOVA test followed by Bonferroni's post-test. ** $p < 0.01$, *** $p < 0.001$ vs saline treatment; °°° $p < 0.01$ vs 2cm transplanted mice; ### $p < 0.001$ vs 1 cm transplanted mice.

4.5 PM-NPCs transplanted in Parkinson's disease

4.5.1 Loss of function correlate with loss of striatal dopamine

The effect of MPTP administration on TH-positive neurons and axons in the nigrostriatal system was evaluated at 10 days after MPTP administration. Panel A of figure 4.6 TH immunoreactivity in striatum and in SN pars compacta (SNpc) of controls and MPTP-treated mice. As is well known, MPTP causes a highly significant loss in TH-positive cell bodies and axons. The quantification shows that the reduction is higher than 50% (Fig 4.6A). Ventral tegmental area (VTA) provided the internal control zone, since VTA dopaminergic neurons were affected by MPTP to a much lesser extent than SNpc neurons (Liang, 2004). In addition to the neuropathological changes, we observed that striatal DA and related DOPAC and HVA metabolites (Phani, 2010) were reduced by MPTP exposure (Fig. 4.26B). Three behavioral tests were performed in support of the histological and biochemical data (Fig 4.26C). The horizontal grid test allowed assessment of the forepaw faults in healthy and MPTP-treated mice. The behavioral impairment was already marked as early as 1 day after MPTP administration with 73 percent of forepaw faults ($p < 0.001$ vs control mice, CTRL). This behavioral impairment remained significantly high throughout the experimental period (Fig 4.26C). Through the vertical grid test, we assessed the time required by the mouse to turn around and descend the grid once positioned on the top. Following MPTP treatment, mice hesitated and remained on the top of the grid much longer, therefore the time required to turn and descend from the top to the bottom of the grid was much longer from day 1 (Fig 4.26C). The time was exactly 112.8 ± 19.4 sec for MPTP-treated mice and 14.1 ± 7.76 sec for controls ($p < 0.001$). At later times, after the second injection of MPTP, mice required even more time to perform the test (126.33 ± 14.2), while in controls it was only slightly higher (20.5 ± 4.5 sec). The olfactory impairment is a classic symptom in Parkinson disease. In our experimental protocol, olfactory capabilities were evaluated at day 10 after the second MPTP administration (Fig 4.26C). MPTP-treated mice did not find and bite the buried chip as quickly as controls (MPTP= 350.0 ± 10.58 sec; CTRL= 100.8 ± 19.44 sec; $p < 0.001$).

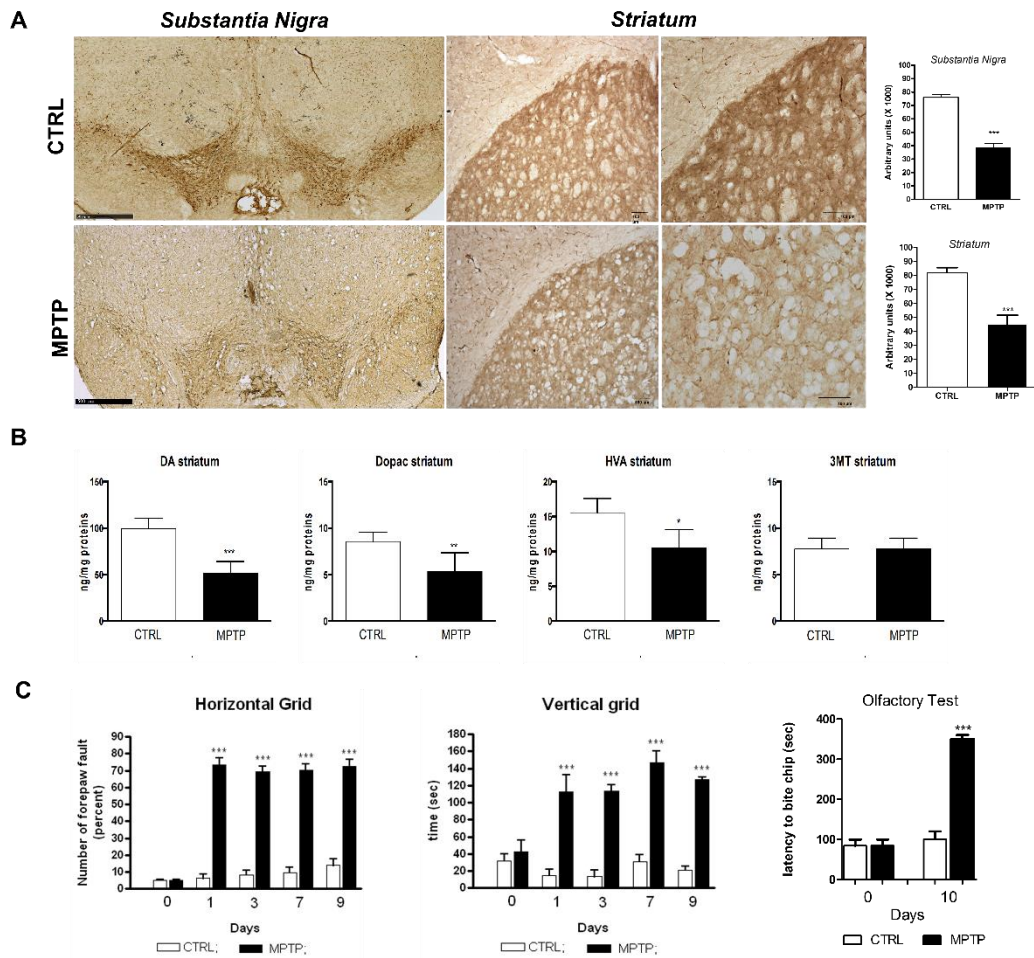


Figure 4.26. The applied paradigm of MPTP impairs nigrostriatal dopamine neurons and causes functional impairment in mice.

(A) TH immunoreactivity performed on brain coronal sections of mice intoxicated or not with MPTP (bars =100 μ m). TH-ir was evaluated at day 10. Quantification was made by ImageJ picture analysis. *** $p < 0.001$ vs CTRL. (B) DA, DOPAC, HVA, and 3-MT striatum levels in control and MPTP intoxicated mice (day 10). Values are expressed as mean \pm SD of three independent experiments ($n = 5$ mice in each group). (C) Evaluation of functional impairment was performed by means of three different behavioral tests (inverted grid, vertical grid and olfactory tests). Data are expressed as mean \pm SD of 3 independent experiments.

4.5.2 PM-NPCs transplantation and recovery of function

In order to evaluate the effects of intrastriatal injection of PM-NPCs (2.5×10^5 cells/ 5μ l; see Materials and Methods for details) on functional recovery of MPTP treated mice, the behavioral tests described above were performed (Fig 4.27). Three days after cell injection, the percentage of forepaw faults of PM-NPCs-transplanted mice was 42.6 ± 9.6 % (horizontal grid test) compared to 69.8 ± 5 % of saline-treated ($p < 0.001$ vs CTRL; $p < 0.001$ vs MPTP saline-treated). The early improvement observed in PM-NPCs-transplanted mice was then maintained

throughout the period of observation, while saline-treated MPTP mice gradually worsened, reaching the maximum deficit 8 days after treatment with values similar to untreated MPTP-mice. The difference between cell-treated and saline-treated groups was even more conspicuous, when their motor coordination ability was tested by means of the vertical grid test. At 3 days after transplantation, animals showed a significant improvement in the time required for turning and descending the grid (62.7 ± 8.4 sec), while the time employed by MPTP-treated mice was almost twice as long (112.7 ± 2.7 sec), even worse than MPTP alone. The deficit was comparable between these two latter groups at day 8. The functional improvement promoted by PM-NPCs treatment steadily increased reaching values similar to controls (healthy mice) within two weeks after cell injection (Figure 1A). The loss of olfactory capabilities caused by MPTP was also evaluated after the PM-NPCs infusion. The improvement was observed as soon as 3 days after transplantation and was maintained throughout the observational period (Fig 4.27A). The histology performed at two weeks after transplantation shows that TH-positive cell bodies of the SN were less detectable after MPTP intoxication, and the total TH-immunoreactivity was reduced to about 30%. In contrast, it was as high as 60% after PM-NPCs infusion (Fig 4.27B). The neuroprotective effects of exogenous PM-NPCs were also present in SNpc contralateral to the injection site (Fig 4.27C). Histological evaluation showed that the reduced number of TH profiles after MPTP in the not treated group was not due to neural loss (Fig 4.28).

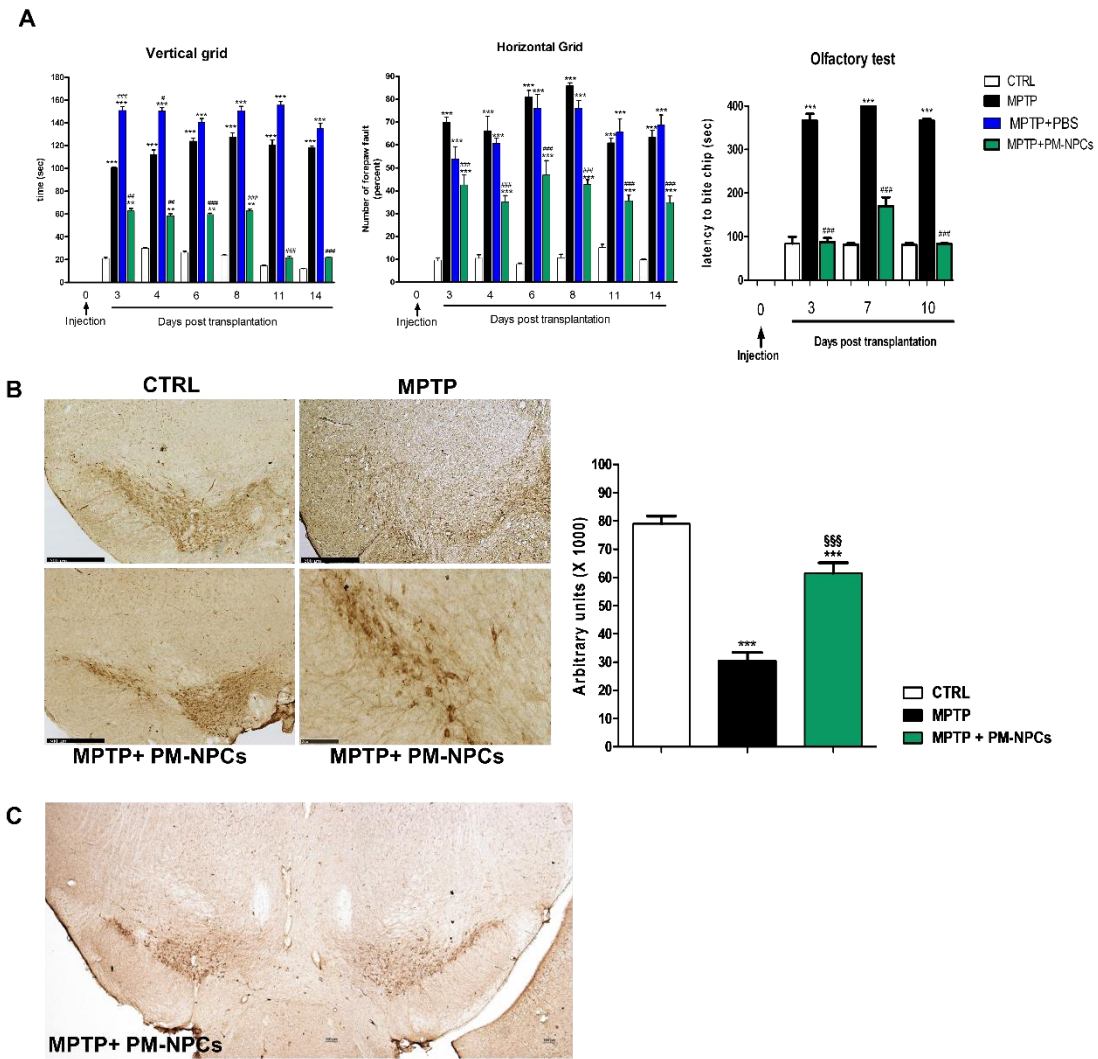


Figure 4.27. PM-NPCs injection promotes recovery of function and protects SN from degeneration.

(A) Vertical grid test. PM-NPCs treated animals recover the motor deficit and climb down quickly from the grid. Horizontal grid test. PM-NPCs treated mice reduces the percentage of forepaw faults per step. Olfactory test. PM-NPCs treated animals recover the olfactory capabilities. Two observers in blind rated each trial for vertical grid, forepaw faults per step and bite of the buried chip. Data are expressed as mean \pm SD (n= sixty mice for CTRL, MPTP and MPTP + PM-NPCs groups; n= six mice MPTP+PBS group). We determined the statistical differences by means of one-way ANOVA test followed by Bonferroni post-test. *** $p < 0.001$ vs CTRL; ### $p < 0.001$; # $p < 0.01$; # $p < 0.05$ vs MPTP. (B) SN coronal slices of CTRL mice, MPTP mice treated or not with PM-NPCs were immune-decorated with anti-TH antibody (bars = 500 μ m; and 100 μ m). Quantification was made by ImageJ picture analysis. *** $p < 0.001$ vs CTRL, §§§ $p < 0.001$ vs MPTP. (C) Reconstruction image of whole mid-brain coronal section relative to MPTP mouse treated with PM-NPCs. Section was immune-decorated with anti-TH antibody (bars = 100 μ m).

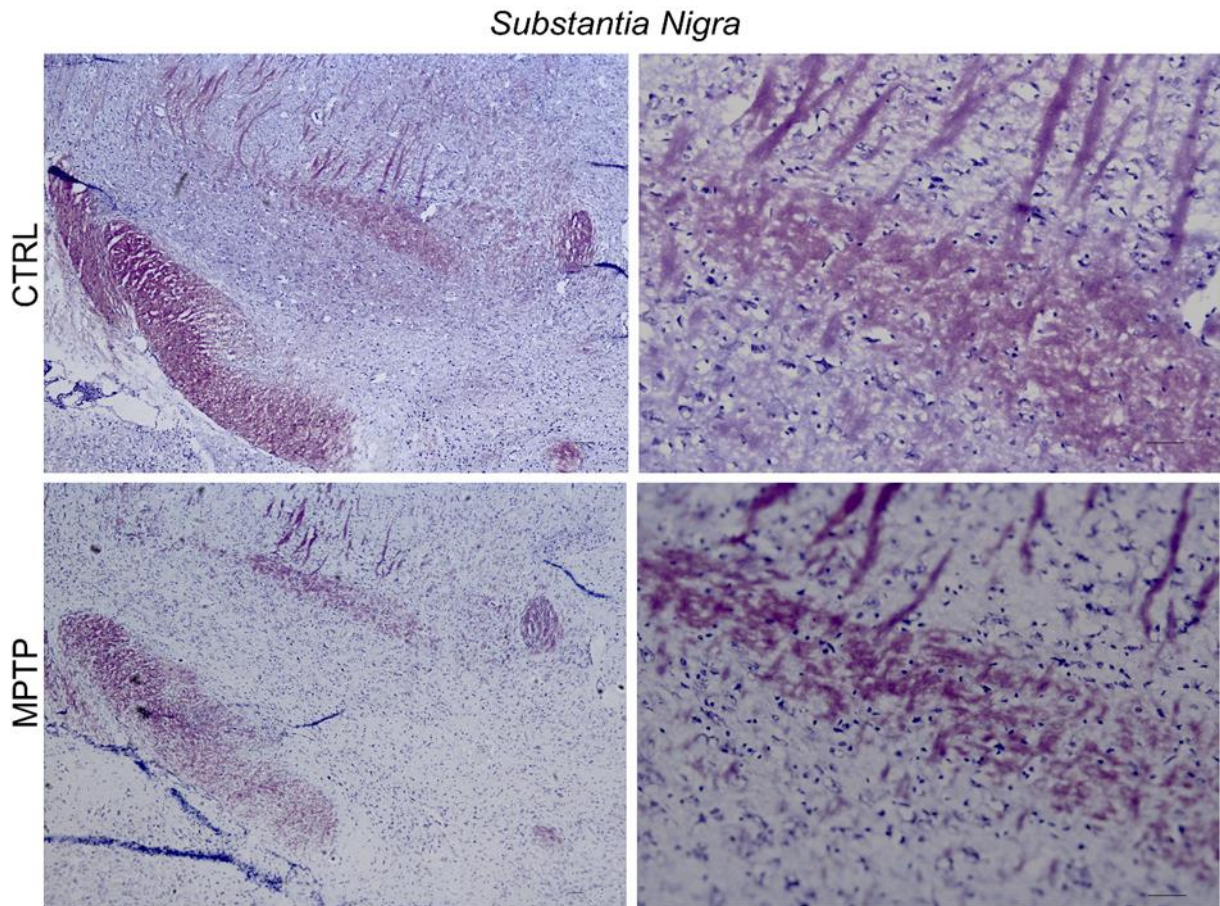


Figure 4.28. Cresyl violet staining of SNpc neurons.

Cresyl violet staining was performed on brain coronal sections of healthy mice (CTRL) or mice intoxicated with MPTP (MPTP) at the end of observational period (day 14 post transplantation) (bars =100 μ m). Cresyl violet staining was performed by following the procedure described by Goldberg and co-workers (Goldberg, 2011).

4.5.3 Reduced striatal levels of dopamine

Tissue levels of dopamine and its metabolites were determined by HPLC (see Materials and Methods). MPTP exposure caused a 50% reduction of dopamine in both the left and right striatum that was maintained up to the end of experimentation period (24 days after 1st MPTP administration). Such a loss was not modified by PM-NPCs transplantation (Fig 4.29A). Therefore, the behavioral recovery promoted by PM-NPCs occurs in absence of any restoration of DA. DOPAC, HVA and 3-MT were also reduced bilaterally, and remained as such unaffected by treatment. 5-hydroxytryptamine, 5-HIAA, and norepinephrine did not change after MPTP exposure and cell transplantation (Fig 4.29B). However, with the loss of striatal DA and DA

synapses there is a dramatic decrease in the expression of both dopamine and norepinephrine transporters, as assessed by real time RT-PCR (Table 4.1). Such reduced levels of mRNA were increased ten and six fold respectively by PM-NPCs (Table 4.1). In addition, TH expression was augmented by 18 fold (Table 4.1). This may suggest that transplantation could have improved synaptic efficacy in the striatum.

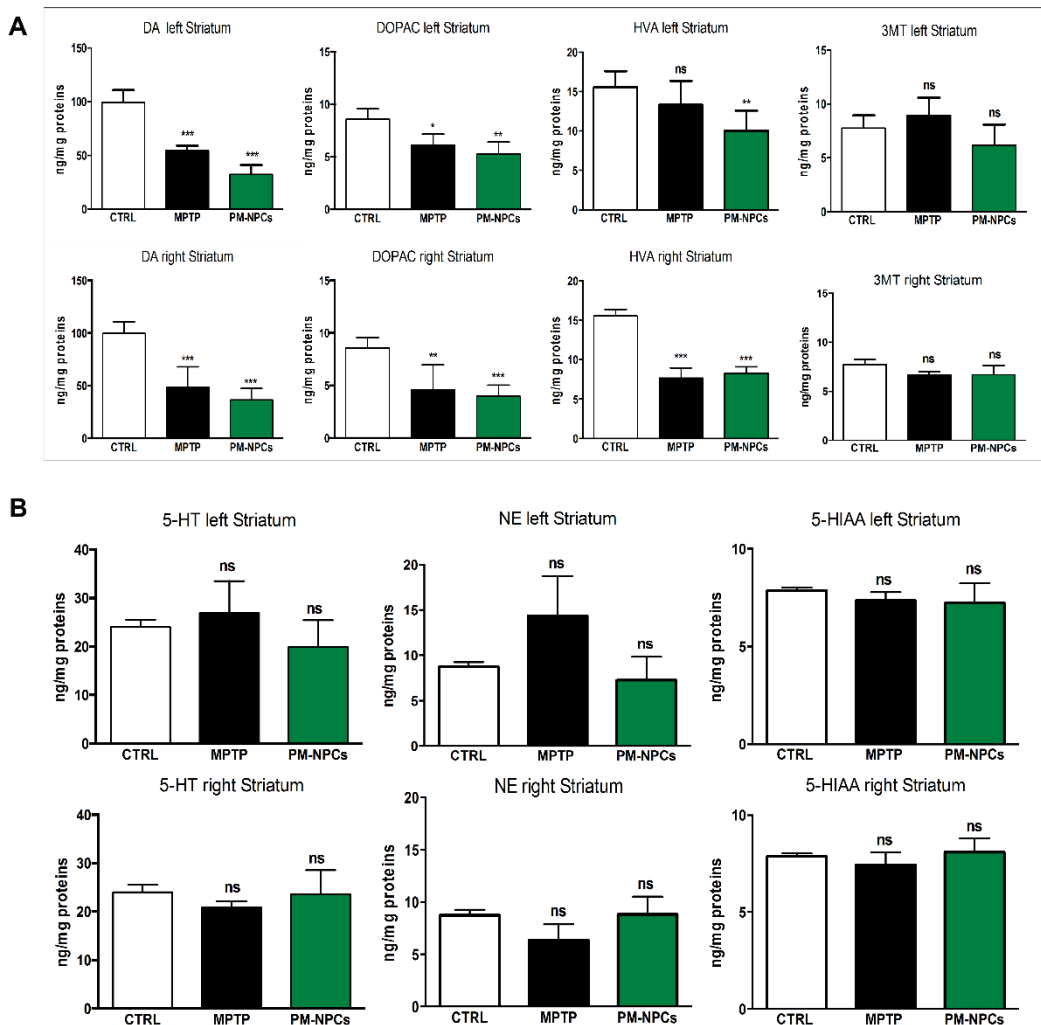


Figure 4.29. Striatal levels of neurotransmitters after PM-NPCs transplantation.

The determination was performed 2 weeks after cells transplantation (day 14 post-injection). (A) Levels of DA, DOPAC, HVA, and 3-MT were determined separately in the left (ipsilateral to the injection) and right (contralateral to the injection site) striatum. (B) Levels of 5-hydroxytryptamine (5-HT), norepinephrine (NE) and 5-Hydroxyindoleacetic acid (5-HIAA) were determined separately in the left and right striatum. Data are expressed as mean of three experiments \pm SD ($n =$ nine mice in each group); *** $p < 0.001$; ** $p < 0.01$; * $p < 0.05$ vs CTRL.

Left striatum	CTRL	MPTP+PBS	MPTP+PM-NPCs 7 days
NET	1± 0	0,78 E-02 ± 0,29E-03 (p<0.001 vs CTRL)	5,9E-02 ± 0,14E-02 (p<0.001 vs MPTP+PBS; p<0.001 vs CTRL)
DAT	1± 0	0,93 E-02 ± 0,08E-01 (p<0.001 vs CTRL)	9,99E-02 ± 0,12E-02 (p<0.001 vs MPTP+PBS; p<0.001 vs CTRL)
TH	1± 0	0,94E-01 ± 0,47 E-02 (p<0.001 vs CTRL)	31,8 E-02 ± 0,79E-02 (p<0.001 vs MPTP+PBS; p<0.001 vs CTRL)

Table 4.1. DAT, TH, and NET mRNA expression levels 7 days after treatment with PM-NPCs or PBS.

mRNA levels was evaluated by real time RT-PCR. Each group was composed of three mice; three quantitative (Q)-RT-PCRs in each experiment was performed, each sample was run in triplicate. 18S ribosomal RNA was used as reference gene. Values represent the number of fold increase versus control and is reported as mean ± SD.

4.5.4 Localization of transplanted PM-NPCs

Healthy and lesioned animal brains with or without PM-NPCs injection were sectioned. A large portion (78.50 ± 7.5 %) of the 2.5 x 10⁵ cells injected into the left striatum of each animal were still present 2 weeks after transplantation. The vast majority (69.56 ± 4.5 %) of GFP-positive transplanted PM-NPCs were within the striatum (Fig 4.30A). Grafted PM-NPCs appeared rather differentiated with an oval soma and abundant neuritic processes, even 30 µm long (Fig 4.30B). As expected, the axonal TH immunoreactivity resulted significantly decreased into the striatum of MPTP-treated animals (Fig 4.30A), and such a loss was slightly affected by cell transplantation (Fig 4.30A). However, a high number of PM-NPCs resulted strongly labelled by anti-TH antibodies (see arrows in Fig 4.30C). The quantitative evaluation of total TH immunoreactivity in the striatum resulted slightly higher in transplanted animals, probably because of the presence of transplanted cells.

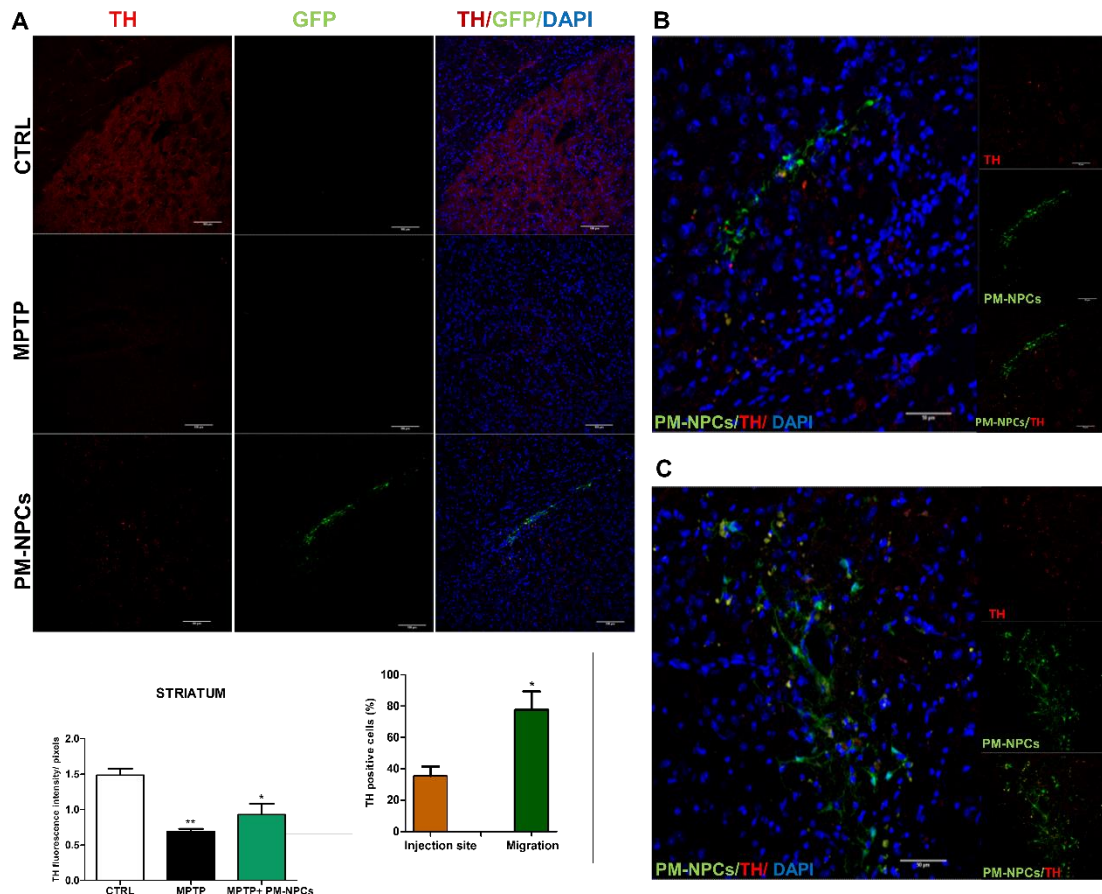


Figure 4.30. Intra-striatal localization of PM-NPCs.

(A) Confocal images of tyrosine hydroxylase-labeled (TH; Red) coronal striatum sections of control animals (CTRL), MPTP injected mice and MPTP injected mice treated with PM-NPCs (Green). Pictures refer to animals sacrificed 2 weeks after cells transplantation. Nuclei are stained in blue (DAPI) (bars= 100 μ m). Coronal cryostat sections of CTRL, MPTP and MPTP+PM-NPCs were quantitatively evaluated and the number of TH positive cells was determined as described in materials and methods. Results are expressed as percentage of TH positive cells per HPF. For the quantification we considered sections from at least three animals per group. Values represent average \pm SD. ** $p < 0.01$, * $p < 0.05$. (B) and (C) Magnified details (bars = 50 μ m) of MPTP+ PM-NPCs injected mice striatum coronal sections stained with TH(red). GFP is showed in green and nuclei are stained in blue (DAPI). Co-expression of the cytoplasmic protein TH (red) and GFP (green) within a cell suggests dopaminergic differentiation of the transplanted PM-NPCs within the injured mouse brain.

4.5.5 Astroglisis and cytokines changes

Inflammation is part of the physiological response to MPTP as also indicated by astroglia activation. Figure 4 shows that the density reactive GFAP-positive cellular profiles was markedly increased in striatum of MPTP mice (Fig 4.31A); such an augmentation was significantly reduced in the striatum ipsilateral to the cell injection site. Differently, the astroglisis was unaffected in the contralateral striatum (Fig 4.31A). The quantification

confirmed the visual impression that GFAP-positive cells were reduced in the striatum ipsilateral to PM-NPCs injection site (Fig 4.31A). We also evaluated the extent of macrophages infiltration in the striatum, which resulted, increased after MPTP (Fig 4.31B). As for astrogliosis, the staining for MOMA (MOuseMAcrophages) was normalized in the striatum were PM-NPCs were infused. While in the contralateral the counteractive effect of PM-NPCs was attenuated (Fig 4.31B). Several reports had shown that exogenous applied stem cells have anti-inflammatory properties (Carelli 2014 and 2015; Aggarwal, 2005; Ortiz, 2007; Martino, 2006). It is possible that the PM-NPCs restorative action could be mediated by anti-inflammatory activity. Here we observed that MPTP caused a marked cytokines mRNAs increase in both left and right striatum that was attenuated by the application of PM-NPCs (Table 4.2). The effect was quite remarkable for TNF-alpha, and IL-6. The reduction of IL-15 expression was modest and did not reach statistical significance. In addition, also, NGF increased in the striatum of MPTP mice and its expression was significantly reduced by cell transplantation, while BDNF was unaffected. In contrast, in the right striatum (contralateral to the transplant), the anti-inflammatory action of PM-NPCs was less marked, with changes not statistically significant for IL-1-alpha, TNF-alpha, IL-6, and IL-15. Only NGF mRNA expression was also clearly reduced in the right striatum (Table 4.2).

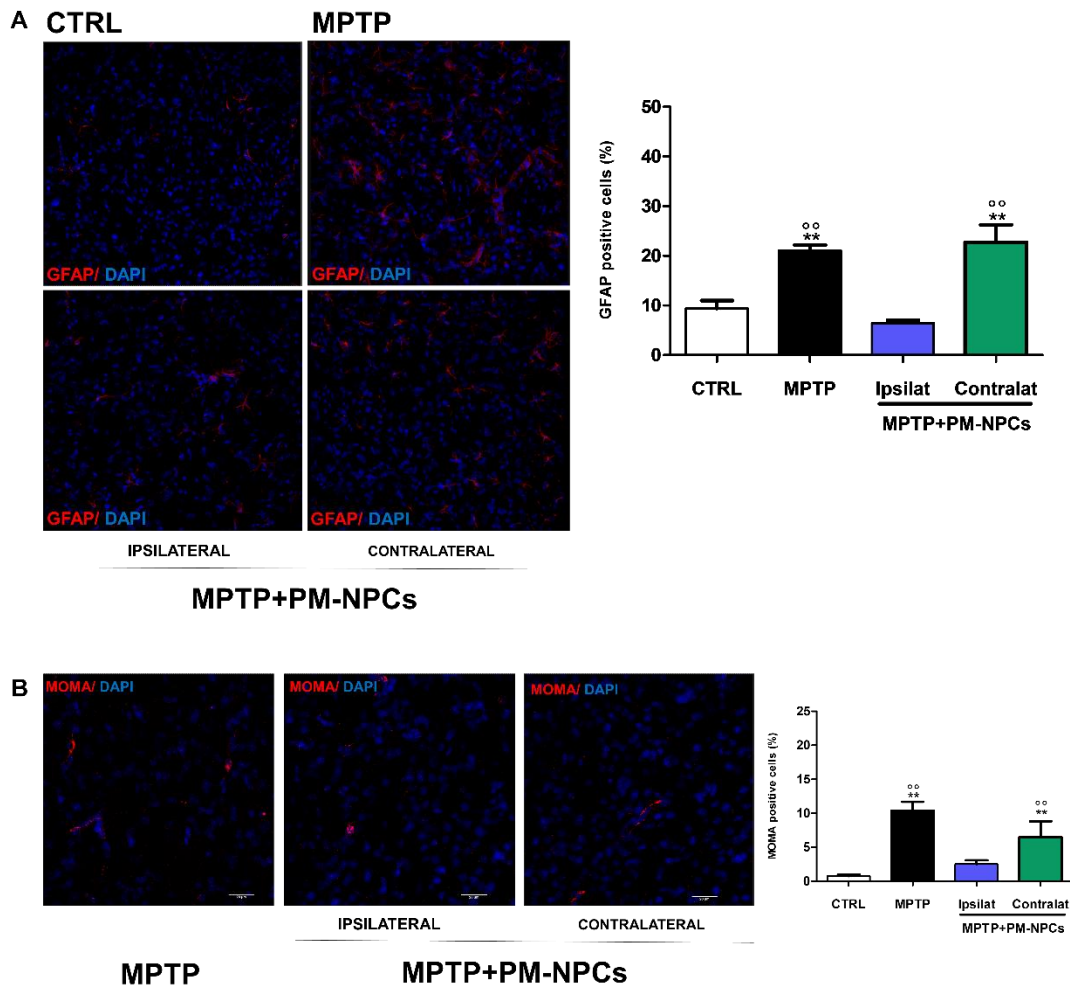


Figure 4.31. Striatal GFAP Immunoreactive-Positive Profiles after PM-NPCs transplantation PM-NPCs reduce the extent of astrogliosis in the MPTP damaged striatum.

Confocal images of (A) GFAP-labeled (Red) and (B) MOMA-labeled (Red) coronal striatum sections of control animals (CTRL), MPTP injected mice and MPTP injected mice treated with PM-NPCs. Pictures refer to animals sacrificed 2 weeks after cells transplantation. Nuclei are stained in blue (DAPI) (bars= 100 μ m). Quantification of GFAP (A) and MOMA (B) positive cells. The percentage of cells positive to GFAP and MOMA are reported in the graph. Data are expressed as mean of six different fields for each condition \pm SD (n= two mice each group; three fields/mouse). $^{\circ\circ}$ p<0.01 vs MPTP+PM-NPCs ipsilateral; ** p<0.01 vs CTRL.

Left striatum	CTRL	MPTP+PBS	MPTP+PM-NPCs
IL-1 alpha	1 ± 0	1.063 ± 0.09 (ns vs CTRL)	1.764 ± 0.486 (ns vs MPTP+PBS; ns vs CTRL)
TNF-alpha	1 ± 0	9,89 ± 2,38 (p<0.01 vs CTRL)	3,22 ± 0.67 (p<0.05 vs MPTP+PBS; P<0.05 vs CTRL)
IL-6	1 ± 0	5.655 ± 0.92 (p<0.01 vs CTRL)	3.7361 ± 0.39 (p<0.05 MPTP+PBS; p<0.05 vs CTRL)
IL-15	1 ± 0	4.6202 ± 0.83 (p<0.01 vs CTRL)	3.481 ± 0.693 (ns vs MPTP+PBS; p<0.05 vs CTRL)
NGF	1 ± 0	4.866 ± 0.4844 (p<0.001 vs CTRL)	2.2256 ± 0.643 (p<0.001 vs MPTP+PBS; p<0.05 vs CTRL)
BDNF	1 ± 0	5.8256 ± 0.831 (p<0.01 vs CTRL)	4.1657 ± 0.787 (ns vs MPTP+PBS; p<0.05 vs CTRL)

Table 4.2 Cytokines mRNA expression levels 7 days after treatment with PM-NPCs or PBS.

Expression of cytokines mRNA levels was evaluated by real time RT-PCR. Each group was composed of three mice; three quantitative (Q)-RT-PCRs in each experiment was performed, each sample was run in duplicate per and a parallel PCR for the gene of interest and the reference gene 18S. Values represent the number of fold increase versus control and is reported as mean ± SD.

4.5.6 PM-NPCs migratory processes

Previous reports had shown that that transplanted stem cells can migrate into the host striatum (7, 26), here we observed that grafted PM-NPCs migrate from the injection site across the striatum (Fig 4.32). In 2 weeks PM-NPCs had migrated up to 3125.72 µm from the site of injection following a ventral direction (Fig 4.32A). In addition, the re-assembly of serial pictures from longitudinal sections, obtained by confocal acquisitions, demonstrates that PM-NPCs moved away from the site of injection following rostra-caudal and rostra-ventral pathways, which appeared to be specific (Fig 4.32B) for distances longer than 1 mm. These directions of migrations were monitored and quantified in three animals, and the migration pathways were highly comparable. It therefore appears that some specific signals capable of directing the cellular migratory process must exist. Furthermore, when transversal brain sections were used,

we observed that the PM-NPCs migrated beyond the borders of the striatum and SN pars compacta, and that ipsilateral and contralateral to the injection site was reached (Fig 4.32C). Here, the transplanted cells are intermingled with endogenous TH-positive neurons (Fig 4.32D and 4.32E).

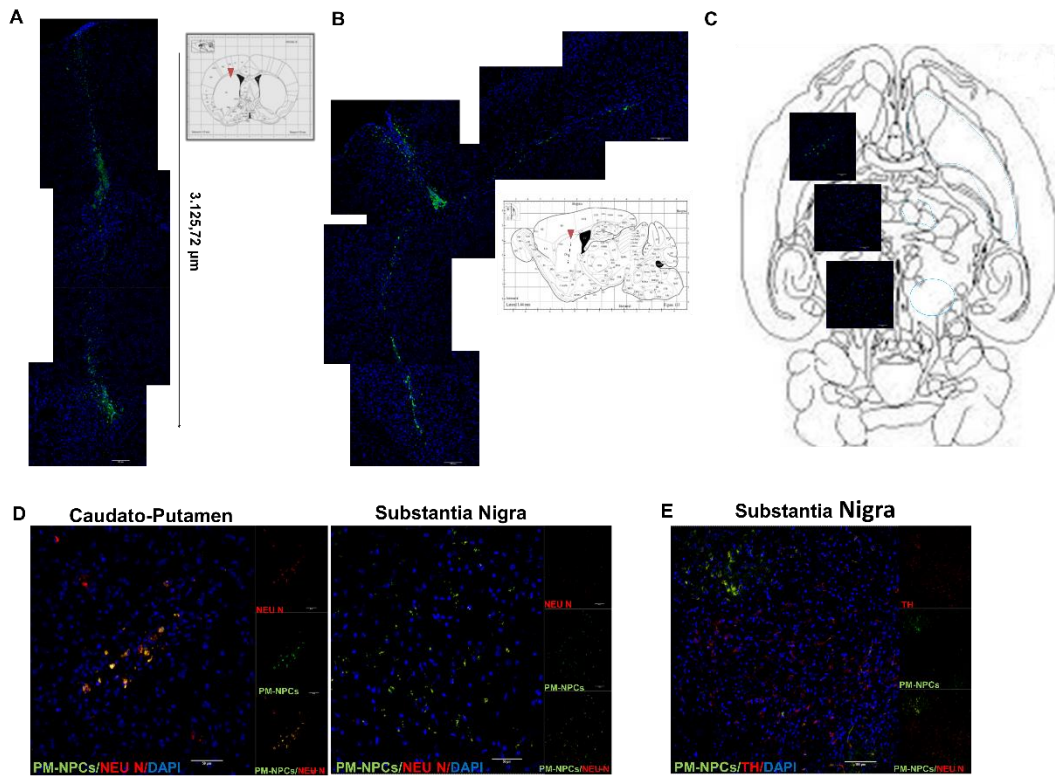


Figure 4.32. Injected PM-NPCs migrate throughout the striatum and reach the Substantia Nigra.

Confocal images of intrastriatal distribution PM-NPCs (green) 2 weeks after transplantation in coronal (A), longitudinal (B), and transversal sections(C) of PM-NPCs injected parkinsonian mouse brains. Transplanted neural precursors (green) migrate for many microns in the striatum following both ventral and caudal directions. (D) and (E) Magnification of brain coronal sections obtained from PM-NPCs injected parkinsonian mice stained with anti-NeuN or anti-TH (red), GFP is showed in green and nuclei are stained in blue (bars= 100 μ m for TH; 50 μ m for NeuN).

4.5.7 Expression of typical markers by transplanted PM-NPCs

Close to the injection site a higher number of cells were positive to Nestin (precursor cell marker), while most migrated PM-NPCs resulted positively marked by anti-NeuN and anti-MAP2 antibodies (markers of neuronal differentiation) (Fig 4.33). Here only a lower percentage of cells was positive to NG2 (marker of oligodendrocytes precursors) and Nestin. The quantification shows that migrated grafted cells differentiated in this proportion: 81.88 % \pm 2.3 % of GFP positive cells resulted positive for NeuN and 62% for MAP-2, while 38.77% \pm 3.8 % of GFP positive cells were positive for NG2 and 36% for Nestin (Fig 4.33). Therefore, PM-

NPCs migration is correlated with a higher differentiation (Fig 4.33A). We also found that a large amount of transplanted cells expressed a marker related to dopamine synthesis, such as TH (47.88% \pm 11%, in 511 analyzed cells). The cholinergic marker ChAT, which is expressed by striatal excitatory interneurons, was found in 58.33% \pm 8% of the 489 analyzed cells, and a relative lower amount of cells expressed GABA (35% \pm 4%, in 354 analyzed cells) (Fig 4.33).

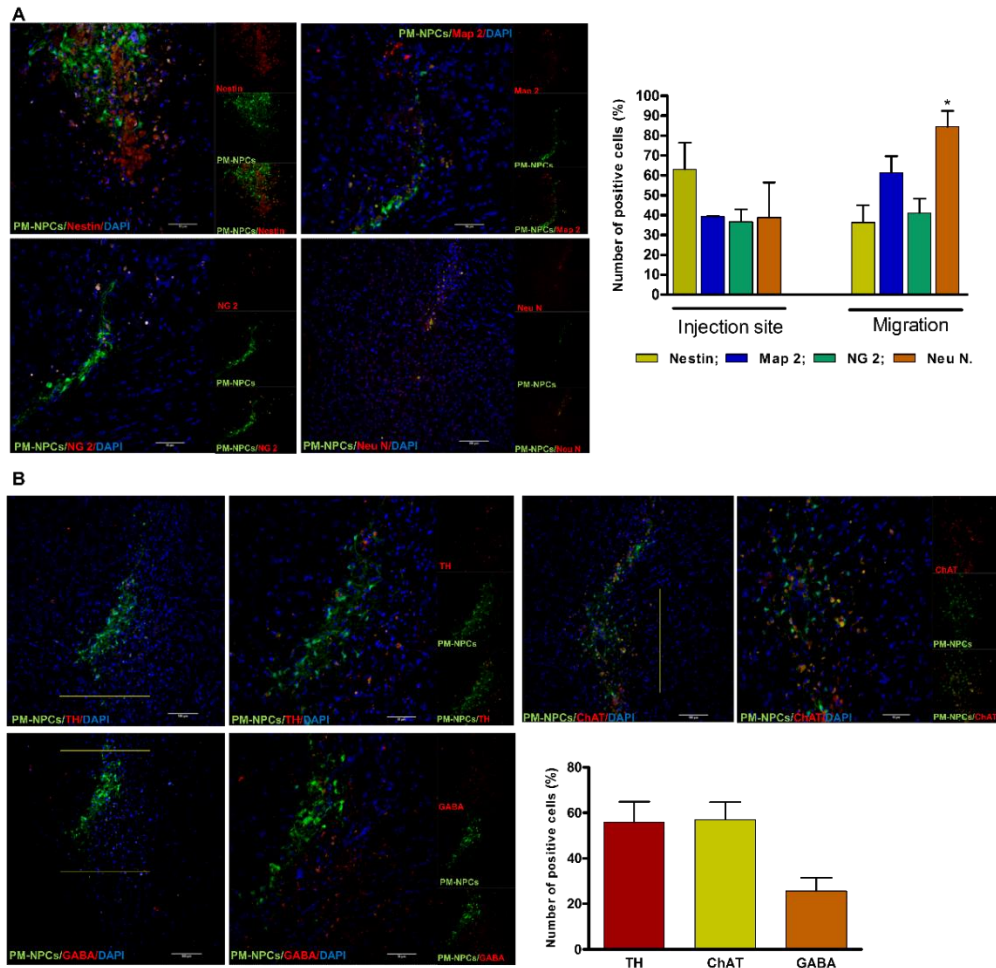


Figure 4.33. Most PM-NPCs adopted a neuronal fate when transplanted into Striatum of MPTP mice and express neuron specific markers. (A) Confocal images of striatal coronal sections stained with neural differentiation specific markers (MAP-2, NeuN, NG2 and nestin). The immunostaining is showed in red. PM-NPCs are showed in green (GFP). Nuclei are stained in blue (DAPI). Images were taken two weeks after PM-NPCs injection. Quantification of neural fate markers expression 2 weeks after transplantation. The percentage of cells co-expressing specific investigated marker and GFP is reported in the graph. Data are expressed as mean of six different fields for each condition \pm SD (n= two mice each group; 3 fields/mouse). Scale bar represents 100 and 500 μ m. (B) Confocal images of coronal striatum sections of MPTP mice treated with PM-NPCs (Green) stained with Tyrosine Hydroxylase (TH; red), Choline Acetyl Transferase (ChAT; Red) and gamma-aminobutyric acid (GABA; red). Co-expression of ChAT (red), GABA (red) and GFP (green) within a cell suggests that transplanted neural precursors differentiate also into cholinergic- and GABAergic neurons within the injured mouse brain. Nuclei are stained in blue (DAPI), scale bar represent 500 μ m. For the quantification, we considered sections from two animals per group (3 fields/animal). The percentage of cells co-expressing specific investigated marker and GFP is reported in the graph. Values represent mean \pm SD.

4.5.8 Is PM-NPCs action mediated by EPO?

We had previously reported that PM-NPCs differentiation was dependent on the autocrine release of EPO (Carelli, 2014), so we then determined whether the striatal functional recovery promoted by PM-NPCs was also mediated by EPO. PM-NPCs inoculation was performed with or without co-administration of anti-EPO or anti-EPOR specific antibodies at comparable concentration previously used in vitro (3µg/ml, respectively). The data show that the addition of either antibodies obliterated the positive effect of PM-NPCs administration above described (Fig 4.34). Such a counteractive effect was observed with both behavioral motor tests. As a further control, we administered EPO alone through the same route. The administration of recombinant human-EPO (rh-EPO; 1U/gr) in MPTP parkinsonian mice significantly improved the behavioral impairment as early as 3 days after injection, as cells did in both tests (Fig 4.34). The intrastriatal injection of anti-EPO and anti-EPOR antibodies alone did not modify the animal behavioral impairment caused by MPTP. These data suggest that the positive action of PM-NPCs in MPTP mice was likely due to EPO release by transplanted PM-NPCs (Fig 4.34).

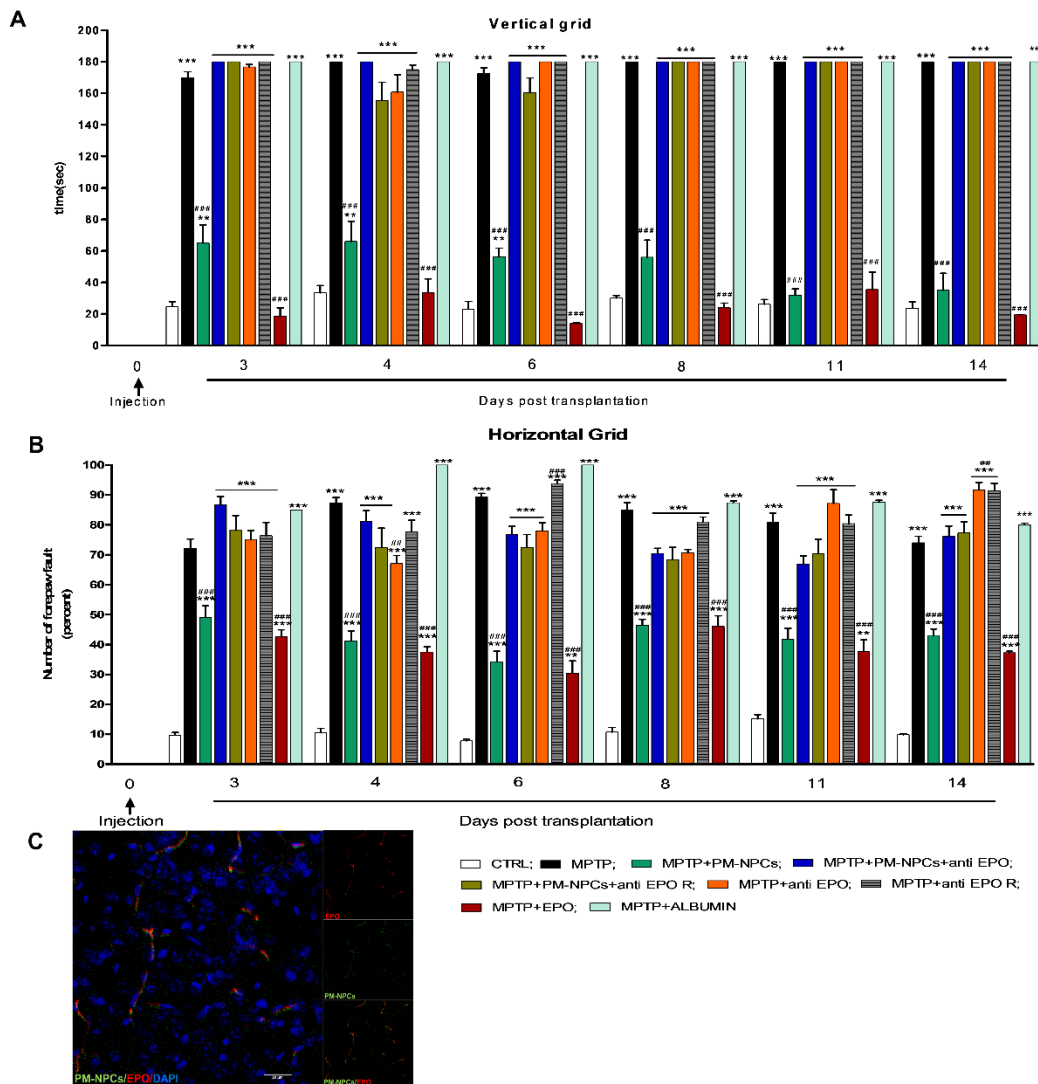


Figure 4.34. Erythropoietin released by transplanted PM-NPCs promotes functional recovery.

(A) Vertical grid test and (B) Horizontal grid test showed an increase in activity for MPTP animals transplanted with PM-NPCs and Erythropoietin (EPO) in comparison with MPTP animals that received specific antibodies against Erythropoietin (anti-EPO) and EPO receptor (Anti-EPO R). Data are expressed as mean of three different experiments \pm SD (n= five animals for each group). We determined the statistical differences by means of one-way ANOVA test followed by Bonferroni post-test. $***p < 0.001$; $**p < 0.01$ vs CTRL; $###p < 0.001$; $##p < 0.01$ vs MPTP. (C) Confocal images of coronal striatum sections of MPTP + PM-NPCs (Green) mice stained with Erythropoietin (EPO; red). Nuclei are stained in blue (DAPI), scale bar represents 20 μ m.

5. Discussion

The development of neuroprotective and restorative therapies remains a major unfulfilled medical need. In this regard to prevent further neuronal damage through the attenuation of secondary degeneration and promote repair and recovery of function in SCI, a stem cell-based therapy provides a promising therapeutic approach. Their characteristic abilities to self-renew and differentiate into any cell type in the body, justify the intense efforts on investigating application in cell therapy of stem cells [Furlan, 2011; Gorio, 2002; Sahni, 2010; Marfia, 2011; Thuret, 2006]. Cell-based therapeutics for spinal cord injury could affect tissue and/or functional outcomes in different manners: (i) differentiation and functional integration of new cells into spared spinal cord circuitry, (ii) increased sparing of host neurons, myelin, and axons, and/or decreased host glial scarring, and (iii) increased host-mediated axonal regeneration or remyelination.

In this study we evaluated the potential therapeutic of the Post Mortem Neural Precursor Cells (PM-NPCs) (Marfia, 2011) in the treatment of the acute traumatic spinal cord lesion. In cell therapy of spinal cord injury have been used different types of cells such as embryonic (Bottai, 2010), mesenchymal (Cizkova, 2006), hematopoietic (Koshizuka, 2004), Neural (Bottai, 2008; Abematsu, 2010), Schwann (Schaal, 2007) and oligodendrocyte ensheathing cells (OECs) (Richter and Roskams, 2008). Neural stem cells / precursor are the most used, probably because it already directed towards a neural phenotype, and then already programmed to differentiate in a appropriate manner to regenerate nerve cells damaged by the trauma. Following intravenous administration, the PM-NPC reach the injury site through the bloodstream, the ematospinalbarrier exceed, which has been deeply affected by the injury and subsequent inflammatory response (Maikos and Shreiber, 2007). Unlike neural cell / classic precursors (Bottai, 2008), the PM-NPCs are not phagocytized by macrophages during the first weeks in the damaged bone and integrate the parenchyma injured edge; then they differentiate into neuronal sense and create a neural tissue inside the spinal cord damaged (Carelli, 2015). The morphological examination of the injured cord showed that PM-NPCs are developed into newly formed neurons, which largely have differentiated in a cholinergic phenotype. The transplanted cells formed in the injured bone a sort of circular section with a one-millimeter diameter, this is mainly made up of differentiated PM-NPCs, and there is a real tissue reorganization within the lesioned area, with a structure highly suitable for supporting regenerative events.

The morphological differentiate framework of injured tissue is associated with a major functional recovery of hind limbs. This recovery was quantified through the Basso Mouse Scale (Basso, 2006) and was observed that the ability to use the hindlimbs increases rapidly from the seventh day, reaching the biggest value after three weeks post lesion and remaining constant. The mice treated

with saline solution, instead, show a markedly lower recovery. An imported recovery of motor function is a common factor that is found in most of the studies on spinal cord injury using a cell-mediated therapy (Barakat, 2005; Firouzi, 2006; Ramon-Cueto, 2000; Moreno-Flores, 2006; Setoguchi, 2004; Ziv, 2006; Bottai, 2008; Bambakidis and Miller, 2004; Carelli, 2014; Carelli, 2015). The cytoarchitecture of bone marrow in the injury site improves by PM-NPCs transplantation, the extension of necrotic tissue is significantly reduced in the treated mice and in the areas of scarring is inserted the new nerve tissue formed by stem cells. The PM-NPCs cytoprotection extends to the white matter, in particular 0.5 mm caudal from the lesion this structure is similar to the control mice, while animals treated with PBS show a myelin density significantly reduced. The preservation of the white matter can explain the increased recovery of motor function after treatment with PM-NPCs. Although in this type of injury the corticospinal tract (CST) is seriously compromised, there are sections of the same pathways which run to the spine: the dorsolateral corticospinal tract (LCST) (Steward, 2004) and the ventral corticospinal tract (VCST) (Brosamle and Schwab, 1997), though, normally they have a less importance function than the CST can replace the functions after spinal cord injury (Brosamle and Schwab, 2000). Since these "secondary" ways shall commence in areas of white matter that we have demonstrated be better preserved by PM-NPCs treatment, it could be probably related to better recovery of motor activity observed in the treated mice. A better motor recovery correlated to a greater preservation of the white matter has also been shown in a spinal contusive model that used rats in which was administered recombinant human erythropoietin rhEPO (Vitellaro-Zuccarello, 2007; Vitellaro-Zuccarello, 2008; Gorio, 2002).

Immunohistochemical analysis revealed that the neuroprotective effect of PMNPCs is also effective at the level of the gray substance. In fact, the presence of surviving axonal damage fibers such as: the serotonergic, positive for serotonin (5-HT), and adrenergic processes, positive for tyrosine hydroxylase (TH), as significantly increased in transplanted animals. Gray matter reinnervation in the caudal portions of the spinal cord is indicative of the PM-NPCs ability to transform the injured area in a site appointed to support the regeneration of injured axons, which probably contributes to the functional recovery improvement. It is known that if the neurons are not stimulated by a proper innervation undergo some morphological and physiological changes such as reducing the number of dendrites and the reduction of their ramifications (Bose, 2005). These events can lead cells to atrophy, a mechanism defined transsynaptic degeneration (Eidelberg, 1989; Van De Meent, 2010). This process brings to the loss of synaptic signals and a non-activation of neurons, which become functionally inactive (McComas, 1973; Benecke, 1983).

For this reason is important to preserve not only the motor neurons, but also the greater number of fibers. The treatment with PM-NPCs that preserves a part of fibers catecholaminergic, adrenergic and serotonergic helps to keep the active neurons, and therefore maintain a neural network that contributes to the recovery of motor activity.

In addition to preserve the descending fibers from the encephalon, PM-NPCs have a neuroprotective effect on the gray matter, and in particular, we have shown that they exert their action on the cell neuron bodies that are in the ventral horns where motor neurons reside. Therefore these cells have a three different therapeutic effect on the spinal cord damaged: preserves cell bodies present in the ventral horns where there are motor neurons; preserves the monoaminergic fibers descendants correlated with locomotion control and finally also preserves the white matter in areas where there are important motor pathway that can partially support corticospinal pathway functions damaged. We have also observed that at 4 weeks after the lesion, many PM-NPCs differentiate into neuronal sense and therefore have the ability to integrate in a functional manner in the neural network that re-arranges post trauma (Abematsu, 2010, Xu, 2011) and also contributing in this case to the functionality motor recovery.

The injection of Fluororuby (Lu, 2001) in CST rostral to the lesion showed that in animals treated with the PM-NPCs the fluorescent tracer is transported in an anterograde manner through survival axons of CST that go around the lesion and in part in the caudal level to the injured spinal cord tissue. In transplanted animals, the fluororuby is significantly higher than that observed in mice treated with saline. This shows that the treatment with PM-NPCs provides a favorable environment to nerve regeneration in the injured cord.

Treatment with PM-NPCs also shows a marked reduction of infiltration of neutrophils that is accompanied by a better preservation of bone marrow cytoarchitecture. Neutrophils usually invade the bone marrow damaged 12-24 hours after injury (Popovich, 1997) and release them pro-inflammatory cytokines and reactive oxygen species (Popovich, 1999; Taoka and Nakajima 1998). Similarly, the infiltration of macrophages at the damage site, which usually has its peak 5-7 days after injury (Taoka, 1997) is reduced following administration of PM-NPCs. It was also demonstrated that anti-inflammatory treatments have a high efficacy in reducing selectively early injury mediated by leukocytes in spinal cord injury, leaving the opportunity to attend later with targeted interventions repair and regeneration of damaged tissue (Gorio, 2007; Gris, 2004). Treatment with this type of neural precursors therefore seems to have also a powerful anti-inflammatory effect probably due to factors / cytokines that the cells themselves release in the lesion site.

We have studied the anti-inflammatory effect of PM-NPCs in glial reaction, an event that ever occurs in spinal cord injury (Silver and Miller, 2004; Fitch and Silver, 2008). The glial scar is important to create a barrier that protects the CNS area already damaged from the other damage (Myer, 2006), but on the other hand it was shown that it acts as a real barrier to axonal regeneration (Fitch and Silver, 1997; Fitch and Silver 2008).

The reduction in glial reaction following administration of PM-NPCs, and then the resulting reduction the scar entity, allows to maintain a microenvironment with a reduced quantity of molecules / stimuli for axonal growth inhibitors; which can lead to a greater regeneration of nerve fibers in the long time. The treatment with the PM-NPCs has also influenced the expression of numerous proinflammatory and anti-inflammatory cytokines analyzed, which are not normally produced by the bone marrow (Pineau, 2007) and may therefore play a very important role in response to the spinal cord trauma. It is known that the exogenous administration of different types of cytokines is able to improve the functional recovery after the spinal trauma (Giehl and Tetzlaff, 1,996; Ruitenbergh, 2004; Sayer, 2002) and in fact the increase in the motor recovery promoted by adult NSCs is accompanied by a significant increase the cytokines expression (Bottai, 2008). The increase of the expression of trophic factors into the lesion site cannot be derived directly from NSCs, because *in vitro* cultured tests revealed that there is only a low production of these trophic molecules (Pluchino, 2003). It is possible that the interaction of the cells with the lesion environment will have increased their production of trophic factors (Sroga, 2003).

IL-6 is a major pro-inflammatory cytokines whose expression increases significantly after SCI, this increase was associated with an increase of infiltration of neutrophils, and at an expansion of the neural damaged due to injury (Lacroix, 2002); PM-NPCs reduce significantly the expression in the acute phase of lesion decreasing the damage tissue, however, 7 days after injury, animals treated with cells show an expression of this cytokine that is significantly increased compared to animals treated with PBS. This data is in agree with some results reported in literature which show that in addition to the involvement of IL-6 in the initial phase of the inflammatory response, it can also affect directly and / or indirectly neuronal survival (Marz, 1999). In addition, IL-6 has also been demonstrated to have neuroprotective effects (Loddick, 1998; Allan and Rothwell, 2001) and promote regeneration and axonal sprouting (Hakkoum, 2007). This cytokine has a neurotoxic effect in the acute phase of injury where his activity is antagonized by the PM-NPCs, while in the chronic phase has a positive effect on the neural tissue and the treatment with the cells contributes to increase the expression.

The production of TNF- α to the site of injury increases in a short time from the lesion and its activity is implicated in the damage of secondary type at multiple levels (Wang, 1996; Liefner, 2000; Paterniti, 2009). The expression levels of this cytokine are increased in animals treated with PBS, while treatment with the PM-NPCs maintains significantly low the expression levels in acute phase of damage this activity helps to reduce the effects of secondary damage. A week after the injury, however, the mice treated with the cells show values of TNF- α higher respect to the animals treated with PBS. This effect may explain the improvements observed with the PM-NPCs as is been demonstrated that TNF- α has also a neuroprotective effect (Shohami, 1999) and is indirectly involved in neuronal survival through stimulus for the production of neurotrophic factors such as NGF (Hattori, 1993) and the BDNF (Saha, 2006). The TNF- α was also known to be implicated in the processes of myelination and demyelination, then the improvement in the motor recovery could also be in part due to the effect that TNF- α promotes remyelination axons survived in the lesion (Arnett et al, 2001; Huang, 2002). This hypothesis is supported by the reduction of the motor recovery degree observed following the trauma of the CNS in KO mice for the expression of TNF- α or its receptor (Sullivan, 1999).

LIF is a cytokine that has been shown to have pro-inflammatory effects. It is considered one of the most potent mediators of the initial phase of the inflammatory response following CNS injury. It has been demonstrated to be essential for the initial recruitment of macrophages and neutrophils (Sugiura, 2000) and is one of the main molecules that regulates the glia response following cortical damage (Sugiura, 2000). In addition, in this case the treatment with the PM-NPCs reduces the expression of this cytokine in the first hour after SCI so antagonize a damaged effect spinal cord.

As it happens, however, with IL-6 and TNF- α , also with LIF at the end of acute phase of the damage we can observe high level of this cytokine in the animals treated with cells compared to the mice treated with PBS. The literature support our data, it has been demonstrated that the administration of exogenous LIF at the end of acute injury leads to a shutdown of the oligodendrocytes death through upregulation of anti-apoptotic molecules and to a downregulation of those pro-apoptotic, with a consequent reduction of demyelination, and then reduction of molecules inhibiting axonal growth (Azari, 2006). We then observed that three major pro-inflammatory molecules such as IL-6, TNF- α and LIF have a negative effect in the acute phase post injury, but are instead very important for the next phase in which they can participate in neuroprotective and regenerative processes. The treatment with the PM-NPCs rule perfectly the activity of these cytokines, reduce the expression when they have a damage effect on neural tissue and promoting it when they can make a positive contribution.

MIP 2 is a major chemotactic factors and activation of neutrophils. Her overproduction in the injured spinal cord is associated to the infiltration of neutrophils suggesting that this mediator plays a key role in the recruitment of inflammatory cells after SCI (Bethea, 2000; Gris, 2004). In the acute phase after injury the MIP 2 expression increases compared to the controls, as is already known from the literature. The treatment with PM-NPCs antagonizes this increase, maintaining the expression levels of the cytokine to values similar to control animals. BDNF is a neurotrophin that has neuroprotective effects in vivo (Novikova, 2000) and stimulates axonal regrowth (Oudega and Hagg, 1999; Zhou and Shine,2003). It was shown that the local administration of BDNF may revertatrophy of neuronal cell bodies in the red nucleus induced by SCI (Ruitenberg, 2004) and that it may also prevent the degeneration of the ascending sensory fibers(Sayer et al, 2002). The treatment with PM-NPCs leads to a significant increase in the expression ofBDNF in the acute phase of injury, while later there are no differences in the two types of treatments.

Although NGF is an important neurotrophin which is very important for the processes ofneuronal survival (Cao, 2002) and regeneration (Oudega and Hagg, 1996) that are established following CNS traumaand (Grilll,1997). Its expression is always increased in response to the spinal cord injury (Brown, 2004), and, we have not found in the acute phasesignificant differences in the animals treated with PBS compared to those treated withPM-NPCs. In later stage, we observed that treatment with thePM-NPCs maintains the expression of NGF to higher values, whichprobably contributes regenerative effect that we found.

In this study the effect of PM-NPCs transplantation has been also investigated on experimental models of another neurodegenerative disease due to the loss of the specific population of neurons such as in Parkinson's disease. After intra-striatal infusion, more than 75% of PM-NPCs survive in the striatum, and differentiate mostly in neuronal-like cells. Such differentiation is higher for those cells that have migrated to more distal sites from the injection point: 60% MAP-2 positive and above than 80% NeuN-positive. Most of PM-NPCs transdifferentiated in TH positive cells, and a large percentage of these were positive for GABA and ChAT. Some had migrated throughout the striatum reaching the SN. At 10 days after MPTP administration mice made several errors in forepaw placement on the horizontal grid test, were practically unable to descend properly from the top of the vertical grid, and showed a severe impairment in the olfactory test. Such stable deficits were promptly reversed when PM-NPCs were administered. Within 3- 4 days the recovery was highly significant and with another 4 days, the behavioral parameters were practically identical to the control animals without any lesions. Such a recovery was likely independent from any

improvement in striatal dopamine content, since the loss, caused by MPTP intoxication, was unaltered after transplantation. HPLC analysis had unequivocally shown that MPTP administration caused about 50% loss of dopamine content in the striatum, and such a decrease was not modified by PM-NPCs. It is therefore clear that the protective or reparative action of PM-NPCs may not be mediated by the simple recovery of dopamine levels in the striatum, but rather by different mechanisms that may lead to an enhanced efficacy of the synaptic dopaminergic transmission from the surviving striatal axon terminals. Cell treatment had slightly increased striatal TH immunoreactivity that correlates with the higher expression of DAT and NET in the transplanted lesioned mice. Our observations are in line with observations made in MPTP lesioned monkeys, where the amount of DAT activity, investigated with PET neuroimaging, was related to the number of surviving dopaminergic fibers (Hallett, 2015). Moreover, very recent investigations on DAT expression, performed in post-mortem brain sections of PD patients treated with fetal mesencephalic grafts, highlighted that the expression of DAT decreases with time after transplantation (Hallett, 2014). This decrease had been related to the loss of efficacy in long-term fetal mesencephalic grafts (Barker, 2013; Hallett, 2015; Hantraye, 1992). The improved functionality of the surviving DA axons as a PM-NPCs mechanism of action is also supported by the fact that, after transplantation, the SN cell bodies do not die and re-acquire the expression of TH, which was strongly reduced 10 days after MPTP treatment. It should be noted that PM-NPCs migrate to SN ipsilateral and contralateral to the injection site.

PM-NPCs have the peculiar properties of releasing erythropoietin (EPO), which is critical factor for their own differentiation (Marfia, 2011). So it is conceivable that the release of such a neuro-protective factor may also have a favorable impact on the striatum dopaminergic functions and, consequently, on behavioral recovery. The EPO neuroprotective effects are very well known and supported by a large body of literature showing that in vivo administration of EPO promotes recovery of function after CNS lesions (Gorio, 2002; Brines, 2008). Moreover, it has been shown that the rh-EPO or EPO analogs administration in the rodent model of PD had neuroprotective and neuro-rescue effects (Jia, 2014; Tayra, 2013; Erbas, 2015). Since PM-NPCs-mediated behavioral recovery was prevented by the blockade of EPO or EPOR, we believe that EPO may be the effector of PM-NPCs transplants. This may have a dual effect on the striatum microenvironment. One related to both a local neuroprotective action on neurons and neural processes affected by MPTP, and the stimulation of a migratory response of endogenous stem cells towards the area of PM-NPCs accumulation. EPO has been shown to direct the migration of endogenous stem cells towards EPO reach source (Erbas, 2015; Shingo, 2000). The other local action of EPO maybe anti-inflammatory, mitigating the inflammatory reaction to MPTP as indicated by there-expression of TH by MPTP-

lesioned SN neurons. A similar effect was observed after a septo-hippocampal lesion, where septal neurons recovered ChAT positivity following NGF or BDNF infusion (Morse, 1993). We have observed that PM-NPCs reduce both inflammatory cytokines and reactive GFAP-positive gliosis and macrophages infiltration caused by MPTP ipsilateral to the injection site. A similar result was obtained in experimental traumatic spinal cord injury after treatment with PM-NPCs (21) or EPO (Gorio, 2002). These counteractive effects on astrogliosis are quite relevant, since these cells are positively activated in PD and produce an elevated level of inflammatory cytokines and reactive oxygen species (Block, 2007); such an activation is correlated with increased neural death (McGeer, 1988; Sofroniew, 2005).

In conclusion, we found that treatment with PM-NPCs could limit the effects of secondary degeneration of the traumatic injury in the spinal cord through a significant reduction in the area affected by neurodegenerative process and with the preservation of the white matter rostral and caudal to the lesion. The PM-NPCs also have an important anti-inflammatory effect that is expressed with a strong reduction of reactive gliosis and a decrease infiltration of neutrophils and macrophages in the lesion. The PM-NPCs modulate the expression of cytokines reducing the effect of those pro-inflammatory and increasing the function of those neurotrophic / anti-inflammatory. The treatment of the injured cord with these cells promotes the formation of a favorable environment that leads to neuronal differentiation of the cells themselves and to a vigorous axon regeneration that passes the site of injury as demonstrated by the injection of fluororuby at the cervical level of the corticospinal tract. In fact, animals treated with the cells show a greater number of axons with tracer caudal to the lesion, indicating a significant axonal regrowth through the site of injury. The multiple effects that have the PM-NPCs on the damaged spinal cord will lead to a good therapeutic result which is expressed in a significant improvement in the recovery of motor function.

Moreover PM-NPCs markedly improve morphological, biochemical and behavioral dysfunctions caused by MPTP intoxication. This effect may be mediated by local EPO release, which mitigates neuro-inflammatory events leading to recovery of function. Therefore, transplantable natural unmodified cells capable of releasing anti-inflammatory factors may represent a promising path for the treatment of neurodegenerative disorders.

6. Bibliography

1. Abbaszadeh HA, Tiraihi T, Noori-Zadeh A, Delshad AR et al. Human ciliary neurotrophic factor-overexpressing stable bone marrow stromal cells in the treatment of a rat model of traumatic spinal cord injury. *Cytotherapy*.(2015) 17(7):912-21.
2. Abematsu M, Tsujimura K, Yamano M, Saito M et al. Neurons derived from transplanted neural stem cells restore disrupted neuronal circuitry in a mouse model of spinal cord injury. *J Clin Invest*. (2010)120: 3255-3266.
3. Adelman DM, Simon MC. Hypoxic gene regulation in differentiating ES cells. *Methods Mol Biol*. (2002) 185: 55-62.
4. Aggarwal S, Pittenger MF. Human mesenchymal stem cells modulate allogeneic immune cell responses. *Blood*. (2005) 105:1815-1822.
5. Allan SM and Rothwell NJ. Cytokines and acute neurodegeneration. *Nat Rev Neurosci*, (2001) 2: 734-744.
6. Alvarez-Fischer D, Guerreiro S, Hunot S, Saurini F, Marien M, Sokoloff P et al. Modelling Parkinson-like neurodegeneration via osmotic minipump delivery of MPTP and probenecid. *J Neurochem*. (2008) 107: 701–711.
7. American Spinal Injury Association Chicago. American spinal injury association, international standards for neurological classifications of spinal cord injury (revised). (2000): 1–23.
8. Anderson DK, Means ED, Waters TR, Green ES. Microvascular perfusion and metabolism in injured spinal cord after methylprednisolone treatment. *J Neurosurg*. (1982) 56: 106-113.
9. Arnett HA, Mason J, Marino M, Suzuki K, Matsushima GK, Ting JP. TNF alpha promotes proliferation of oligodendrocyte progenitors and remyelination. *Nat Neurosci*. (2001) 4(11):1116-22.
10. Azari MF, Profyris C, Karnezis T, Bernard CC et al. Leukemia inhibitory factor arrests oligodendrocyte death and demyelination in spinal cord injury. *J NeuropatholExp Neurol*. (2006) 65, 914-929.

11. Badiola N, Malagelada C, Llecha N, Hidalgo J, Comella JX, Sabriá J, Rodríguez-Alvarez J. Activation of caspase-8 by tumour necrosis factor receptor 1 is necessary for caspase-3 activation and apoptosis in oxygen-glucose deprived cultured cortical cells. *Neurobiol Dis.* (2009) 35(3):438-47.
12. Baptiste DC, Fehlings MG. Pharmacological approaches to repair the injured spinal cord. *J Neurotrauma.* (2006) 23(3-4): 318-34.
13. Barakat DJ, Gaglani SM, Neravetla SR, Sanchez AR et al. Survival, integration, and axon growth support of glia transplanted into the chronically contused spinal cord. *Cell Transplant.* (2005) 14: 225-240.
14. Barakat DJ, Gaglani SM, Neravetla S., Sanchez AR et al. Survival, integration, and axon growth support of glia transplanted into the chronically contused spinal cord. *Cell Transplant.* (2005) 14: 225-240.
15. Barker RA, Barrett J, Mason SL, Björklund A. Fetal dopaminergic transplantation trials and the future of neural grafting in Parkinson's disease. *Lancet Neurol.* (2013) 12:84-91.
16. Barker RA, Barrett J, Mason SL, Björklund A. Fetal dopaminergic transplantation trials and the future of neural grafting in Parkinson's disease. *Lancet Neurol.* (2013) 12: 84-91.
17. Barker RA, de Beaufort I. Scientific and ethical issues related to stem cell research and interventions in neurodegenerative disorders of the brain. *Prog Neurobiol* (2013) 110: 63-73.
18. Barker RA. Developing stem cell therapies for Parkinson's disease: waiting until the time is right. *Cell Stem Cell.* (2014) 15: 539-542.
19. Barone FC, Arvin B, White RF, Miller A et al Tumor necrosis factor-alpha. A mediator of focal ischemic brain injury. *Stroke.* (1997) 28(6):1233-44.
20. Basso DM et al. Basso Mouse Scale for locomotion detects differences in recovery after spinal cord injury in five common mouse strains. *J Neurotrauma.* (2006) 23 (5): 635–59.
21. Beirowski B, Adalbert R, Wagner D, Grumme DS et al. The progressive nature of Wallerian degeneration in wild-type and slow Wallerian degeneration (WldS) nerves. *BMC Neurosci.* (2005) 6: 6

22. Bellermand M and Fouad K. Spontaneous locomotor recovery in spinal cord injured rats is accompanied by anatomical plasticity of reticulospinal fibers. *Eur J Neurosci.* (2006) 23: 1988-1996.
23. Bethea JR. Spinal cord injury-induced inflammation: a dual-edged sword. *Prog Brain Res.* (2000) 128: 33-42.
24. Beyer Nardi N and da Silva Meirelles L. Mesenchymal stem cells: isolation, in vitro expansion and characterization. *HandbExpPharmacol.* (2006) 174: 249-82.
25. Bianco JJ, Perry C, Harkin DG, Mackay-Sim A, Feron F. Neurotrophin 3 promotes purification and proliferation of olfactory ensheathing cells from human nose. *Glia* (2004) 45: 111-123.
26. Bjorklund LM, Sanchez-Pernaute R, Chung S et al. Embryonic stem cells develop into functional dopaminergic neurons after transplantation in a Parkinson rat model. *Proc Natl Acad Sci.* (2002) 99: 2344–2349.
27. Block ML, Hong JS. Chronic microglial activation and progressive dopaminergic neurotoxicity. *BiochemSoc Trans* (2007) 35:1127–1132.
28. Bose P, Parmer R, Reier PJ and Thompson FJ. Morphological changes of the soleus motoneuron pool in chronic midthoracic contused rats. *Exp Neurol.* (2005) 191: 13-23.
29. Bottai D, Cigognini D, Madaschi L, Adami R, Nicora E, Menarini M, Di Giulio A M, Gorio A. Embryonic stem cells promote motor recovery and affect inflammatory cell infiltration in spinal cord injured mice. *Exp. Neurol.* (2010) 223: 452-463.
30. Bottai D, Madaschi L, Di Giulio AM, Gorio A. Viability-dependent promoting action of adult neural precursors in spinal cord injury. *Mol Med.* (2008) 14(9-10): 634-44.
31. Bracken MB, Collins WF, Freeman DF, Shepard MJ et al. Efficacy of methylprednisolone in acute spinal cord injury. *JAMA* (1984) 251: 45-52
32. Bracken MB, Holford TR. Effects of timing of methylprednisolone or naloxone administration on recovery of segmental and long-tract neurological function in NASCIS 2. *J Neurosurg.* (1993) 79(4): 500-7.

33. Bracken MB, Shepard MJ, Collins WF, Holford TR et al. A randomized, controlled trial of methylprednisolone or naloxone in the treatment of acute spinal-cord injury. Results of the Second National Acute Spinal Cord Injury Study. *N Engl J Med* (1990) 322: 1405-1411.
34. Brines M, Cerami A. Erythropoietin-mediated tissue protection: reducing collateral damage from the primary injury response. *J Intern Med.* (2008) 264:405-432.
35. Brines ML, Ghezzi P, Keenan S, Agnello D et al. Erythropoietin crosses the blood-brain barrier to protect against experimental brain injury. *Proc Natl AcadSci USA.* (2000) 97: 10525-10531.
36. Brosamle C and Schwab ME. Cells of origin, course, and termination patterns of the ventral, uncrossed component of the mature rat corticospinal tract. *J Comp Neurol.* (1997) 386: 293-303.
37. Brosamle C and Schwab ME. Ipsilateral, ventral corticospinal tract of the adult rat: ultrastructure, myelination and synaptic connections. *J Neurocytol.* (2000) 29: 499-507.
38. Brown A, Ricci MJ and Weaver LC. NGF message and protein distribution in the injured rat spinal cord. *Exp Neurol.* (2004) 188: 115-127.
39. Buehr M, Meek S, Blair K, Yang J, Ure J, Silva J et al Capture of authentic embryonic stem cells from rat blastocysts. *Cell.* (2008) 135: 1287–1298.
40. Burns RS, Chiueh CC, Markey SP, Ebert MH, Jacobowitz DM, Kopin IJ. A primate model of Parkinsonism: selective destruction of dopaminergic neurons in the pars compacta of the substantia nigra by N-methyl-4-phenyl-1,2,3,6-tetrahydropyridine. *Proc Nat Acad Sci USA.* (1983) 80: 4546–4550.
41. Cao X, Tang C and Luo Y. Effects of nerve growth factor on N-methyl-D-aspartate receptor after spinal cord injury in rats. *Chin J Traumatol.* (2002) 5: 228-231.
42. Carelli S, Giallongo T, Gerace C, De Angelis A, Basso MD, Di Giulio AM, Gorio A. Neural stem cell transplantation in experimental contusive model of spinal cord injury. *J Vis Exp.* (2014) 94 (a).
43. Carelli S, Giallongo T, Latorre E, Caremoli, F et al. A. Adult Mouse Post Mortem Neural Precursors survive, differentiate, counteract cytokine production and promote functional

- recovery after transplantation in experimental traumatic spinal cord. *J Stem Cell Res Transplant.* (2014) 1(2): 1008 (b).
44. Carelli S, Giallongo T, Marfia G et al. Exogenous adult postmortem neural precursors attenuate secondary degeneration and promote myelin sparing and functional recovery following experimental spinal cord injury. *Cell Transplant.* (2015) 24(4): 703-19.
 45. Chapman A R, Scala C C. Evaluating the first-in-human clinical trial of a human embryonic stem cell-based therapy. *Kennedy Inst EthicsJ.* (2012) 22(3): 243–261.
 46. Chiba K, Trevor A, Castagnoli N, Jr. Metabolism of the neurotoxic tertiary amine, MPTP, by brain monoamine oxidase. *Biochem Biophys Res Commun.* (1984) 120: 574–578
 47. Chirugiavol 2, *Chirurgia specialistica*, 3° edizione – Dionigi R. - Ed. Massori p. 1926-1935
 48. Choi C, Benveniste EN. Fas ligand/Fas system in the brain: regulator of immune and apoptotic responses. *Brain Res Brain Res Rev.* (2004) 44(1):65-81.
 49. Cizkova D, Rosocha J, Vanicky I, et al. Transplants of human mesenchymal stem cells improve functional recovery after spinal cord injury in the rat. *Cell Mol Neurobiol.* (2006) 26: 1167–80.
 50. Cloutier F, Siegenthaler M M, Nistor G, Keirstead H S. Transplantation of human embryonic stem cell-derived oligodendrocyte progenitors into rat spinal cord injuries does not cause harm. *Regen Med.* (2006) 1(4): 469–479.
 51. Conley BJ, Young JC, Trounson AO, Mollard R. Derivation, propagation and differentiation of human embryonic stem cells. *Int. J. Biochem. Cell Biol.* (2004) 36: 555–567.
 52. Cornelius C, Crupi R, Calabrese V, Graziano A et al. Traumatic brain injury: oxidative stress and neuroprotection. *Antioxid Redox Signal.* (2013) 19(8):836-53.
 53. Cui YF, Hargus G, Xu JC, et al. Embryonic stem cell-derived L1 overexpressing neural aggregates enhance recovery in Parkinsonian mice. *Brain.* (2010) 133:189-204.

54. Davis AE, Campbell SJ, Wilainam P, Anthony DC. Post conditioning with lipopolysaccharide reduces the inflammatory infiltrate to the injured brain and spinal cord: a potential neuroprotective treatment. *Eur J Neurosci.* (2005) 22: 2441-2450.
55. Davis GC, Williams AC, Markey SP, Ebert MH, Caine ED, Reichert CM et al. Chronic Parkinsonism secondary to intravenous injection of meperidine analogues. *Psychiatry Res* (1979) 1: 249–254.
56. Diaz-Ruiz A, Rios C, Duarte I, Correa D et al. Cyclosporin-A inhibits lipid peroxidation after spinal cord injury in rats. *Neurosci Lett.* (1999) 266: 61–64.
57. Diaz-Ruiz A, Vergara P, Perez-Severiano F, Segovia J et al. Cyclosporin-A inhibits inducible nitric oxide synthase activity and expression after spinal cord injury in rats. *Neurosci Lett.* (2004) 357: 49–52.
58. Doi D, Samata B, Katsukawa M, et al. Isolation of human induced pluripotent stem cell-derived dopaminergic progenitors by cell sorting for successful transplantation. *Stem Cell Reports.* (2014) 2: 337-350.
59. Donnelly DJ, Popovich PG. Inflammation and its role in neuroprotection, axonal regeneration and functional recovery after spinal cord injury. *Exp Neurol.* (2008) 209(2):378-88.
60. Dumont RJ, Verma S, Okonkwo DO, Hurlbert RJ et al. Acute spinal cord injury, part II: contemporary pharmacotherapy. *Clin Neuropharmacol.* (2001) 24: 265-279.
61. Duncan ID, Milward EA. Glial cell transplants: experimental therapies of myelin diseases. *Brain Pathol.* (1995)5(3): 301-10.
62. Eidelberg E, Nguyen LH, Polich R and Walden JG. Transsynaptic degeneration of motoneurons caudal to spinal cord lesions. *Brain Res Bull.* (1989) 22: 39-45.
63. Emerit J, Edeas M, Bricaire F. Neurodegenerative diseases and oxidative stress. *Biomedicine & Pharmacotherapy.* (2004) 58:39–46.
64. Erbaş O, Çınar BP, Solmaz V, et al. The neuroprotective effect of erythropoietin on experimental Parkinson model in rats. *Neuropeptides* (2015) 49:1-5.

65. Erbayraktar S, Grasso G, Sfacteria A, Xie QW. Asialoerythropoietin is a nonerythropoietic cytokine with broad neuroprotective activity in vivo. *Proc Natl AcadSci USA*. (2003) 100: 6741–6746.
66. Faravelli I, Bucchia M, Rinchetti P, Nizzardo M, Simone C, Frattini E, Corti S. Motor neuron derivation from human embryonic and induced pluripotent stem cells: experimental approaches and clinical perspectives. *Stem Cell Res Ther*. (2014) 5(4): 87.
67. Fehlings MG, Rao SC, Tator CH, Skaf G, Arnold P et al. The optimal radiologic method for assessing spinal canal compromise and cord compression in patients with cervical spinal cord injury. Part II: Results of a multicenter study. *Spine* (1999) 24: 605-613.
68. Fehlings MG, Tator CH, Linden RD. The effect of nimodipine and dextran on axonal function and blood flow following experimental spinal cord injury. *J Neurosurg*. (1989) 71: 403–416.
69. Fitch MT and Silver J. CNS injury, glial scars, and inflammation: Inhibitory extracellular matrices and regeneration failure. *Exp Neurol*.(2008) 209: 294-301.
70. Fitch MT and Silver J. Glial cell extracellular matrix: boundaries for axon growth indevelopment and regeneration. *Cell Tissue Res*.(1997) 290: 379-384.
71. Fornai F, Schluter OM, Lenzi P, Gesi M, Ruffoli R, Ferrucci M et al. Parkinson-like syndrome induced by continuous MPTP infusion: convergent roles of the ubiquitin-proteasome system and a-synuclein. *Proc Natl Acad Sci USA*. (2005) 102: 3413–3418.
72. Freeman WM, Walker SJ, Vrana KE. Quantitative RT-PCR: pitfalls and potential. *Biotechniques*. (1999) 124-5.
73. Fu ES and Tummala RP. Neuroprotection in brain and spinal cord trauma. *CurrOpinAnaesthesiol* (2005) 18: 181-187.
74. Furlan JC, Noonan V, Cadotte DW, Fehlings MG. Timing of decompressive surgery of spinal cord after traumatic spinal cord injury: an evidence-based examination of pre-clinical and clinical studies. *J Neurotrauma*. (2011) 28: 1371-99.
75. G. Raisman. Olfactory ensheathing cells — another miracle cure for spinal cord injury? *Nature Reviews Neuroscience*. (2001) 2(5): 369–375.

76. Gaviria M, Privat A, D'Arbigny P, Kamenka J, Hato, H, Ohanna F. Neuroprotective effects of a novel NMDA antagonist, gacyclidine, after experimental contusive spinal cord injury in adult rats. *Brain Res.* (2000) 874: 200–209.
77. Geisler FH, Dorsey FC, Coleman WP. Recovery of motor function after spinal-cord injury-- a randomized, placebo-controlled trial with GM-1 ganglioside. *N Engl J Med* (1991) 324: 1829-1838.
78. Gerardo-Nava J, Mayorenko II, Grehl T, Steinbusch HW, Weis J, Brook GA. Differential pattern of neuroprotection in lumbar, cervical and thoracic spinal cord segments in an organotypic rat model of glutamate-induced excitotoxicity. *J Chem Neuroanat.* (2013) 53:11-7.
79. Gibrat C, Saint-Pierre M, Bousquet M, Levesque D, Rouillard C, Cicchetti F. Differences between subacute and chronic MPTP mice models: investigation of dopaminergic neuronal degeneration and a-synuclein inclusions. *J Neurochem* (2009) 109: 1469–1482.
80. Giehl KM and Tetzlaff W. BDNF and NT-3, but not NGF, prevent axotomy-induced death of rat corticospinal neurons in vivo. *Eur J Neurosci.* (1996) 8: 1167-1175.
81. Glinka Y, Gassen M, Youdim MB. Mechanism of 6- hydroxydopamine neurotoxicity. *J Neural Transm Suppl* (1997) 50: 55–66.
82. Goldberg NR, Haack AK, Lim NS, Janson OK, Meshul CK. Dopaminergic and behavioral correlates of progressive lesioning of the nigrostriatal pathway with 1-methyl-4-phenyl-1,2,3,6-tetrahydropyridine. *Neuroscience.* (2011) 180:256-271.
83. Gonzalez-Lara LE et al. The use of cellular magnetic resonance imaging to track the fate of iron-labeled multipotent stromal cells after direct transplantation in a mouse model of spinal cord injury. *Mol Imaging Biol.* (2010) 13 (4): 702-11.
84. Goodman & Gilman's 2011. *The Pharmacological Basis of Therapeutics*, 12 edition.
85. Gorio A, Gokmen N, Erbayraktar S, et al. Recombinant human erythropoietin counteracts secondary injury and markedly enhances neurological recovery from experimental spinal cord trauma. *Proc Natl AcadSci U S A.* (2002) 99:9450-9455.

86. Gorio A, Gokmen N, Erbayraktar S, Yilmaz O et al. Recombinant human erythropoietin counteracts secondary injury and markedly enhances neurological recovery from experimental spinal cord trauma. *Proc Natl AcadSci U S A.* (2002) 99: 9450-5.
87. Gorio A, Madaschi L, Zadra G, Marfia G, Cavalieri B, Bertini R and Di Giulio AM. Reparixin, an inhibitor of CXCR2 function, attenuates inflammatory responses and promotes recovery of function after traumatic lesion to the spinal cord. *J PharmacolExpTher.* (2007) 322: 973-981.
88. Gorio A, Torrente Y, Madaschi L, Di Stefano AB et al. Fate of autologous dermal stem cells transplanted into the spinal cord after traumatic injury (TSCI). *Neuroscience.* (2004) 125: 179-189.
89. Gorio A, Vergani L, Ferro L, Prino G, Di Giulio AM. Glycosaminoglycans in nerve injury: II. Effects on transganglionic degeneration and on the expression of neurotrophic factors. *J Neurosci Res.* (1996) 46(5): 572-80.
90. Gorio A. Ganglioside enhancement of neuronal differentiation, plasticity and repair. *CRC Crit Rev ClinNeurobiol* (1986) 2: 241-296.
91. Greenwood HL, Thorsteinsdottir H, Perry G, Renihan J, Singer PA, et al. Regenerative medicine: New opportunities for developing countries. *Int J Biotechnol*(2006) 8: 60–77.
92. Grill RJ, Blesch A and Tuszynski MH. Robust growth of chronically injured spinal cord axons induced by grafts of genetically modified NGF-secreting cells. *Exp Neurol.* (1997) 148: 444-452.
93. Gris D, Marsh DR, Oatway MA, Chen Y et al. Transient blockade of the CD11d/CD18 integrin reduces secondary damage after spinal cord injury, improving sensory, autonomic, and motor function. *J Neurosci.* (2004) 24: 4043–4051.
94. Gris D, Marsh DR, Oatway MA, Chen Y et al. Transient blockade of the CD11d/CD18 integrin reduces secondary damage after spinal cord injury, improving sensory, autonomic, and motor function. *J Neurosci.* (2004) 24, 4043-4051.
95. Gritti A, Frölichsthal-Schoeller P, Galli R, Parati EA et al. Epidermal and fibroblast growth factors behave as mitogenic regulators for a single multipotent stem cell-like population

- from the subventricular region of the adult mouse forebrain. *J Neurosci.* (1999) 19(9): 3287-97.
96. Gritti A, Parati EA, Cova L, Frolichsthal P. Multipotential stem cells from the adult mouse brain proliferate and self-renew in response to basic fibroblast growth factor. *J Neurosci.* (1996) 16: 1091-1100.
97. Gudehithlu KP, Duchemin AM, Tejawani GA, Neff NH, Hadjiconstantinou M. Preproenkephalin mRNA and methionine-enkephalin increase in mouse striatum after 1-methyl-4-phenyl-1,2,3,6-tetrahydropyridine treatment. *J Neurochem*(1991) 56: 1043–1048.
98. Hakkoum D, Stoppini L and Muller D. Interleukin-6 promotes sprouting and functional recovery in lesioned organotypic hippocampal slice cultures. *J Neurochem.* (2007) 100: 747-757.
99. Hallett PJ, Cooper O, Sadi D, et al. Long-term health of dopaminergic neuron transplants in Parkinson's disease patients. *Cell Rep.* (2014) 7:1755-1761.
100. Hallett PJ, Cooper O, Sadi D, et al. Long-term health of dopaminergic neuron transplants in Parkinson's disease patients. *Cell Rep.* (2014) 7: 1755-1761.
101. Hallett PJ, Deleidi M, Astradsson A et al. Successful function of autologous iPSC-derived dopamine neurons following transplantation in a non-human primate model of Parkinson's disease. *Cell Stem Cell.* (2015) 16:269-274.
102. Hallett PJ, Deleidi M, Astradsson A et al. Successful function of autologous iPSC-derived dopamine neurons following transplantation in a non-human primate model of Parkinson's disease. *Cell Stem Cell* (2015) 16: 269-274.
103. Halliwell B. The wanderings of a free radical. *Free Radic Biol Med* (2009) 46: 531–542.
104. Hantraye P, Brownell AL, Elmaleh D et al. Dopamine fiber detection by [¹¹C]-CFT and PET in a primate model of parkinsonism. *Neuroreport.* (1992) 3:265-268.
105. Happel RD, Smith KP, Banik NL, Powers JM et al. Ca²⁺-accumulation in experimental spinal cord trauma. *Brain Res.* (1981) 211(2):476-479

106. Haque NS, LeBlanc CJ, Isacson O. Differential dissection of the rat E16 ventral mesencephalon and survival and reinnervation of the 6-OHDA-lesioned striatum by a subset of aldehyde dehydrogenase-positive TH neurons. *Cell Transplant.* (1997) 6: 239–248.
107. Hashimoto T, Fukuda N. Effect of thyrotropin-releasing hormone on the neurologic impairment in rats with spinal cord injury: treatment starting 24 h and 7 days after injury. *Eur J Pharmacol.* (1991) 203: 25–32.
108. Hassouna I, Wickert H, Zimmermann M, Gillardon F (1996). Increase in bax expression in substantia nigra following 1-methyl-4-phenyl-1,2,3,6-tetrahydropyridine (MPTP) treatment of mice. *Neurosci Lett* 204: 85–88.
109. Hattori A, Tanaka E, Murase K, Ishida et al. Tumor necrosis factor stimulates the synthesis and secretion of biologically active nerve growth factor in non-neuronal cells. *J Biol Chem.* (1993) 268: 2577-2582.
110. Hebert G, Arsaut J, Dantzer R, Demotes-Mainard J. Time-course of the expression of inflammatory cytokines and matrix metalloproteinases in the striatum and mesencephalon of mice injected with 1-methyl-4-phenyl-1,2,3,6-tetrahydropyridine, a dopaminergic neurotoxin. *Neurosci Lett.* (2003) 349: 191–195.
111. Heinemann AW, Yarkony GM, Roth EJ, Lovell L et al. Functional outcome following spinal cord injury. A comparison of specialized spinal cord injury center vs general hospital short-term care. *Arch Neurol.* (1989) 46(10):1098-1102.
112. Herrmann JE, Imura T, Song B, et al. STAT3 is a critical regulator of astrogliosis and scar formation after spinal cord injury. *J Neurosci.* (2008) 28: 7231–7234.
113. Higuchi R, Fockler C, Dollinger G, Watson R. Kinetic PCR analysis: Real-Time monitoring of DNA amplification reactions. *Biotechnology.* (1993) 1026-1030.
114. Hill CE, Beattie MS and Bresnahan JC. Degeneration and sprouting of identified descending supraspinal axons after contusive spinal cord injury in the rat. *Exp Neurol.* (2001) 171: 153-169.
115. Hofstetter CP, Holmström NA, Lilja JA, Schweinhardt P et al. Allodynia limits the usefulness of intraspinal neural stem cell grafts: Directed differentiation improves outcome. *Nat. Neurosci.* (2005) 8: 346–353.

116. Horvath LL, Galimi F, Gage FH, et al. Fate of endogenous stem/progenitor cells following spinal cord injury. *J Comp Neurol.* (2006) 498: 525–38.
117. Hur JW, Cho TH, Park DH, Lee JB, Park JY, Chung YG. Intrathecal transplantation of autologous adipose-derived mesenchymal stem cells for treating spinal cord injury: A human trial. *J Spinal Cord Med.* (2015) [Epubahead of print]
118. Hyun I. Big bang theory: more reason to scrap Bush's stem cell policy. *Hastings Cent Rep.* (2008) 38(6): 5-6.
119. Ibarra A, Correa D, Willms K, Merchant MT et al. Effects of cyclosporin-A on immune response, tissue protection and motor function of rats subjected to spinal cord injury. *Brain Res.* (2003) 979: 165–178.
120. Jackson-Lewis V, Przedborski S. Protocol for the MPTP mouse model of Parkinson's disease. *Nat Protoc* (2007) 2: 141–151.
121. Janowski M et al. Neurotransplantation in mice: The concordance-like position ensures minimal cell leakage and widespread distribution of cells transplanted into the cistern magna. *Neuroscience Letter.* (2008) 430 (2): 169-174.
122. Javitch JA, D'Amato RJ, Strittmatter SM, Snyder SH. Parkinsonism-inducing neurotoxin, N-methyl-4-phenyl-1,2,3,6 -tetrahydropyridine: uptake of the metabolite N-methyl-4-phenylpyridine by dopamine neurons explains selective toxicity. *Proc Natl Acad Sci USA.* (1985) 82: 2173–2177.
123. Jenner P. Clues to the mechanism underlying dopamine cell death in Parkinson's disease. *J Neurol Neurosurg Psychiatry* (1989) 52 (Suppl.): 22–28.
124. Jia Y, Mo SJ, Feng QQ, et al. EPO-dependent activation of PI3K/Akt/FoxO3a signalling mediates neuroprotection in in vitro and in vivo models of Parkinson's disease. *J MolNeurosci.* (2014) 53:117-124.
125. Johannessen JN, Chiueh CC, Burns RS, Markey SP. Differences in the metabolism of MPTP in the rodent and primate parallel differences in sensitivity to its neurotoxic effects. *Life Sci.* (1985) 36: 219–224.

126. Jorgensen J, Ahn J, Aboushaala K, Singh K. Current concepts in the use of stem cells for the treatment of spinal cord injury. *Semin Spin Surg.* (2015) 27: 90 – 92
127. Juul SE, Anderson DK, Li Y, Christensen RD. Erythropoietin and erythropoietin receptor in the developing human central nervous system. *Pediatr Res.* (1998) 43: 40-49.
128. Juurlink BH and Paterson PG. Review of oxidative stress in brain and spinal cord injury: suggestions for pharmacological and nutritional management strategies. *J Spinal Cord Med.* (1998) 21: 309–334.
129. Kaptanoglu E, Tuncel M, Palaoglu S, Konan A, Demirpençe E, Kiliç K. Comparison of the effects of melatonin and methylprednisolone in experimental spinal cord injury. *J Neurosurg.* (2000) 93: 77-84.
130. Karunakaran S, Saeed U, Mishra M, Valli RK, Joshi SD, Meka DP et al. (2008). *Selective activation of p38 mitogen-activated protein kinase in dopaminergic neurons of substantia nigra leads to nuclear translocation of p53 in 1-methyl-4-phenyl-1,2,3,6-tetrahydropyridine-treated mice. J Neurosci 28: 12500–12509.*
131. Kefalopoulou Z, Politis M, Piccini P, et al. Long-term clinical outcome of fetal cell transplantation for Parkinson disease: two case reports. *JAMA Neurol.* (2014) 71: 83-87.
132. Keirstead HS, Nistor G, Bernal G, et al. Human embryonic stem cell-derived oligodendrocyte progenitor cell transplants remyelinate and restore locomotion after spinal cord injury. *J Neurosci.* (2005) 25(19): 4694–4705.
133. Kim JH, Auerbach JM, Rodríguez-Gómez JA et al. Dopamine neurons derived from embryonic stem cells function in an animal model of Parkinson's disease. *Nature* (2002) 4: 50-56.
134. Kokoszka JE, Coskun P, Esposito LA, Wallace DC. Increased mitochondrial oxidative stress in the Sod2 (+/-) mouse results in the age-related decline of mitochondrial function culminating in increased apoptosis. *Proc Natl Acad Sci USA.* (2001) 98: 2278-2283.
135. Kriks S, Shim JW, Piao J et al. Dopamine neurons derived from human ES cells efficiently engraft in animal models of Parkinson's disease. *Nature.* (2011) 480: 547–551.
136. Kriks, S. et al. Dopamine neurons derived from human ES cells efficiently engraft in animal models of Parkinson's disease. *Nature.* (2011) 480: 547–551.

137. Kunikowska G, Jenner P. 6-Hydroxydopamine-lesioning of the nigrostriatal pathway in rats alters basal ganglia mRNA for copper, zinc- and manganese-superoxide dismutase, but not glutathione peroxidase. *Brain Res* (2001) 922: 51–64
138. Kurkowska-Jastrzebska I, Wronska A, Kohutnicka M, Czlonkowski A, Czlonkowska A. The inflammatory reaction following 1-methyl-4-phenyl-1,2,3, 6-tetrahydropyridine intoxication in mouse. *Exp Neurol*. (1999) 156: 50–61.
139. Lacroix S, Chang L, Rose-John S and Tuszynski MH. Delivery of hyper-interleukin-6 to the injured spinal cord increases neutrophil and macrophage infiltration and inhibits axonal growth. *J Comp Neurol*. (2002) 454: 213-228.
140. Langston JW, Ballard P, Tetrud JW, Irwin I. Chronic Parkinsonism in humans due to a product of meperidine-analog synthesis. *Science*. (1983) 219: 979–980.
141. Langston JW, Ballard P. Parkinsonism induced by 1-methyl-4-phenyl-1,2,3,6-tetrahydropyridine (MPTP): implications for treatment and the pathogenesis of Parkinson's disease. *Can J Neurol Sci*. (1984) 11: 160–165.
142. Lau YS, Meredith GE . From drugs of abuse to Parkinsonism. The MPTP mouse model of Parkinson's disease. *Methods Mol Med*. (2003) 79: 103–116.
143. Leist M, Ghezzi P, Grasso G, Bianchi R et al. Derivatives of erythropoietin that are tissue protective but not erythropoietic. *Science* (2004) 305: 239–242.
144. Li J and Lepski G. Cell transplantation for spinal cord injury: a systematic review. *Biomed Res Int*. (2013) 2013:786475.
145. Li S, Jiang Q, Stys PK. Important role of reverse Na(+)-Ca(2+) exchange in spinal cord white matter injury at physiological temperature. *J Neurophysiol*. (2000) 84(2):1116-1119.
146. Liang CL, Nelson O, Yazdani U et al. Inverse relationship between the contents of neuromelanin pigment and the vesicular monoamine transporter-2: human midbrain dopamine neurons. *J Comp Neurol*. (2004) 473:97-106.
147. Liefner M, Siebert H, Sachse T, Michel U, Kollias G and Bruck W. The role of TNF α during Wallerian degeneration. *J Neuroimmunol*, (2000) 108: 147-152.

148. Lima C, Pratas-Vital J, Escada P, Hasse-Ferreira A, Capucho C, Peduzzi JD. Olfactory Mucosa Autografts in Human Spinal Cord Injury: A Pilot Clinical Study. *The Journal of Spinal Cord Medicine*. (2006) 29(3): 191-203.
149. Lindvall O, Brundin P, Widner H, et al. Grafts of fetal dopamine neurons survive and improve motor function in Parkinson's disease. *Science*. (1990) 247: 574–577.
150. Lipton SA, Rosenberg PA. Excitatory amino acids as a final common pathway for neurologic disorders. *N Engl J Med*. (1994) 330(9):613-22.
151. Liu J, Akay T, Hedlund PB, Pearson KG, Jordan LM. Spinal 5-HT7 receptors are critical for alternating activity during locomotion: in vitro neonatal and in vivo adult studies using 5-HT7 receptor knockout mice. *J Neurophysiol*. (2009) 102(1): 337-48.
152. Liu SL, Qu Y, Stewart TJ, Howard MJ, Chakraborty S, Holekamp TF, McDonald JW. Embryonic stem cells differentiate into oligodendrocytes and myelinate in culture and after spinal cord transplantation. *Proc Natl Acad Sci U S A*. (2000) 97(11): 6126-31.
153. Livak KJ, Flood SJ, Marmaro J, Giusti W, Deetz K. Oligonucleotides with fluorescent dyes at opposite ends provide a quenched probe system useful for detecting PCR product and nucleic acid hybridization. *PCR Methods Appl*. (1995) 357-362.
154. Loddick SA, Turnbull AV and Rothwell NJ. Cerebral interleukin-6 is neuroprotective during permanent focal cerebral ischemia in the rat. *J Cereb Blood Flow Metab*. (1998) 18: 176-179.
155. Long JB, Martinez-arizala A, Petras JM, Holaday JW. Endogenous opioids in spinal cord injury: a critical evaluation. *Cent Nerv Syst Trauma*. (1986) 3: 295–315.
156. Lorber B, Chew DJ, Hauck SM, Chong RS et al. Retinal glia promote dorsal root ganglion axon regeneration. *PLoS One*. (2015) 10(3):e0115996.
157. Lukovic D, Moreno Manzano V, Stojkovic M, Bhattacharya S S, Erceg S. Concise review: human pluripotent stem cells in the treatment of spinal cord injury. *Stem Cells* . (2012) 30 (9): 1787–1792.

158. Luthman J, Fredriksson A, Lewander T, Jonsson G, Archer T. Effects of d-amphetamine and methylphenidate on hyperactivity produced by neonatal 6-hydroxydopamine treatment. *Psychopharmacology (Berl)*. (1989) 99: 550–557.
159. Ma, L. et al. Human embryonic stem cell-derived GABA neurons correct locomotion deficits in quinolinic acid-lesioned mice. *Cell Stem Cell*. (2012) 10: 455–464.
160. Maier IC and Schwab ME. Sprouting, regeneration and circuit formation in the injured spinal cord: factors and activity. *Philos Trans R Soc Lond B Biol Sci*. (2006) 361: 1611-1634.
161. Maikos JT and Shreiber DI. Immediate damage to the blood-spinal cord barrier due to mechanical trauma. *J Neurotrauma*. (2007) 24: 492-507.
162. Manuale di chirurgia vol 1- Stipa A. – Ed. Monduzzi p. 1385-1395.
163. Marsden CD. Movement disorders. In: Weatherall DJ, Ledingham JGG, Warrell DA, eds. *Oxford textbook of medicine*. Vol 3, New York: Oxford University Press Inc. (1996) 3998-4022.
164. Martin GR. Isolation of a pluripotent cell line from early mouse embryos cultured in medium conditioned by teratocarcinoma stem cells. *Proc Natl Acad Sci USA* (1981) 78: 7634–7638.
165. Martínez-Cerdeño V, Noctor SC, Espinosa A, et al. Embryonic MGE precursor cells grafted into adult rat striatum integrate and ameliorate motor symptoms in 6-OHDA-lesioned rats. *Cell Stem Cell* (2010) 6: 238-250.
166. Martino G, Pluchino S. The therapeutic potential of neural stem cells. *Nat Rev Neurosci*. (2006) 7:395-406.
167. Marz P, Heese K, Dimitriades-Schmutz B, Rose-John S and Otten U. Role of interleukin-6 and soluble IL-6 receptor in region-specific induction of astrocytic differentiation and neurotrophin expression. *Glia*. (1999) 26: 191-200.
168. Mazzi EA, Reams RR, Soliman KF. The role of oxidative stress, impaired glycolysis and mitochondrial respiratory redox failure in the cytotoxic effects of 6-hydroxydopamine in vitro. *Brain Res*. (2004) 1004: 29–44.

169. McComas AJ, Sica RE, Upton AR and Aguilera N. Functional changes in motoneurons of hemiparetic patients. *J NeurolNeurosurg Psychiatry*. (1973) 36: 183-193.
170. McCreedy DA, Sakiyama-Elbert SE. Combination therapies in the CNS: engineering the environment. *Neurosci Lett*. (2012)519(2):115-21.
171. McDonald J W, Liu X Z, Qu Y, et al. Transplanted embryonic stem cells survive, differentiate and promote recovery in injured rat spinal cord. *Nat Med*. (1999) 5(12): 1410–1412.
172. McDonald JW, Becker D, Sadowsky CL, Jane JA et al. Late recovery following spinal cord injury. Case report and review of the literature. *J Neurosurg*. (2002) 97: 252-265.
173. McGeer PL, Itagaki S, Boyes BE, McGeer EG. Reactive microglia are positive for HLA-DR in the substantia nigra of Parkinson's and Alzheimer's disease brains. *Neurology* (1988) 38:1285–1291.
174. Meredith GE, Totterdell S, Beales M, Meshul CK. Impaired glutamate homeostasis and programmed cell death in a chronic MPTP mouse model of Parkinson's disease. *Exp Neurol* (2009) 219: 334–340.
175. Merriam WF, Taylor TK, Ruff SJ, McPhail MJ. A reappraisal of acute traumatic central cord syndrome. *J Bone Joint Surg Br*. (1986) 68: 708–713.
176. Molcanyi M, Riess P, Bentz K, Maegele M et al. Trauma-associated inflammatory response impairs embryonic stem cell survival and integration after implantation into injured rat brain. *J Neurotrauma*. (2007) 24(4): 625-37.
177. Moreno-Flores MT, Bradbury EJ, Martin-Bermejo MJ, Agudo M et al A clonal cell line from immortalized olfactory ensheathing glia promotes functional recovery in the injured spinal cord. *MolTher*.(2006) 13: 598-608.
178. Mori S, Matsui T, Kuze B, Asanome M, Nakajima K, et al. Cerebellar-induced locomotion: reticulospinal control of spinal rhythm generating mechanism in cats. *Ann N Y Acad Sci*. (1998) 860: 94-105.

179. Morse JK, Wiegand SJ, Anderson K, et al. Brain-derived neurotrophic factor (BDNF) prevents the degeneration of medial septal cholinergic neurons following fimbria transection. *J Neurosci.* (1993) 13:4146-4156.
180. MSKTC. Spinal Cord Injury (SCI) Facts and Figures at a Glance. 2014 (https://www.nscisc.uab.edu/PublicDocuments/fact_figures_docs/Facts%202014.pdf).
181. Mukhida K, Mendez I, McLeod M, et al. Spinal GABAergic transplants attenuate mechanical allodynia in a rat model of neuropathic pain. *Stem Cells.* (2007) 25: 2874–85.
182. Murrell W, Wetzig A, Donnellan M, Féron F, Burne T, Meedeniya A, Kesby J, Bianco J, Perry C, Silburn P, Mackay-Sim A. Olfactory mucosa is a potential source for autologous stem cell therapy for Parkinson's disease. *Stem Cells.* (2008) 26(8): 2183-92.
183. Musina RA, Bekchanova ES, Sukhikh GT. Comparison of Mesenchymal Stem Cells Obtained from Different Human Tissues. *Bulletin of Experimental Biology and Medicine.* (2005) 139 (4): 504–509.
184. Newey ML, Sen PK, Fraser RD. The long-term outcome after central cord syndrome: a study of the natural history. *J Bone Joint Surg Br.* (2000) 82: 851–855.
185. Nivet E, Vignes M, Girard SD, Pierrisnard C, Baril N, Devèze A, Magnan J, Lanté F, Khrestchatsky M, Féron F, Roman FS. Engraftment of human nasal olfactory stem cells restores neuroplasticity in mice with hippocampal lesions. *J Clin Invest.* (2011) 121(7): 2808-20.
186. Noble LJ, Wrathall JR: Distribution and time course of protein extravasation in the rat spinal cord after contusive injury. *Brain Res.* (1989) 482:57–66.
187. Novikova L, Garris BL, Garris DR, Lau YS. Early signs of neuronal apoptosis in the substantia nigra pars compacta of the progressive neurodegenerative mouse 1-methyl-4-phenyl-1,2,3,6 tetrahydropyridine/probenecid model of Parkinson's disease. *Neuroscience.* (2006) 140: 67–76.
188. Novikova LN, Novikov LN and Kellerth JO. Survival effects of BDNF and NT-3 on axotomized rubrospinal neurons depend on the temporal pattern of neurotrophin administration. *Eur J Neurosci.* (2000) 12: 776-780.

189. Ortiz LA, Dutreil M, Fattman C et al. Phinney DG. Interleukin 1 receptor antagonist mediates the antiinflammatory and antifibrotic effect of mesenchymal stem cells during lung injury. *Proc Natl AcadSci U S A.* (2007)104:11002.
190. Ottobriani L et al. Magnetic resonance imaging of stem cell transplantation in injured mouse spinal cord. *Cell R4.* (2014) 2 (3): e963.
191. Oudega M and Hagg T. Nerve growth factor promotes regeneration of sensory axons into adult rat spinal cord. *Exp Neurol.* (1996)140: 218-229.
192. Oudega M and Hagg T. Neurotrophins promote regeneration of sensory axons in the adult rat spinal cord. *Brain Res* (1999) 818: 431-438.
193. Oyinbo CA. Secondary injury mechanisms in traumatic spinal cord injury: a nugget of this multiply cascade. *ActaNeurobiolExp (Wars).* (2011) 71(2):281-99.
194. Park E, Velumian AA, Fehlings MG. The role of excitotoxicity in secondary mechanisms of spinal cord injury: a review with an emphasis on the implications for white matter degeneration. *J Neurotrauma.* (2004) 21(6):754-74.
195. Parr AM, Tator CH and Keating A. Bone marrow-derived mesenchymal stromal cells for the repair of central nervous system injury. *Bone Marrow Transplant.* (2007) 40: 609-619.
196. Paterniti I, Genovese T, Crisafulli C, Mazzon, E. Treatment with green tea extract attenuates secondary inflammatory response in an experimental model of spinal cord trauma. *NaunynSchmiedebergs ArchPharmacol* (2009) 380: 179-192.
197. Pêgo AP, Kubinova S, Cizkova D, Vanicky I, Mar FM, Sousa MM, Sykova E. Regenerative medicine for the treatment of spinal cord injury: more than just promises? *J Cell Mol Med.* (2012) 16(11): 2564-82.
198. Perumal AS, Gopal VB, Tordzro WK, Cooper TB, Cadet JL . Vitamin E attenuates the toxic effects of 6-hydroxydopamine on free radical scavenging systems in rat brain. *Brain Res Bull* (1992) 29: 699–701.
199. Petitjean ME, Pointillart V, Dixmierias F, Wiart L et al. Medical treatment of spinal cord injury in the acute stage. *Ann Fr Anesth Reanim.* (1998) 17: 114 122
200. Petit-Zeman S Regenerative medicine. *Nat Biotechnol.*(2001) 19: 201–206.

201. Phani S, Gonye G, Iacovitti L. VTA neurons show a potentially protective transcriptional response to MPTP. *Brain Res.* (2010) 9:1-13.
202. Pineau I, Lacroix S: Proinflammatory cytokine synthesis in the injured mouse spinal cord: multiphasic expression pattern and identification of the cell types involved. *J Comp Neurol.* (2007) 500:267–285.
203. Pitts LH, Ross A, Chase GA, Faden AI. Treatment with thyrotropin-releasing hormone (TRH) in patients with traumatic spinal cord injuries. *J Neurotrauma* (1995) 12: 235–243.
204. Pluchino S, Quattrini A, Brambilla E, Gritti A et al. Injection of adult neurospheres induces recovery in a chronic model of multiple sclerosis. *Nature.* (2003) 422: 688-694.
205. Popovich PG, Jones TB. Manipulating neuroinflammatory reactions in the injured spinal cord: back to basics. *Trends Pharmacol Sci.* (2003) 24(1): 13-7.
206. Popovich PG, Wei P and Stokes BT. Cellular inflammatory response after spinal cord injury in Sprague-Dawley and Lewis rats. *J Comp Neurol.* (1997) 377: 443-464.
207. Popovich PG, Wei P, Stokes BT. Cellular inflammatory response after spinal cord injury in Sprague-Dawley and Lewis rats. *J Comp Neurol.* (1997) 377: 443–464.
208. Pothakos K, Kurz MJ, Lau YS. Restorative effect of endurance exercise on behavioral deficits in the chronic mouse model of Parkinson's disease with severe neurodegeneration. *BMC Neurosci.* (2009) 10: 6.
209. Povlishock JT, and Kontos HA. The role of oxygen radical in the pathobiology of traumatic brain injury. *Human Cell.* (1992) 5: 345–353.
210. Precht TA, Phelps RA, Linseman DA, Butts BD et al. The permeability transition pore triggers Bax translocation to mitochondria during neuronal apoptosis. *Cell Death Differ.* (2005) 12(3):255-65.
211. Ramón-Cueto A and Avila J. Olfactory ensheathing glia: properties and function. *Brain Research Bulletin.* (1998) 46 (3): 175–187.
212. Ramon-Cueto A, Cordero MI, Santos-Benito FF, and Avila J. Functional recovery of paraplegic rats and motor axon regeneration in their spinal cords by olfactory ensheathing glia. *Neuron.* (2000) 25: 425-435.

213. Rawson NE and Gomez G. Cell and molecular biology of human olfaction. *Microscopy Research and Technique*. (2002) 58(3): 142.
214. Riachi NJ, LaManna JC, Harik SI. Entry of 1-methyl-4-phenyl-1,2,3,6-tetrahydropyridine into the rat brain. *J Pharmacol Exp Ther* (1989) 249: 744–748.
215. Richter MW and Roskams AJ. Olfactory ensheathing cell transplantation following spinal cord injury: hype or hope? *Exp Neurol*. (2008) 209: 353-367.
216. Ríos C, Orozco-Suarez S, Salgado-Ceballos H, Mendez-Armenta M, Nava-Ruiz C, Santander I, Barón-Flores V, Caram-Salas N, Diaz-Ruiz A. Anti-Apoptotic Effects of Dapsone After Spinal Cord Injury in Rats. *Neurochem Res*. (2015) 40(6):1243-51.
217. Romanyuk N, Amemori T, Turnovcova K, et al. Using human fetal neural stem cells or human induced pluripotent stem cell derived neural precursors for the treatment of experimental spinal cord injury. 8th IBRO World Congress of Neuroscience. Florence, Italy, 2011.
218. Rosenberg LJ, Teng YD, Wrathall JR. Effects of the sodium channel blocker tetrodotoxin on acute white matter pathology after experimental contusive spinal cord injury. *J Neurosci*. (1999) 19: 6122–6133.
219. Rowland JW, Hawryluk GW, Kwon B, Fehlings MG. Current status of acute spinal cord injury pathophysiology and emerging therapies: promise on the horizon. *Neurosurg Focus*. (2008) 25(5):E2.
220. Ruitenberg MJ, Blits B, Dijkhuizen PA, teBeek ET et al. Adeno-associated viral vector mediated gene transfer of brain-derived neurotrophic factor reverses atrophy of rubrospinal neurons following both acute and chronic spinal cord injury. *Neurobiol Dis*. (2004) 15: 394-406.
221. Safford K and Rice H. Stem Cell Therapy for Neurologic Disorders: Therapeutic Potential of Adipose-Derived Stem Cells. *Current Drug Targets*. (2005) 6(1): 57–62.
222. Saha RN, Liu X and Pahan K. Up-regulation of BDNF in astrocytes by TNF-alpha: a case for the neuroprotective role of cytokine. *J Neuroimmune Pharmacol*. (2006) 1: 212-222.

223. Sahni V, Kessler JA. Stem cell therapies for spinal cord injury. *Nat Rev Neurol.* (2010) 6: 363-72.
224. Sakanka M, Wen TC, Matsuda S, Masuda S et al. In vivo evidence that erythropoietin protects neurons from ischemic damage. *Proc Natl AcadSci USA.* (1998) 95: 4635-4640.
225. Saporito MS, Thomas BA, Scott RW. MPTP activates c-Jun NH(2)-terminal kinase (JNK) and its upstream regulatory kinase MKK4 in nigrostriatal neurons in vivo. *J Neurochem.* (2000) 75: 1200–1208.
226. Sayer FT, Oudega M and Hagg T. Neurotrophins reduce degeneration of injured ascending sensory and corticospinal motor axons in adult rat spinal cord. *Exp Neurol* (2002) 175: 282-296.
227. Schaal SM, Kitay BM, Cho KS, Lo TP Jr et al. Schwann cell transplantation improves reticulospinal axon growth and forelimb strength after severe cervical spinal cord contusion. *Cell Transplant.* (2007) 16: 207-228.
228. Schofield BR, Schofield RM, Sorensen KA, Motts SD. On the use of retrograde tracers for identification of axon collaterals with multiple fluorescent retrograde tracers. *Neuroscience.* (2007) 146(2):773-83.
229. Schultzberg M, Dunnett SB, Bjorklund A, et al. Dopamine and cholecystokinin immunoreactive neurons in mesencephalic grafts reinnervating the neostriatum: evidence for selective growth regulation. *Neuroscience.* (1984) 12: 17–32.
230. Schwartz G, Fehlings MG. Evaluation of the neuroprotective effects of sodium channel blockers after spinal cord injury: improved behavioral and neuroanatomical recovery with riluzole. *J Neurosurg Spine.* (2001) 94: 245–256.
231. Scivoletto G. and Di Donna V. Prediction of walking recovery after spinal cord injury. *Brain Res Bull* (2009) 78 (1): 43-51.
232. Sekhon LH, Fehlings MG. Epidemiology, demographics, and pathophysiology of acute spinal cord injury. *Spine (Phila Pa 1976).* (2001) 15(26):S2-12.

233. Setoguchi T, Nakashima K, Takizawa T, Yanagisawa M et al Treatment of spinal cord injury by transplantation of fetal neural precursor cells engineered to express BMP inhibitor. *Exp Neurol.* (2004) 189: 33-44.
234. Sharma HS. Pathophysiology of blood-spinal cord barrier in traumatic injury and repair. *Curr Pharm Des.* (2005) 11(11):1353-89.
235. Shingo T, Sorokan ST, Shimazaki T, Weiss S. Erythropoietin regulates the in vitro and in vivo production of neuronal progenitors by mammalian forebrain neural stem cells. *J Neurosci.* (2001) 21: 9733-9743.
236. Shingo T, Sorokan ST, Shimazaki T, Weiss S. Erythropoietin regulates the in vitro and in vivo production of neuronal progenitors by mammalian forebrain neural stem cells. *J Neurosci* (2000) 21:9733-9743.
237. Shohami E, Ginis I and Hallenbeck JM. Dual role of tumor necrosis factor alpha in brain injury. *Cytokine Growth Factor Rev.*(1999) 10: 119-130.
238. Silva NA, Sousa N, Reis RL, Salgado AJ. From basics to clinical: a comprehensive review on spinal cord injury. *Prog Neurobiol.* (2014) 114:25-57.
239. Silver J and Miller JH. Regeneration beyond the glial scar. *Nat Rev Neurosci.* (2004) 5: 146-156.
240. Skene JH, Jacobson RD, Snipes GJ, McGuire C.B et al A protein induced during nerve growth (GAP-43) is a major component of growth-cone membranes (1986) 233(4765): 783-786.
241. Sofroniew MV. Reactive astrocytes in neural repair and protection. *Neuroscientist.* (2005) 11:400-407.
242. Spillantini MG, Crowther RA, Jakes R, Hasegawa M, Goedert M. Alpha-Synuclein in filamentous inclusions of Lewy bodies from Parkinson's disease and dementia with lewy bodies. *Proc Natl Acad Sci USA.* (1998) 95: 6469-73.
243. Spillantini MG, Schmidt ML, Lee VM, Trojanowski JQ, Jakes R, Goedert M. Alpha-synuclein in Lewy bodies. *Nature.* (1997) 388: 839-40.

244. Sroga JM, Jones TB, Kigerl KA, McGaughy VM and Popovich PG. Rats and mice exhibit distinct inflammatory reactions after spinal cord injury. *J Comp Neurol.* (2003) 462: 223-240.
245. Steward O, Zheng B, Ho C, Anderson K and Tessier-Lavigne M. The dorsolateral corticospinal tract in mice: an alternative route for corticospinal input to caudal segments following dorsal column lesions. *J Comp Neurol.* (2004) 472: 463-477.
246. Stirling DP, Khodarahmi K, Liu J, McPhail LT et al. Minocycline treatment reduces delayed oligodendrocyte death, attenuates axonal dieback, and improves functional outcome after spinal cord injury. *J Neurosci.* (2004) 24: 2182–2190.
247. Stocum DL. Tissue restoration through regenerative biology and medicine. *Adv Anat Embryol Cell Biol.* (2004) 176(III-VIII): 1-101.
248. Stoodley, M.A. Pathophysiology of syringomyelia. *J Neurosurg.* (2000) 92: 1069-1070; author reply 1071-1063.
249. Stys PK. White matter injury mechanisms. *Curr Mol Med.* (2004) 4: 113-130.
250. Sugiura S, Lahav R, Han J, Kou SY, Banner LR et al. Leukaemia inhibitory factor is required for normal inflammatory responses to injury in the peripheral and central nervous systems in vivo and is chemotactic for macrophages in vitro. *Eur J Neurosci.* (2000) 12: 457-466.
251. Sullivan PG, Bruce-Keller AJ, Rabchevsky AG, Christakos S et al. Exacerbation of damage and altered NF-kappaB activation in mice lacking tumor necrosis factor receptors after traumatic brain injury. *J Neurosci.* (1999) 19, 6248-6256.
252. Sundberg M, Bogetofte H, Lawson T, et al. Improved cell therapy protocols for Parkinson's disease based on differentiation efficiency and safety of hESC-, hiPSC-, and non-human primate iPSC-derived dopaminergic neurons. *Stem Cells.* (2013) 31: 1548-1562.
253. Tabar V, Studer L. Pluripotent stem cells in regenerative medicine: challenges and recent progress. *Nat Rev Genet.* (2014) 15(2):82-92.
254. Takahashi K, Tanabe K, Ohnuki M et al. Induction of pluripotent stem cells from adult human fibroblasts by defined factors. *Cell.* (2007) 131: 861–872.

255. Takami T, Oudega M, Bates ML, et al. Schwann cell but not olfactory ensheathing glia transplants improve hindlimb locomotor performance in the moderately contused adult rat thoracic spinal cord. *J Neurosci.* 2002; 22: 6670–81.
256. Tanhoffer RA, Yamazaki RK, Nunes EA, Pchevozniki AI et al. Glutamine concentration and immune response of spinal cord-injured rats. *J Spinal Cord Med.* (2007) 30(2):140-146.
257. Taoka Y and Okajima K. Spinal cord injury in the rat. *Prog Neurobiol.* (1998) 56: 341-358.
258. Taoka Y, Okajima K, Uchiba M, Murakami K et al. Role of neutrophils in spinal cord injury in the rat. *Neuroscience.* (1997) 79(4):1177-82.
259. Taoka Y, Okajima K, Uchiba M, Murakami K et al. Role of neutrophils in spinal cord injury in the rat. *Neuroscience.* (1997) 79: 1177–1182.
260. Taoka Y, Okajima K, Uchiba M, Murakami K et al. Role of neutrophils in spinal cord injury in the rat. *Neuroscience.* (1997) 79:1177-1182.
261. Tarkowski E, Rosengren L, Blomstrand C, Wikkelso C et al. Intrathecal release of pro- and anti-inflammatory cytokines during stroke. *Clin Exp Immunol.* (1997) 110(3):492-9.
262. Tator CH, Fehlings MG. Review of clinical trials of neuroprotection in acute spinal cord injury. *Neurosurg Focus.* (1999) 15 (6):1-8.
263. Tator CH, Fehlings MG. Review of the secondary injury theory of acute spinal cord trauma with emphasis on vascular mechanisms. *J Neurosurg.* (1991) 75(1):15-26.
264. Tayra TJ, Kameda M, Yasuhara T, et al. The neuroprotective and neurorescue effects of carbamylated erythropoietin Fc fusion protein (CEPO-Fc) in a rat model of Parkinson's disease. *Brain Res.* (2013) 1502:55-70.
265. Tetzlaff W, Okon EB, Karimi-Abdolrezaee S, et al. A systematic review of cellular transplantation therapies for spinal cord injury. *J Neurotrauma.* (2011) 28: 1611–82.
266. Thomas AJ, Nockels RP, Pan HQ, Shaffrey CI, Chopp M. Progesterone is neuroprotective after acute experimental spinal cord trauma in rats. *Spine (Phila Pa 1976)* (1999) 24: 2134-2138.

267. Thomson JA, Itskovitz-Eldor J, Shapiro SS, Waknitz MA, Swiergiel JJ, Marshall VS et al. Embryonic stem cell lines derived from human blastocysts. *Science*. (1998) 282: 1145–1147.
268. Thuret S, Moon LD, Gage FH. Therapeutic interventions after spinal cord injury. *Nat Rev Neurosci*. (2006) 7: 628-43.
269. Tsui A, Isacson O. Functions of the nigrostriatal dopaminergic synapse and the use of neurotransplantation in Parkinson's disease. *J Neurol*. (2011) 258: 1393-1405.
270. Um JW, Park HJ, Song J, Jeon I, Lee G, Lee PH et al. Formation of parkin aggregates and enhanced PINK1 accumulation during the pathogenesis of Parkinson's disease. *Biochem Biophys Res Commun* (2010) 393: 824–828.
271. Ungerstedt U . 6-Hydroxy-dopamine induced degeneration of central monoamine neurons. *Eur J Pharmacol*. (1968) 5: 107–110.
272. Van De Meent H, Hosman AJ, Hendriks J, Zwarts M, Group ESS and Schubert M. Severe degeneration of peripheral motor axons after spinal cord injury: a European multicenter study in 345 patients. *Neurorehabil Neural Repair*. (2010) 24: 657-665.
273. Venkatesh P, Khushboo C, Kenneth LH. Stem cell treatment for the spinal cord injury – A concise review. *The Indian Journal of Neurotrauma*. (2014) 11: 30-38.
274. Vitellaro-Zuccarello L, Mazzetti S, Madaschi L, Bosisio P et al. Chronic erythropoietin-mediated effects on the expression of astrocyte markers in a rat model of contusive spinal cord injury. *Neuroscience* (2008)151:452–466.
275. Vitellaro-Zuccarello L, Mazzetti S, Madaschi L, Bosisio P et al. Erythropoietin-mediated preservation of the white matter in rat spinal cord injury. *Neuroscience* (2007) 144:865–877.
276. Wang CX, Nuttin B, Heremans H, Dom R and Gybels J. Production of tumor necrosis factor in spinal cord following traumatic injury in rats. *J Neuroimmunol*. (1996) 69: 151-156.
277. Wang M, Lu C, Roisen F. Adult human olfactory epithelial-derived progenitors: a potential autologous source for cell-based treatment for Parkinson's disease. *Stem Cells Transl Med*. (2012) 1(6): 492-502.

278. Wang SJ, Wang KY, Wang WC. Mechanisms underlying the riluzole inhibition of glutamate release from rat cerebral cortex nerve terminals (synaptosomes). *Neuroscience*. (2004) 125: 191–201.
279. Warden P, Bamber NI, Li H, Esposito A et al. Delayed glial cell death following wallerian degeneration in white matter tracts after spinal cord dorsal column cordotomy in adult rats. *Exp Neurol*. (2001) 168: 213-224.
280. Wells JE, Hurlbert RJ, Fehlings MG, Yong VW. Neuroprotection by minocycline facilitates significant recovery from spinal cord injury in mice. *Brain* (2003) 126: 1628–1637.
281. Werhagen L, Aito S, Tucci L, Strayer J, Hultling C. 25 years or more afterspinal cord injury: clinical conditions of individuals in the Florence andStockholm areas. *Spinal Cord*. (2012) 50(3):243-246.
282. Wernig M, Zhao JP, Pruszak J, et al. Neurons derived from reprogrammed fibroblasts functionally integrate into the fetal brain and improve symptoms of rats with Parkinson's disease. *Proc Natl Acad Sci*. (2008) 105: 5856-5861.
283. Wiessner C, Allegrini PR, Ekatodramis D, Jewell UR et al. Increased cerebral infarct volumes in polyglobulic mice overexpressing erythropoietin. *J Cereb Blood Flow Metab*. (2001) 21: 857–864.
284. Xiong Y, Rabchevsky AG, Hall ED. Role of peroxynitrite in secondary oxidative damage after spinal cord injury. *J Neurochem*. (2007) 100(3):639-49.
285. Xu RX, Nakamura T, Nagao S, Miyamoto O, Jin L et al. Specific inhibition of apoptosis after coldinduced brain injury by moderate postinjuryhypothermia. *Neurosurgery* (1998) 43: 107-114.
286. Yang D, Zhang ZJ, Oldenburg M, et al. Human embryonic stem cell-derived dopaminergic neurons reverse functional deficit in parkinsonian rats. *Stem Cells*. (2008) 26: 55–63.
287. Yılmaz T, Kaptanoğlu E. Current and future medical therapeutic strategies for the functional repair of spinal cord injury. *World J Orthop*. (2015) 6(1): 42-55.
288. Yip PK, Malaspina A. Spinal cord trauma and the molecular point of no return. *MolNeurodegener*. (2012) 7:6.

289. Yiu G and He Z. Glial inhibition of CNS axon regeneration. *Nat Rev Neurosci.* (2006) 7(8): 617–627.
290. Young W, DeCrescito V, Flamm ES, Blight AR, Gruner JA. Pharmacological therapy of acute spinal cord injury: studies of high dose methylprednisolone and naloxone. *ClinNeurosurg* (1988) 34: 675-697.
291. Young W. Spinal cord regeneration. *Cell Transplant.* (2014) 23(4-5): 573-611.
292. Yu J, Vodyanik MA, Smuga-Otto K, J. Antosiewicz-Bourget, J.L. Frane, S. Tian, et al. Induced Pluripotent Stem Cell Lines Derived from Human Somatic Cells. *Science.* (2007) 318: 1917–1920.
293. Zhou L and Shine HD. Neurotrophic factors expressed in both cortex and spinal cord induce axonal plasticity after spinal cord injury. *J Neurosci Res.* (2003) 74: 221-226.
294. Ziv Y, Avidan H, Pluchino S, Martino G. and Schwartz M. Synergy between immune cells and adult neural stem/progenitor cells promotes functional recovery from spinal cord injury. *Proc Natl AcadSci U S A.* (2006) 103: 13174-13179.
295. Zuk PA, Zhu M, Mizuno H, Huang J et al. Multilineage Cells from Human Adipose Tissue: Implications for Cell-Based Therapies. *Tissue Engineering.* (2001) 7 (2): 211–228.
296. Zuk PA. Human Adipose Tissue Is a Source of Multipotent Stem Cells, *Molecular Biology of the Cell.* (2002) 13(12): 4279–4295.
297. Tillerson JL, Miller GW. Grid performance test to measure behavioral impairment in the MPTP-treated-mouse model of parkinsonism. *J Neurosci Methods* (2003)123:189-200.
298. Kim ST, Son HJ, Choi JH, et al. Vertical grid test and modified horizontal grid test are sensitive methods for evaluating motor dysfunctions in the MPTP mouse model of Parkinson's disease. *Brain Res* (2010) 1306:176-183.
299. Schintu N, Frau L, Ibba M, et al. Progressive dopaminergic degeneration in the chronic MPTP mouse model of Parkinson's disease. *Neurotox Res* (2009) 16:127–139.

7. Publications

Papers:

- Stephana Carelli*, **Toniella Giallongo***, Claudio Gerace, Anthea De Angelis, Michele D. Basso, Anna Maria Di Giulio, Alfredo Gorio “*Neural stem cell transplantation in experimental traumatic spinal cord injury.*” JoVE. 2014, 94.
- Carelli S., **Giallongo T.**, Latorre E., Caremoli F., Gerace C., Basso M.D., Di Giulio A.M. and Gorio A. *Adult Mouse Post Mortem Neural Precursors Survive, Differentiate, Counteract Cytokine Production and Promote Functional Recovery after Transplantation in Experimental Traumatic Spinal Cord Injury.* J Stem Cell Res Transplant. 2014; 1(2): 1008
- Carelli S. *, Ottobrini L.*, Diceglie C., Lui R. , Merli D., **Giallongo T**, Degrassi A., Russo M., Marfia G., Gianelli U., Bosari S., Clerici M., Lucignani G., Gorio A. “*Magnetic resonance imaging of stem cell-mediated treatment in a mouse model of spinal cord injury*”. CellR4. 2014, 2 (3): e963.
- Carelli* S., **Giallongo* T**, Marfia* G., Merli D., Ottobrini L., BassoM., Di Giulio A. M., and Gorio A. “*Exogenous Adult Post Mortem Neural Precursors attenuate secondary degeneration, and promote myelin sparing and functional recovery following experimental spinal cord injury*”. Cell Transplantation. 2014, 24(4): 703-19.
- Latorre E.*, Carelli S.*, **Giallongo T.**, Caremoli F., Provenzani A., Di Giulio A.M. and Gorio A. *Long-non-coding RNAs and HuR interaction may regulate neural stem cell differentiation.* Submitted to Journal of Stem Cells Research and Therapy 2015.
- Carelli S.*, Caremoli F.*, Latorre E. *, **Giallongo T.**, Colli M., Canazza A., Provenzani A., Di Giulio A.M., and Gorio A. “*Human antigen R binding regulation of SOX2 mRNA in human mesenchymal stem cells*”. Under revision by Molecular Pharmacology, 2015. *equal contribution.
- Carelli S.*, **Giallongo T.***, Cristina Viaggi, Filippo Caremoli, Elisa Latorre, Andrea Raspa, Massimiliano Mazza, Francesca Vaglini, Anna Maria Di Giulio, Alfredo Gorio. “*Recovery of Function in a Model of Parkinson Disease by Exogenous Adult Mouse Post Mortem Neural Precursors: an Erythropoietin Dependent Effect*” In preparation, 2015.

Posters:

- **Giallongo Toniella***, Carelli Stephana*, Latorre Elisa, Gombalova Zuzana, Ottobrini Luisa, Degrassi Anna, Basso Michele, Di Giulio Anna Maria, Gorio Alfredo. *“Exogenous Adult Post Mortem Neural Precursors attenuate secondary degeneration and promote myelin sparing and functional recovery following experimental spinal cord injury”*. 1th Congresso DISS, 13 Nov. 2015. *equal contribution.
- Elisa Latorre*, Stephana Carelli*, **Toniella Giallongo**, Filippo Caremoli, Alessandro Provenzani, Anna Maria Di Giulio, Alfredo Gorio. *“Long-non-coding RNAs and HuR interaction may regulate neural stem cell differentiation”* 1th Congresso DISS, 13 Nov. 2015. *equal contribution.
- Caremoli F.*, De Angelis A.*, Latorre E., **Giallongo T.**, Di Giulio A.M., Carelli S., Gorio A.. *Human adipose-derived stem cells obtained without enzymatic digestion present high multipotent features*. Forum of Italian Researchers on Mesenchymal and Stromal Stem Cells, 6th Meeting FIRST - Milano, May 12th – 13th, 2014 *equal contribution
- **Toniella Giallongo***, Stephana Carelli*, Cristina Viaggi, Claudio Gerace, Danuta Hebda, Giovanni Umberto Corsini, Anna Maria Di Giulio, and Alfredo Gorio. *“Human adipose-derived stem cells promote functional recovery in a mouse model of Parkinson disease and differentiate in TH-positive neurons”*. Forum of Italian Researchers on Mesenchymal and Stromal Stem Cells, 6th Meeting FIRST - Milano, May 12th – 13th, 2014 *equal contribution
- Carelli S., **Giallongo T.**, Viaggi C., Gerace C., Hebda D.M., Caremoli F., Corsini G.U., Di Giulio A.M. and Gorio A. *Exogenous Adult Mouse Post Mortem Neural promote functional recovery in a mouse model of Parkinson disease and differentiate in TH-positive neurons*. Forum of Neuroscience, 9th FENS, Milan July 5-9, 2014
- **Toniella Giallongo***, Stephana Carelli*, Claudio Gerace, Danuta Maria Hebda, Luisa Ottobrini, Elisa Latorre, Michelle Basso, Anna Maria Di Giulio, and Alfredo Gorio *“Exogenous Adult Post Mortem Neural Precursors attenuate secondary degeneration and promote myelin sparing and functional recovery following experimental spinal cord injury”* Forum of Neuroscience, 9th FENS, Milan July 5-9, 2014.
- Carelli S., Caremoli F., De Angelis A., Latorre E., Gerace C., **Giallongo T.**, Di Giulio A.M., Gorio A. *Minimal manipulation of tissues and stem cells to achieve application in regenerative medicine*. Convegno monotematico SIF (Societa Italiana di Farmacologia).

Titolo: “La farmacologia clinica tra impegno nella ricerca e ruolo nel Servizio Sanitario Nazionale”. Napoli, 2-3 ottobre 2014

- Carelli S., Messaggio F., **Giallongo T.**, Caremoli F., Hebda D.M., Colli M., Tremolada C., Trabucchi E., Di Giulio A.M., Gorio A. *Fresh and Frozen Lipogems-derived micro-fractured human adipose tissue generates mesenchymal stem cells with higher differentiation potential and in vivo repair efficacy*. Congress of the Italian Society of Pharmacology (SIF), 2013, Torino.
- Stephana Carelli, Toniella Giallongo¹, Cristina Viaggi, Andrea Raspa, Giovanni Umberto Corsini, Anna Maria Di Giulio and Alfredo Gorio. “Exogenous Adult Mouse Post Mortem Neural promote functional recovery in a mouse model of Parkinson disease and differentiate in TH-positive neurons”; Congress of the Italian Society of Pharmacology (SIF 2013), Torino.
- Carelli S., Messaggio F., **Giallongo T.**, Caremoli F., Hebda D.M., Colli M., Tremolada C., Trabucchi E., Di Giulio A.M., Gorio A. *Fresh and Frozen Lipogems-derived micro-fractured human adipose tissue generates mesenchymal stem cells with higher differentiation potential and in vivo repair efficacy*. International Society of Plastic Regenerative Surgery (ISPRES), 2013, Berlin.
- Stephana Carelli, Toniella Giallongo¹, Cristina Viaggi, Andrea Raspa, Giovanni Umberto Corsini, Anna Maria Di Giulio and Alfredo Gorio. “Exogenous Adult Mouse Post Mortem Neural promote functional recovery in a mouse model of Parkinson disease and differentiate in TH-positive neurons”; International society for stem cell research (ISSCR 2013), Boston .